# Investigations of Group IVA Transition Metal Mediated Carbon-Carbon Bond Forming Reactions

Thesis by

Ernest Byron Wysong

In Partial Fulfillment of the Requirements

for the Degree of

Doctor of Philosophy

California Institute of Technology

Pasadena, California

1990

(Submitted November 27, 1989)

To My Loving Parents

# ACKNOWLEDGEMENTS

I would like to begin at the top and thank my graduate advisor, Bob Grubbs, for allowing me to be a part of his research group and contributing to the success of my graduate education. His keen insight, guidance, and never-ending encouragement was invaluable to me.

I would next like to thank those members of the Grubbs group who taught me the ropes including Bob Waymouth, Joel Hawkins, Dr. Miwako Mori, and Joon Won Park. In addition, I give special thanks to Dr. Phil Hampton and Dr. Jeff Moore for proofreading this thesis and my proposals. Their suggestions and advice have been extremely helpful. I would also like to thank Dave Wheeler for helping countless times with the operation of the "magnificent" Jeol GX400 NMR Spectrometer and always giving sound advice on a variety of subjects. I owe a great deal of thanks to Andy Myers and the entire Myers group for allowing me to participate in their group meetings, as well as giving me great advice about synthetic techniques.

In making my existence at Caltech more bearable, I thank Paul Smith, Floyd Klavetter, Mike Youngquist, and Steve Novick. In the area of music, I thank Bill Bing for giving me the opportunity to further my skills with the trumpet. For adding a new dimension to the last year of my graduate career, I give special thanks to my Pasadena Ballroom Dance buddies; Leslie, Mina, and Sonja.

Finally, I give the deepest thanks to my Mom, Dad and Brother for their constant encouragement and support.

# ABSTRACT

Zirconocene aldehyde and ketone complexes were synthesized in high yield by treatment of zirconocene acyl complexes with trimethylaluminum or diisobutylaluminum hydride. These complexes, which are activated by dialkylaluminum chloride ligands, inserted unsaturated substrates such as alkynes, allenes, ethylene, nitriles, ketenes, aldehydes, ketones, lactones, and acid chlorides with moderate to high conversion. Insertion of aldehyde substrates yielded zirconocene diolate complexes with up to 20:1 (anti:syn) diastereoselectivity. The zirconocene diolates were hydrolyzed to afford unsymmetrical 1,2-diols in 40-80% isolated yield. Unsymmetrical ketones gave similar insertion yields with little or no diastereoselectivity. A high yielding one-pot method was developed that coupled carbonyl substrates with zirconocene aldehyde complexes that were derived from olefins by hydrozirconation and carbonylation. The zirconocene aldehyde complexes also inserted carbon monoxide and gave acyloins in 50% yield after hydrolysis.

The insertion reaction of aryl epoxides with the trimethylphoshine adduct of titanocene methylidene was examined. The resulting oxytitanacyclopentanes were carbonylated and oxidatively cleaved with dioxygen to afford γ-lactones in moderate yields. Due to the instability and difficult isolation of titanocene methylidene trimethylphoshine adducts, a one-pot method involving the addition of catalytic amounts of trimethylphosphine to β,β-dimethyltitanacyclobutane was developed. A series of disubstituted aryl epoxides were examined which gave mixtures of diastereomeric insertion products. Based on these results, as well as

earlier Hammett studies and labeling experiments, a biradical transition state intermediate is proposed. The method is limited to aryl substituted epoxide substrates with aliphatic examples showing no insertion reactivity.

The third study involved the use of magnesium chloride supported titanium catalysts for the Lewis acid catalyzed silyl group transfer condensation of enol silanes with aldehydes. The reaction resulted in silylated aldol products with as many as 140 catalytic turnovers before catalyst inactivation. Low diastereoselectivities favoring the anti-isomer were consistent with an open transition state involving a titanium atom bound to the catalyst surface. The catalysts were also used for the aldol group transfer polymerization of *t*-butyldimethylsilyloxy-1-ethene resulting in polymers with molecular weights of 5000-31,000 and molar mass dispersities of 1.5-2.8. Attempts to polymerize methylmethacrylate using GTP proved unsuccessful with these catalysts.

## TABLE OF CONTENTS

## LIST OF TABLES

## LIST OF FIGURES AND SCHEMES

CHAPTER 1.

# CHAPTER 1

## Reactivity of Zirconium Ketone and Aldehyde Complexes: Insertion of Unsaturated Substrates

## Introduction

Transition-metal ketene and ketone complexes have been proposed as intermediates in the stoichiometric and catalytic reduction of carbon monoxide involving heterogeneous and homogeneous systems.[1] Many homogeneous examples of such complexes have been isolated and characterized.[2] While exploring a new methodology for the synthesis of bis(cyclopentadienyl)titanium enolates, D. A. Straus, of this research group, discovered a general procedure for the formation of zirconium ketene complexes (eq 1).[3]

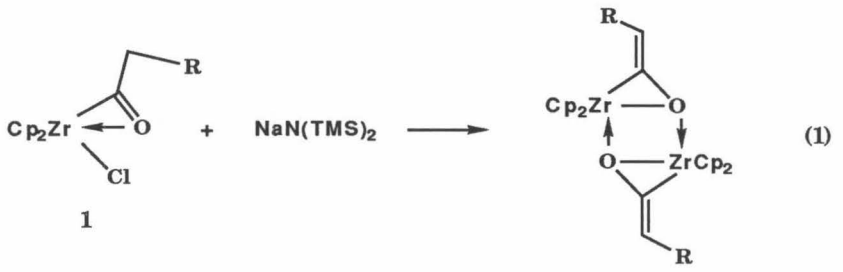


1 (1)

The chemistry of bis(cyclopentadienyl) complexes of early transition-metals is best described by frontier molecular orbital theory (Figure 1). In the case of zirconium, the orbitals $2a_1$ and $b_2$ (the highest occupied molecular orbitals, HOMOs) are used to bind the groups R and Cl in complex **1**, whereas the $1a_1$ is the lowest unoccupied molecular orbital (LUMO) in this 16-electron complex and binds the lone pair of the acyl oxygen atom. In order to attain an 18-electron closed shell, the 16-electron zirconium ketene complexes form very strong dimers by cross donation of oxygen lone pairs into the open coordination sites on the zirconium atoms.

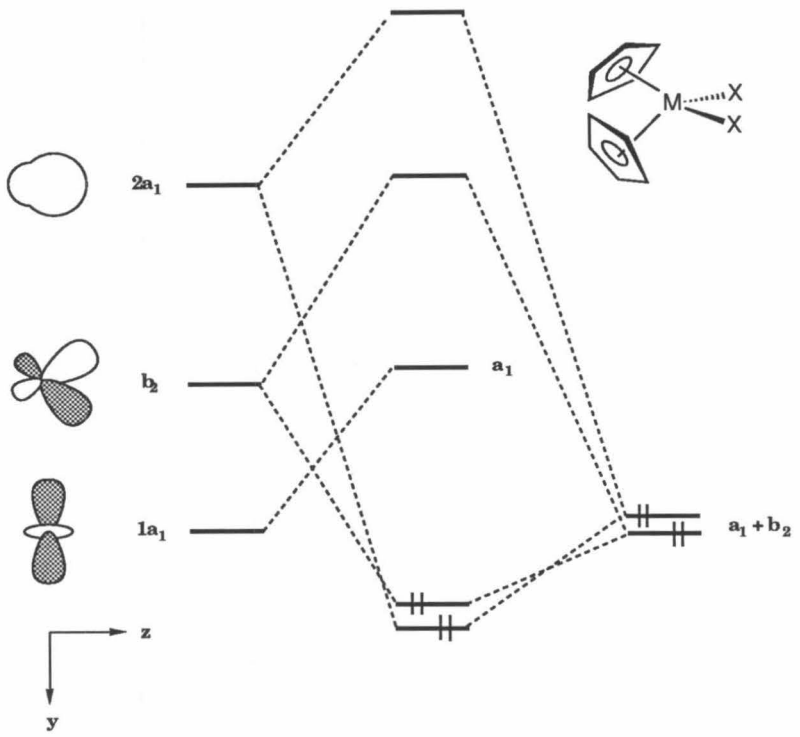


**Figure 1. Bent metallocene frontier MO diagram.**

As a result of dimer formation, the reactivity is diminished. Isolation of the intermediate anionic ketene adduct by Straus, however, provided a reactive species that demonstrated enolate-type behavior (eq 2).[3]

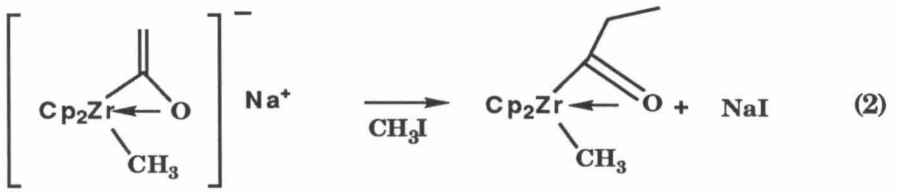


2

Another method that was used to prevent dimerization was the synthesis of zirconium ketene complexes incorporating pentamethylcyclopentadienyl (Cp*) ligands. In this case, the bulky Cp* ligands prevent interactions between the ketene complexes. The pyridine adducts of these complexes demonstrated much higher reactivity with

some important examples summarized in Figure 2.[3] The Cp* ketene complexes react with electron rich unsaturated substrates via insertion into the zirconium-carbon bond.

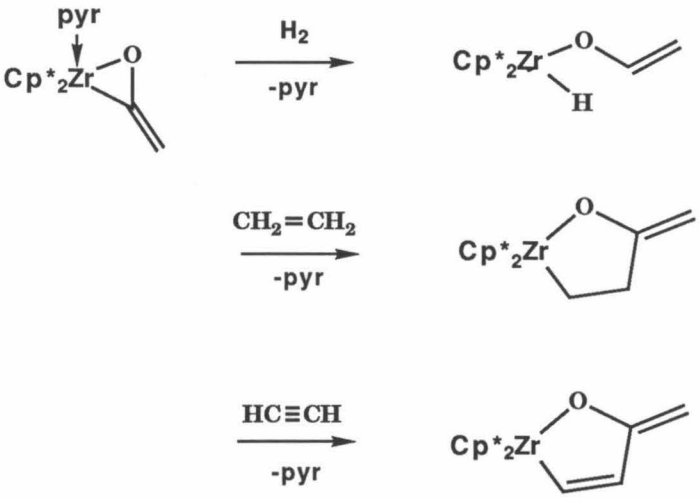


**Figure 2. $Cp^*_2$ Titanium ketene complex reactivity.**

The study of these zirconium ketene complexes was continued by S.C. Ho with the synthesis of bimetallic analogs as shown in equation 3.[4]

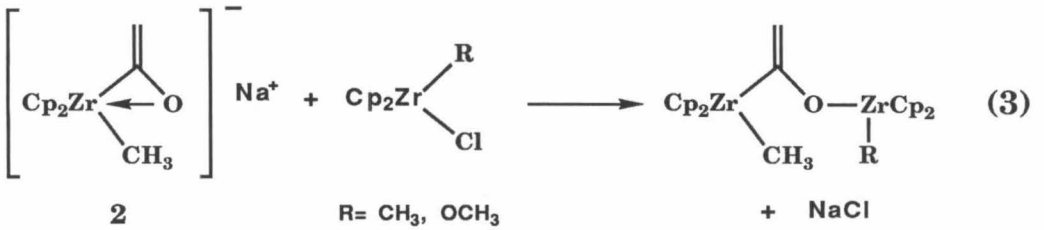


In addition, it was found that complex **2** reacts with zirconocene hydrido chloride via two separate pathways (Figure 3).[4]

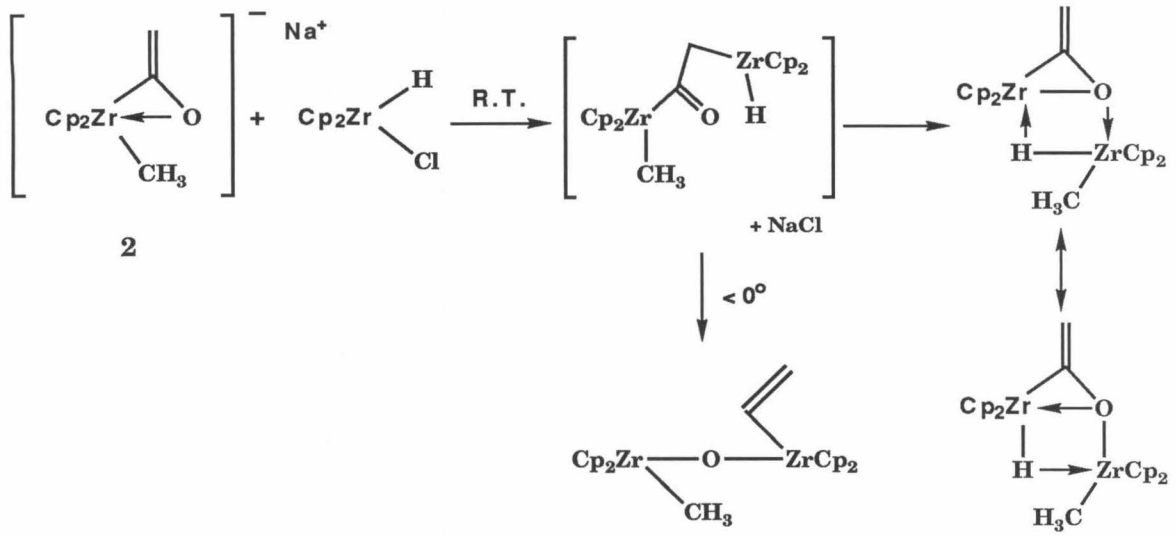


**Figure 3. Zirconium ketene complex reaction with zirconocene hydrido chloride.**

A series of experiments were performed which elucidated the following mechanistic scheme for both reaction pathways (Scheme 1).[4]

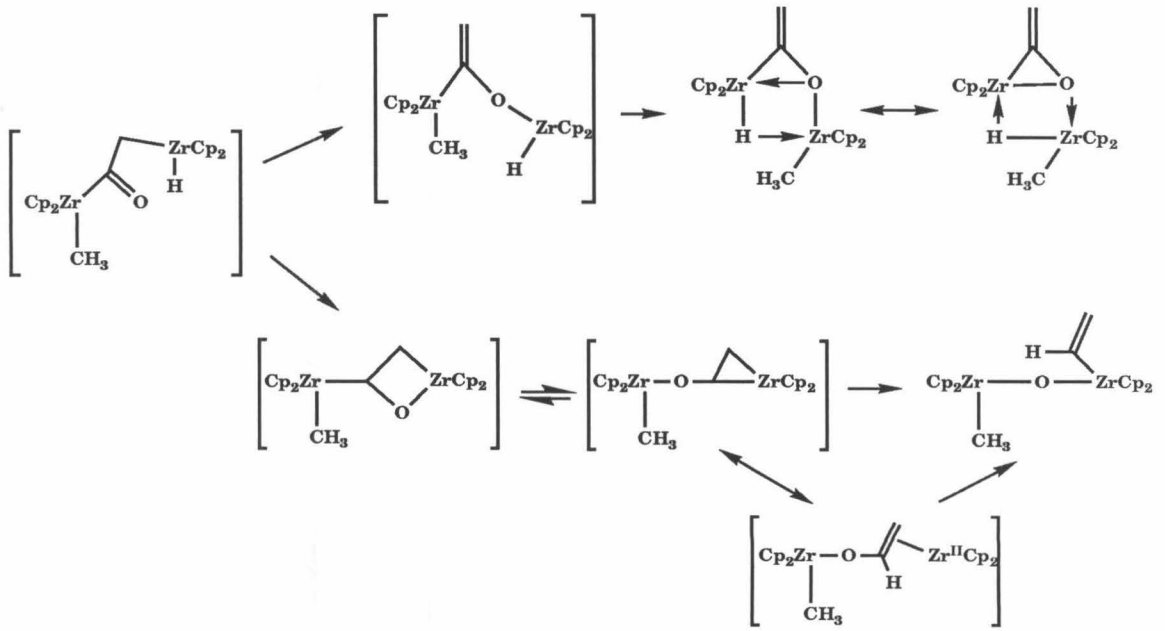

**Scheme 1. Mechanistic scheme for the reaction of zirconium ketene complex (2) with zirconocene hydrido chloride.**

Another aspect of zirconium chemistry within the Grubbs group involves the effect of Lewis acids, such as alkyl aluminums, on the reactivity of transition-metal ketene and ketone complexes. Such Lewis acid cocatalysts are used in a number of industrially important catalytic processes such as Ziegler-Natta polymerization[5] and olefin metathesis.[6] R. M. Waymouth synthesized and characterized trialkylaluminum adducts of zirconium ketene complexes (eq 4).[7]

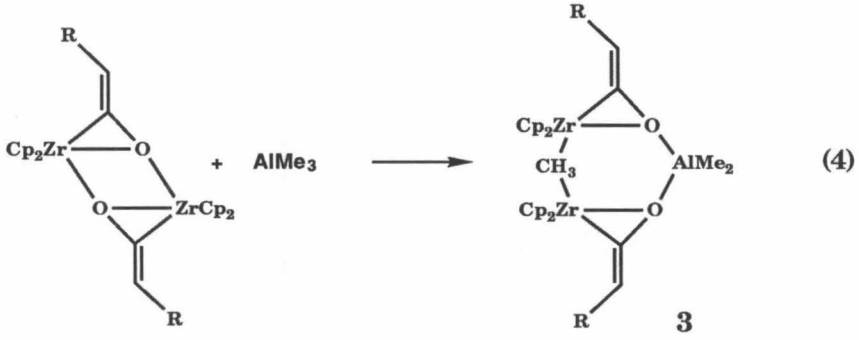


(4)

Complex **3** is interesting in that the methyl group between the two zirconium atoms is close to being planar, thus exhibiting $sp^2$ hybridization.[8] Coordination of the alkylaluminum ligand prevents dimerization and enhances reactivity as shown in Figure 4.[7]

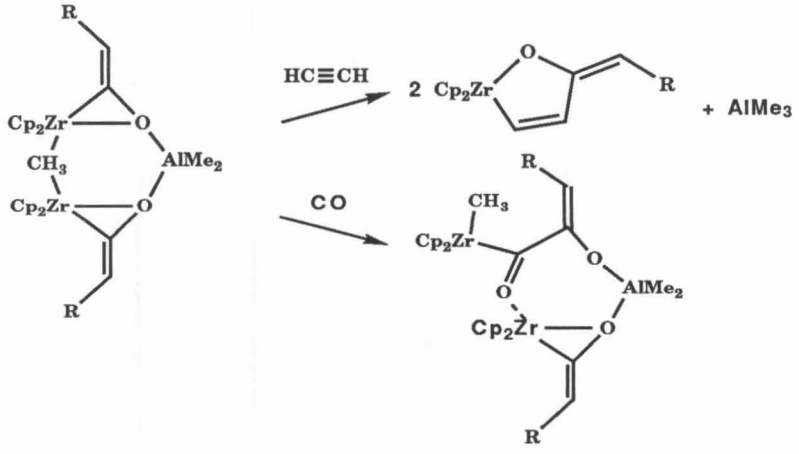


**Figure 4. Trinuclear zirconium ketene complex reactivity.**

Direct treatment of zirconium acyls with trialkyl aluminum reagents results in zirconium ketone complex formation (eq 5)[7].

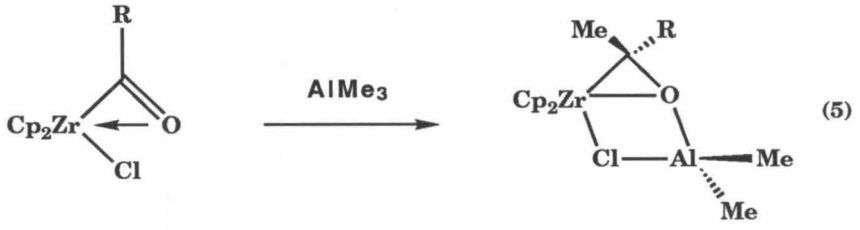


(5)

As with the ketene complexes, the alkyl aluminum ligand stabilizes the zirconium ketone complex and greatly enhances reactivity when compared to dimeric ketone complexes synthesized via independent routes (Figure 5).[9]

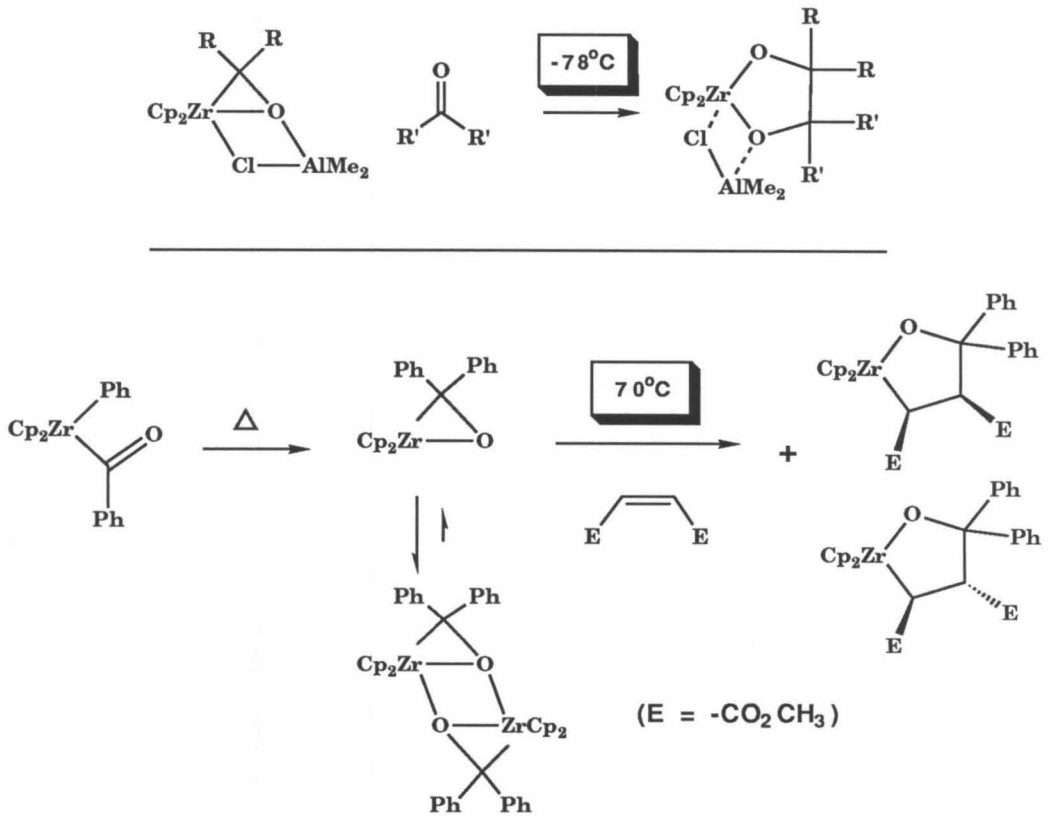


**Figure 5. Comparison of ketone complex reactivities with and without alkylaluminum liagands.**

It is this ability of zirconium ketone complexes, as well as the closely related zirconium aldehyde complexes, to insert unsaturated substrates to form new carbon-carbon bonds that represents the main scope of this chapter. The use of zirconium compounds as synthetic organic reagents has been the subject of much attention recently. Reactions such as hydrozirconation, carbometallation, and carbozirconation have been well-documented (Scheme 2).[10]

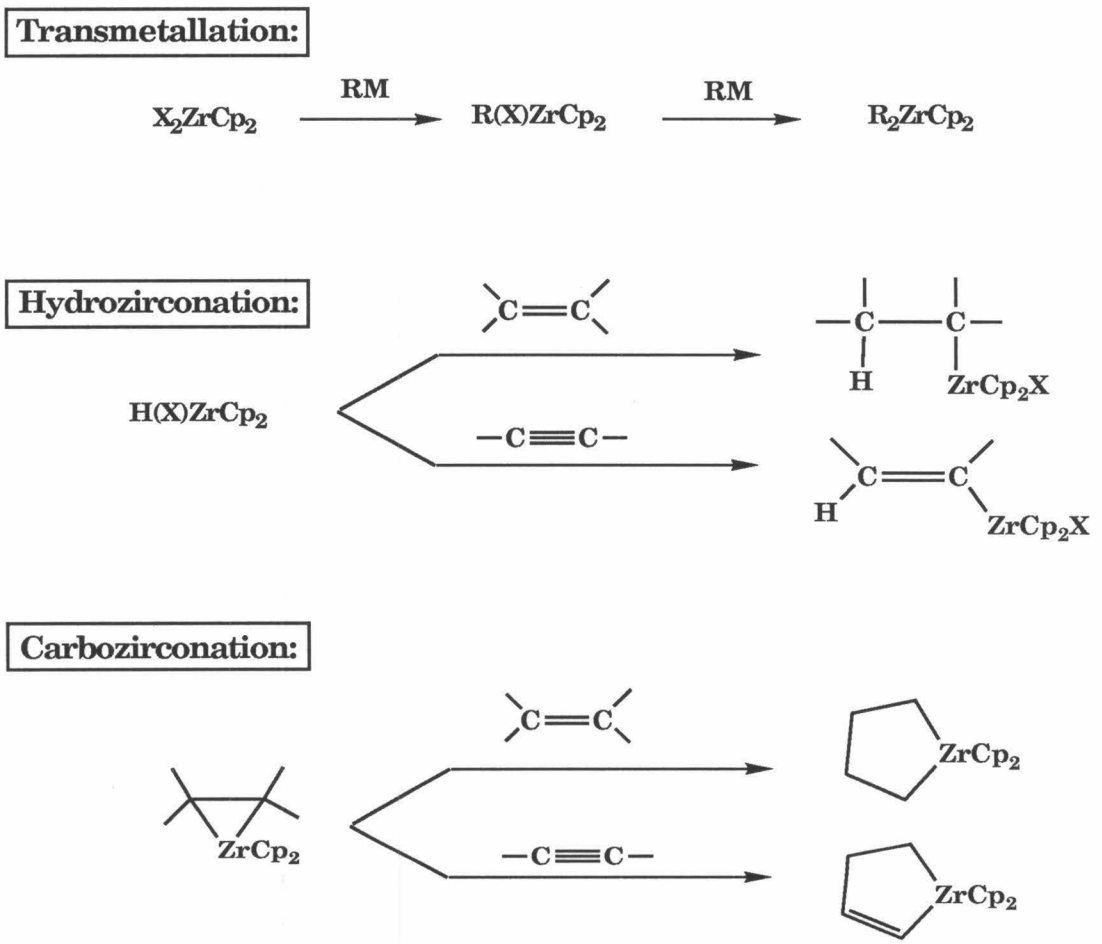


**Scheme 2. Examples of the use of zirconium in organic synthesis.**

Within this chapter, the applications and limitations of zirconium ketone and aldehyde complexes involving insertion reactions with various unsaturated substrates are discussed. In addition, examples are presented which illustrate the chemistry of such compounds with respect to their being models for catalytic CO reduction intermediates.

## Results and Discussion

**Preparation of Zirconium Aldehyde and Ketone Complexes.** In order to explore the potential usefulness of these zirconium reagents for organic synthesis, certain considerations were made. Both zirconium ketone and aldehyde complexes were derived from zirconocene chloro acyls **4**. These zirconium acyls are easily synthesized in high yield from an olefin via hydrozirconation followed by carbonylation (eq 6).[11]

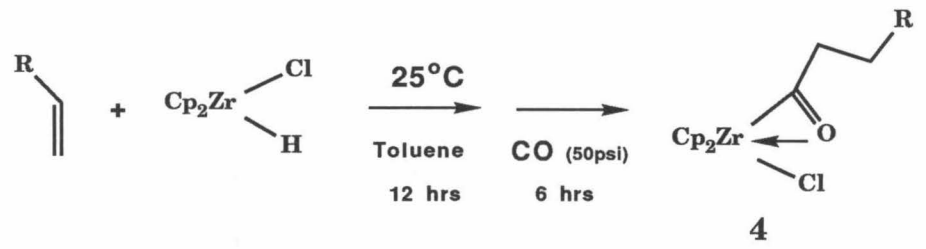


**4** (6)

Due to the commercial availability of the zirconocene hydrido chloride, the bis-cyclopentadienyl analogs were chosen for study as opposed to much more difficult to produce mixed Cp-Cp* and $Cp^*_2$ zirconium systems. Treatment of the zirconium acyl **4a** with one equivalent of trimethylaluminum at 0 °C in aromatic solvents affords the ketone complex **5** in isolated yields of 65-90% (eq 7).[7]

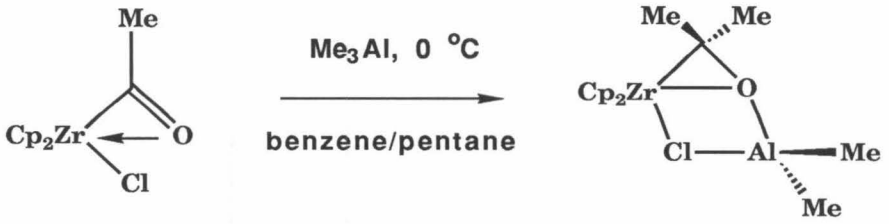


**4a** **5** (7)

In a similar manner, treatment of **4b** or **4c** with one equivalent of diisobutylaluminum hydride (DIBAL) affords the corresponding aldehyde complexes **6b** and **6c** in 80-95% yields (eq 8).

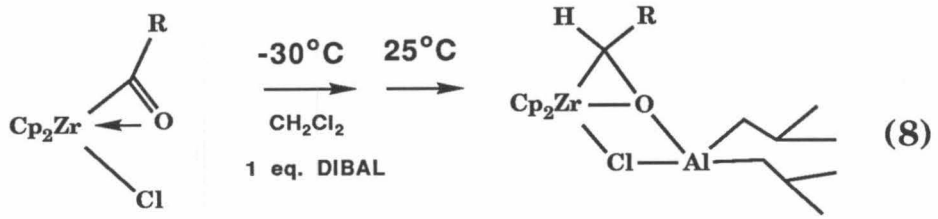


(8)

**4b** R = Ethyl
**c** R = Cyclohexyl

**6a,b** 80-90%

In contrast to the zirconium ketone complexes which can be isolated as pale yellow, temperature sensitive solids, the aldehyde complexes decompose during isolation procedures. As a result, they have been characterized *in situ* by $^{1}H$ and $^{13}C$ NMR, IR, and analysis of hydrolysis products (see experimental section).

The $^{1}H$ NMR spectrum for complex **6b** shows a characteristic resonance at 2.97 ppm due to the aldehydic proton. This $^{1}H$ chemical shift, the $^{13}C$ chemical shift of 87.3 ppm, the $J_{CH}$ coupling constant of 146 Hz, and the absence of a strong absorption around 1650 $cm^{-1}$ in the IR spectra support a metallaoxirane structure as opposed to a $\pi$-complex for this compound (Figure 6).[9,12]

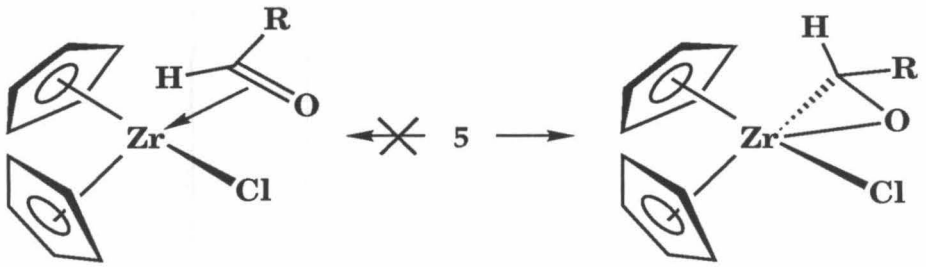


**Figure 6. Zirconocene aldehyde complex structure.**

Selective decoupling $^1H$ NMR experiments show four distinct methyl resonances of the aluminum isobutyl groups indicating that one non-equilibrating diisobutylaluminum chloride ligand is bound to the zirconium stereocenter. As in the case of the ketene and ketone complexes, the diisobutylaluminum chloride ligand apparently serves to stabilize the reactive zirconium aldehyde moiety.

The zirconium aldehyde complexes can be easily formed in toluene, methylene chloride, or chloroform. Due to the high solubility of the zirconium acyl in chlorinated solvents, the cleanest products are obtained from these solvents. This is probably a result of better mixing which reduces side reactions with DIBAL. These complexes give pale yellow solutions which have decomposition half-lives of two and seven days for the ethyl and cyclohexyl analogs respectively.

Although the dialkyl aluminum chloride ligand stabilizes the aldehyde moiety, it also provides a pathway for decomposition as determined by the production of isobutylene and the corresponding zirconium chloro alkoxide **7** (eq 9).

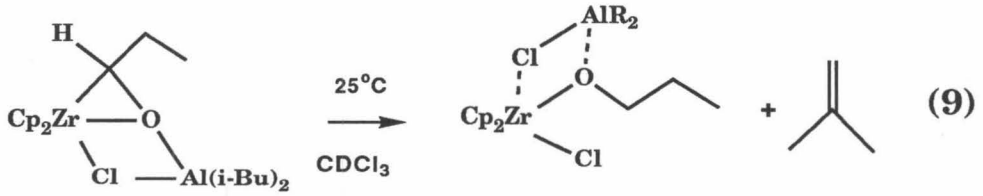


**6b** **7** **(9)**

Apparently, an isobutyl group on the aluminum ligand undergoes a β-hydride elimination reaction followed by a transfer of hydride to the zirconium atom which results in the cleavage of the zirconium-carbon

bond. This process is possibly accelerated by isolation procedures involving a vacuum which would drive the equilibrium of isobutylene production toward decomposition of the complex. In order to test this zirconium hydride hypothesis, the chloro alkoxide was synthesized by literature methods[13] and compared spectroscopically with the product of decomposition. The $^1$H NMR of the decomposition product gave a close match to that of the diisobutylaluminum chloride adduct of the zirconium alkoxide.[14] An exact match is impossible due to the complex nature of the interactions between the zirconium alkoxide and the aluminum by-products present in the decomposition mixture. Another possible pathway for decomposition involves β-hydride elimination of the aldehyde alkyl substituent to form a zirconium enolate. However, no olefin chemical shift is observed in the $^1$H NMR of the decomposition products.

A similar type of reaction is observed during the treatment of complex **6a** with hydrogen in which a zirconium alkoxide is formed. This is reminiscent of the $Cp^*_2$ zirconium ketene chemistry of Straus in which hydrogen cleaves the Zr-carbon bond to yield zirconium hydride enolates. The reaction of **6a** with hydrogen provides additional support for the carbon monoxide reduction mechanism proposed by Wolczanski and Bercaw (Scheme 3).[13,15]

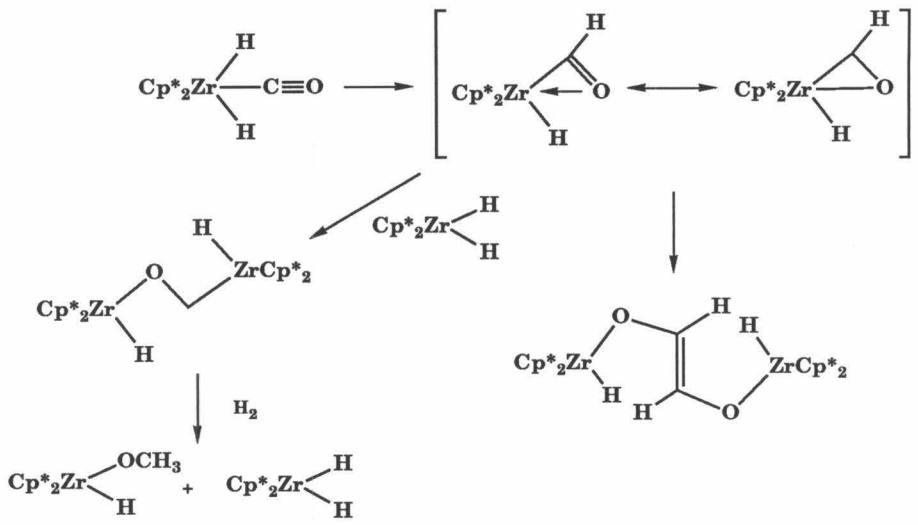

**Scheme 3. Reaction scheme of Cp*zirconocene with carbon monoxide.**

The decomposition chemistry of **6a** is not clean and it is unclear why this process occurs and whether both isobutyl groups undergo elimination. In contrast, the zirconium ketone complexes decompose via a different route which includes the formation of trinuclear complexes of the type isolated by Waymouth. This difference reflects the lack of a β-hydride elimination pathway for the aluminum methyl groups of the dimethylaluminum chloride ligand.

A number of different neutral and anionic hydride reagents including boron examples were tested in an attempt to form zirconium aldehyde complexes via alternative methods. These gave either oligomeric zirconium complexes that were not synthetically useful or no aldehyde product at all. Of the aluminum hydride reagents tried, only DIBAL gives high yields of the desired aldehyde products. It is possible that the comparable electronegativities of aluminum and zirconium play an

important role in providing the stabilization for the aldehyde moiety just as they promote transmetallation reactions between these two metals.[16]

When zirconium complex **4b** is treated with two equivalents of DIBAL, zirconium aldehyde complexes stabilized by dialkylaluminum hydrides are formed (eq 10).

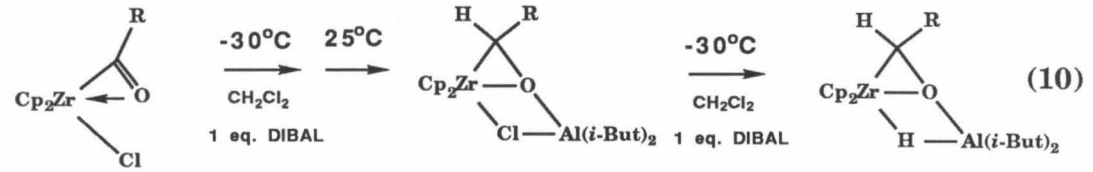


(10)

4b R = Ethyl
c R = Cyclohexyl

These complexes are colorless and react as a latent source of DIBAL.[17] This type of alkyl aluminum hydride displacement was also observed with the trimethylphosphine adduct of titanacene methylidene[18] in which a thermally unstable titanium hydride was formed.[19] Similar types of zirconium hydride complexes have been reported in the literature (Figure 7).[4,7,9,20]

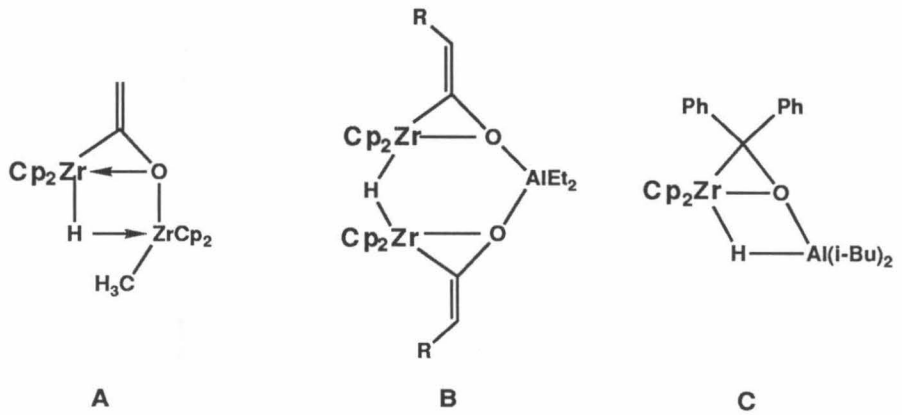


**Figure 7. Zirconocene hydride complexes.**

**Reactivity of Aldehyde Complexes.** The types of reactions that zirconium aldehyde and ketone complexes undergo are quite similar, with aldehyde complexes being more reactive. Due to the wider flexibility of products that can be formed with zirconium aldehyde complexes, in comparison to ketone complexes, the aldehyde complexes became the focus of study concerning synthetic applications. These complexes insert a number of unsaturated substrates as shown in Scheme 4.

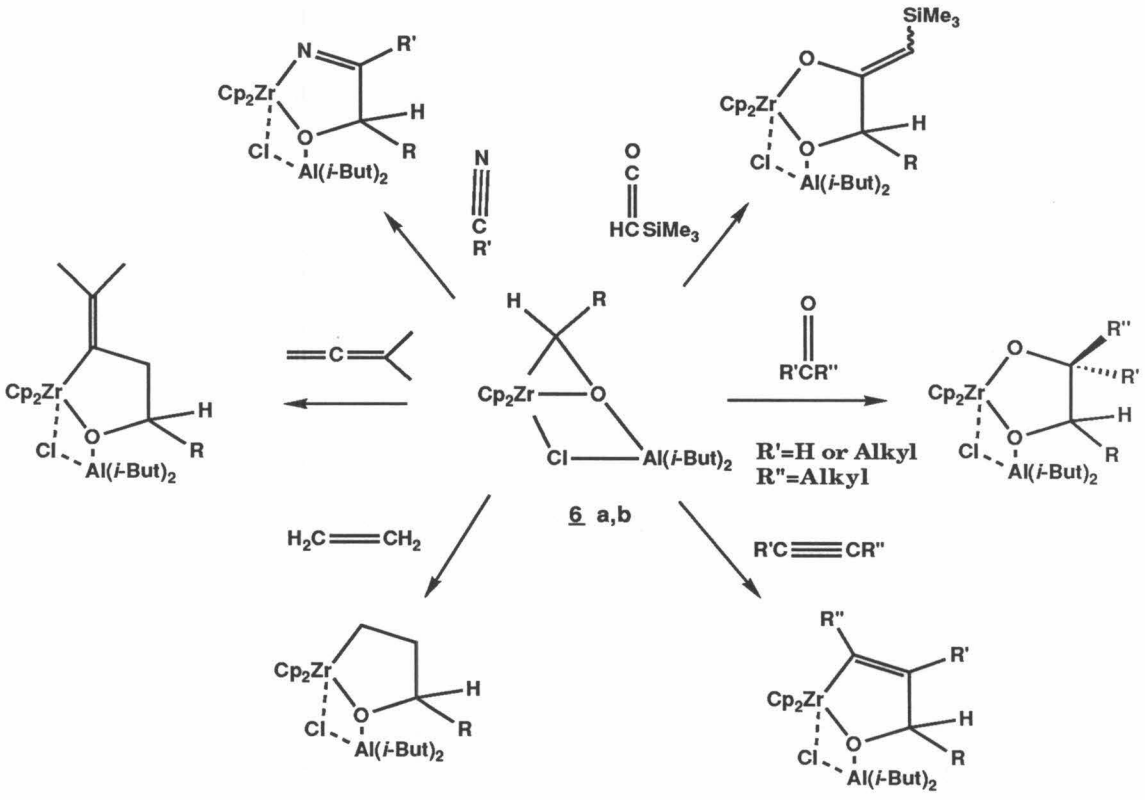


**Scheme 4. Reactivity of zirconium aldehyde complexes.**

In the case of carbonyl substrates, zirconium diolate complexes are formed which can be hydrolyzed to the corresponding 1,2-diol. Whereas most late transition-metal ketone complexes show synthetically useless "head to tail" coupling with carbonyls (Figure 8, path **A**),[21] the highly

oxophilic zirconium examples demonstrate the synthetically productive "head to head" coupling (Figure 8, path **B**).

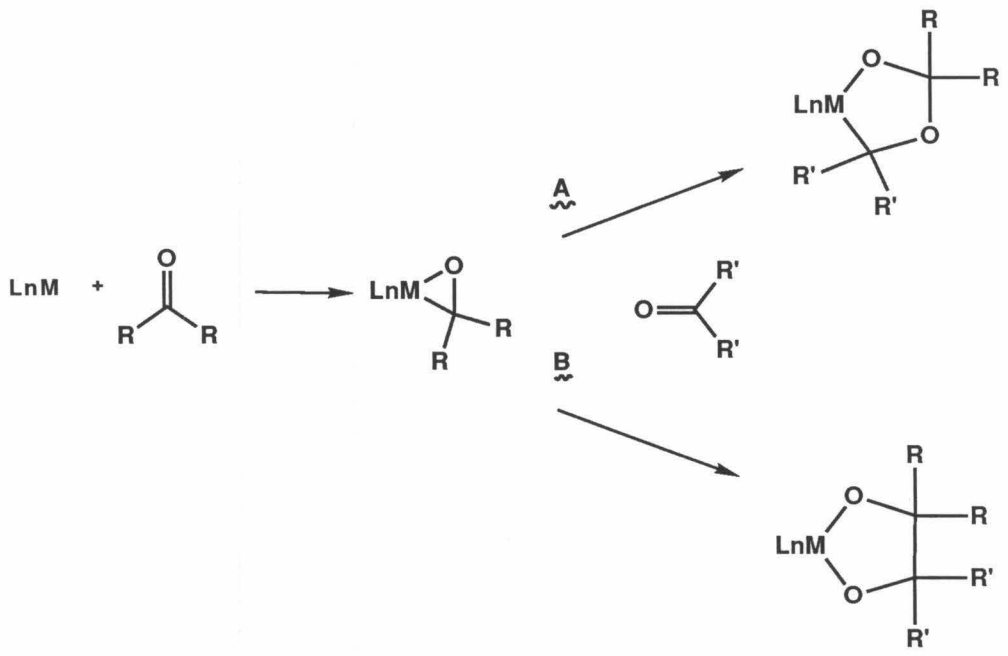


**Figure 8. Transition-metal ketone complex insertion of carbonyls.**

The carbonyl carbon of the zirconium ketone or aldehyde is believed to function as a nucleophile and add to carbonyls in such a manner. The possibility of an electron transfer process, however, has not been ruled out.

By examining the entire reaction scheme of aldehyde complexes with carbonyl compounds, the overall method resembles an unsymmetrical pinacol-type coupling of a metal-bound and a free carbonyl substrate. The 1,2-diol structural unit is an important feature that appears in numerous polyketide natural products of biological significance.[22] Convergent methods of synthesizing unsymmetrical 1,2-diols, such as metal-catalyzed reductive coupling of carbonyl compounds, give moderate to good yields of products with limited stereoselection (Figure 9).[23]

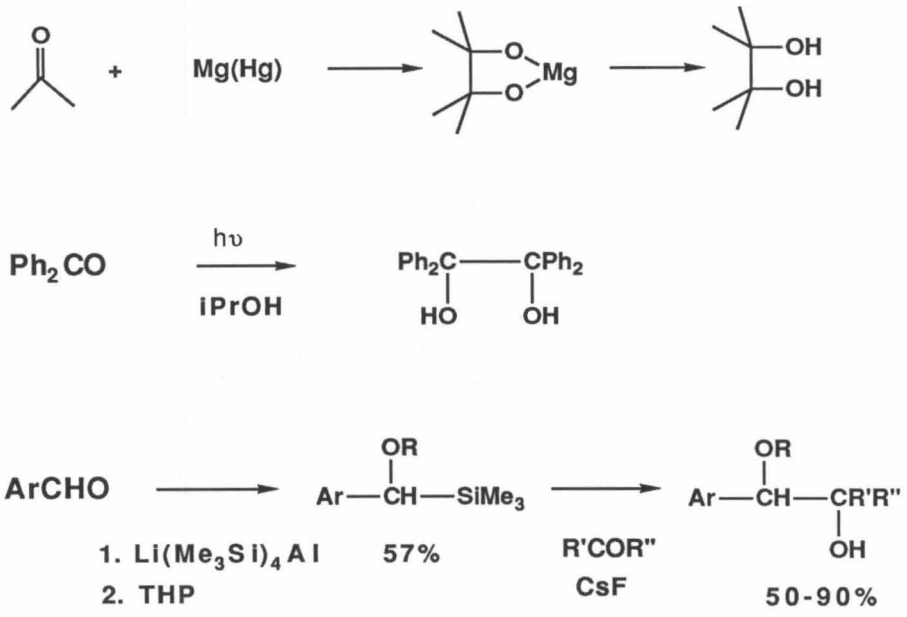


**Figure 9. Pinacol coupling reactions.**

The reaction of aldehydes with zirconium aldehyde complexes offers a method for convergent pinacol type couplings without the statistical problems encountered in many other procedures. Based on the high yields observed in preliminary studies, a series of carbonyl compounds were examined with two zirconium aldehyde substrates (Scheme 5).

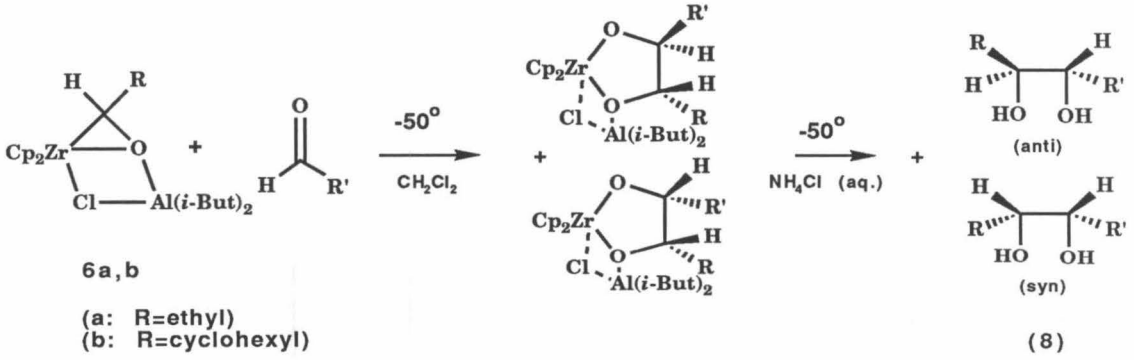


**Scheme 5. Zirconium aldehyde complex aldehyde substrate insertion scheme.**

The complexes chosen represent two steric extremes of alkyl substitution adjacent to the metal center as allowed by the hydrozirconation reaction due to the β-hydride elimination isomerizations of olefin.[24] This represents the first limitation of the method in that all olefins used, whether internal or terminal, will result in terminal zirconium carbonyls. Table 1 illustrates some of the substrates used and the resulting isolated yields of products.

The complexes chosen represent two steric extremes of alkyl substitution adjacent to the metal center as allowed by the hydrozirconation reaction due to the β-hydride elimination isomerizations of olefin.[24] This represents the first limitation of the method in that all olefins used, whether internal or terminal, will result in terminal zirconium carbonyls. Table 1 illustrates some of the substrates used and the resulting isolated yields of products.

| ALDEHYDE | Zirconium-Aldehyde Complex: R = Ethyl (6a) PRODUCT | syn:anti Ratio (Yield %) | R = Cyclohexyl (6b) PRODUCT | syn:anti Ratio (Yield %) |
|---|---|---|---|---|
| 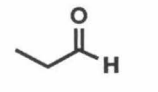 | 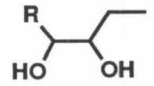 8a | 1:3 (64.6)[a] | 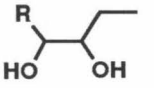 8b | 1:12 (78.9)[a] |
| 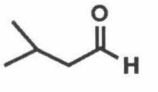 | 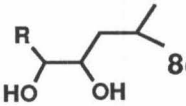 8c | 1:4 (70)[a,c] | 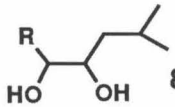 8d | 1:13 (78)[a,c] |
| 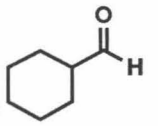 | 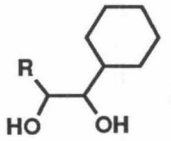 8e | 1:6 (70.4)[a] | 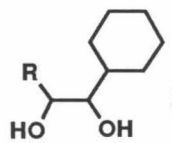 8f | 1:>20 (64.4)[a] |
| 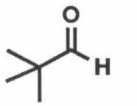 | 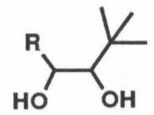 8g | 1:>20(52.2)[b] | N. R. | |
| 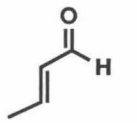 | 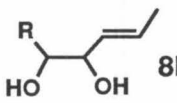 8h | 1:2 (64.4)[b] | 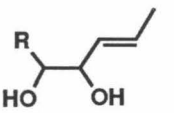 8i | 1:3.5 (45.9)[b] |
| 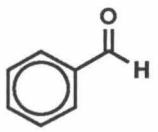 | 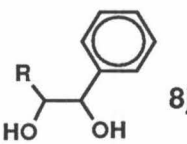 8j | 1:8 (61.7)[b] | 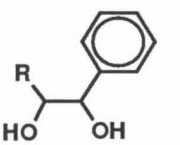 | (<30)[b] |

a) Reaction temp. -78° C in $CH_2Cl_2$, b) Reaction temp. -50° C in $CH_2Cl_2$., c) NMR yield.

**Table 1. Reaction of zirconium aldehyde complexes (6a) and (6b) with aldehydes.**

From the above data, it appears that for aldehydes with aliphatic substituents, steric bulk plays an important role in determining diastereoselectivity. As the size of the alkyl group increases, selectivity

favoring the anti-isomer is enhanced.[25] Interestingly, the size of the alkyl group attached to the zirconium aldehyde moiety affects selectivity to a greater extent than the substituent from the aldehyde. This may be a due to a kinetic effect in which the more reactive zirconium ethyl aldehyde complex gives lower selectivity. Another possible explanation involves the conformation of the cyclohexane ring which may be forced into an axial position by the cyclopentadienyl ligands resulting in a greater shielding of the zirconium metal center.

When steric interactions become large enough, pathways of decomposition dominate and yields diminish. In the case of the reaction between pivaldehyde and the zirconium cyclohexyl aldehyde complex **6b**, no insertion occurs.

The reaction of unsaturated aldehydes required higher temperatures which may reflect the additional energy needed to overcome resonance stabilization. The result was lower diastereoselectivities and, due to increased side reactions, lower yields. No cis-trans isomerization is observed with conjugated olefin examples. During the reaction of some highly conjugated carbonyl and olefin substrates, such as benzaldehyde and styrene, an intense yellow color formed instantly after addition at low temperature. However, no change was observed in the $^1$H NMR that corresponded to insertion. The color gradually disappeared as the insertion proceeds indicating a possible precoordination of the substrate to the zirconium metal center before the reaction occured.

As shown in Scheme 3, complex **6a** inserts ketones to give similar diol products. Dr. M. Mori performed a study on a series of unsymmetrical

ketones in an attempt to control diastereoselectivity. Table 2 shows some ketone substrates that were examined.

| KETONE | Zirconium-Aldehyde Complex<br>R = Ethyl (6a)<br>PRODUCT | Yield %, syn:anti ratio |
|---|---|---|
| 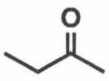 | 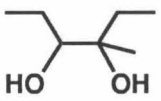 9a | 51.5% , 1:1 [a] |
| 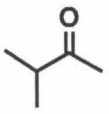 | 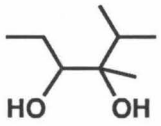 9b | 41.8% , 1:1 [b] |
| 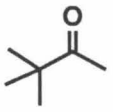 | | N. R. ( 25°) |
| 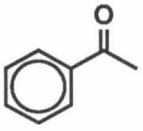 | 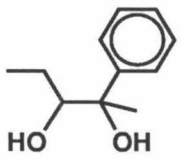 9c | 77.0% , 3:4 [a] |
| 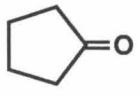 | 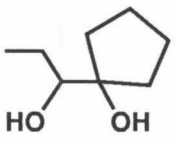 9d | 53.4% [a] |
| 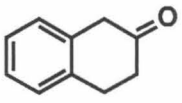 | 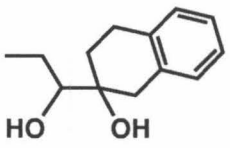 9e | 63.6% , 1:1 [a] |

a) Reaction temp. -50° C in $CH_2Cl_2$
b) Reaction temp. -10° C in $CH_2Cl_2$

**Table 2. Reaction of zirconium aldehyde complex (6a) with various ketones.**

Although the insertion of unsymmetrical ketones with complex **6a** give yields comparable to aldehyde substrates, little or no

diastereoselectivity is observed.[26] Apparently the aldehyde complex is not very sensitive to fine differences in steric bulk. Zirconium aldehyde complex **6b** and zirconium-ketone complexes do not react with unactivated ketones.

In addition to hydrolysis of the zirconium diolate intermediates, other methods were examined to find alternative reactivity. Treatment of the diolate with acetic anhydride and pyridine affords the corresponding mono-protected pinacol in moderate yields (50-60%) (eq 11).[26]

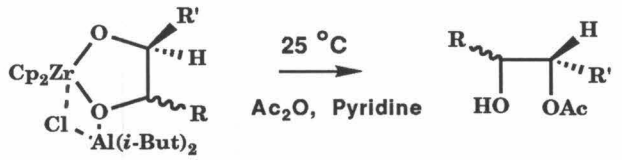


(11)

In order to make this method more useful, the entire reaction scheme was carried out in a one-pot fashion beginning with an olefin. For example, 1-hexene and benzylacetone give the corresponding diol in 78.6% overall yield based on starting olefin (Figure 10).[26]

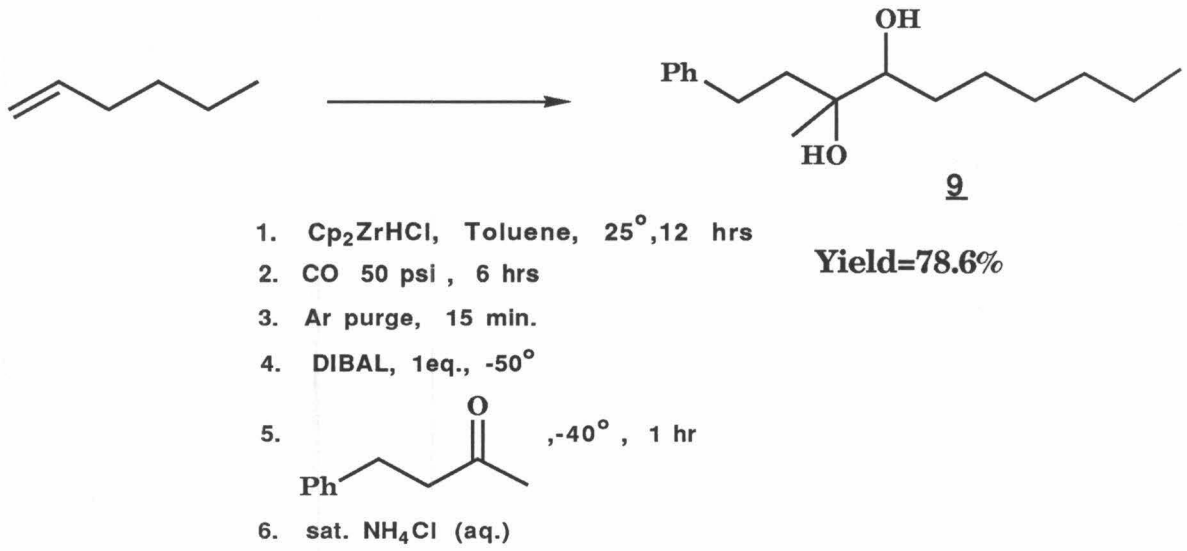


**Figure 10. One-pot reaction of zirconium aldehyde complexes with carbonyls.**

During the development of the one-pot procedure, an interesting side reaction of zirconium aldehyde complexes was discovered. If the reaction mixture is not purged of carbon monoxide after the carbonylation step, the addition of DIBAL results in the formation of unusual organic side products. The reaction was monitored by variable temperature $^1$H NMR and clearly shows a number of zirconocene products are formed and consumed during the course of the insertion. Isolation and characterization of the major hydrolysis products indicate that CO is inserted into the complex, after which several side reactions occur one of which includes Cp ligand migration into the diol product (Scheme 6).

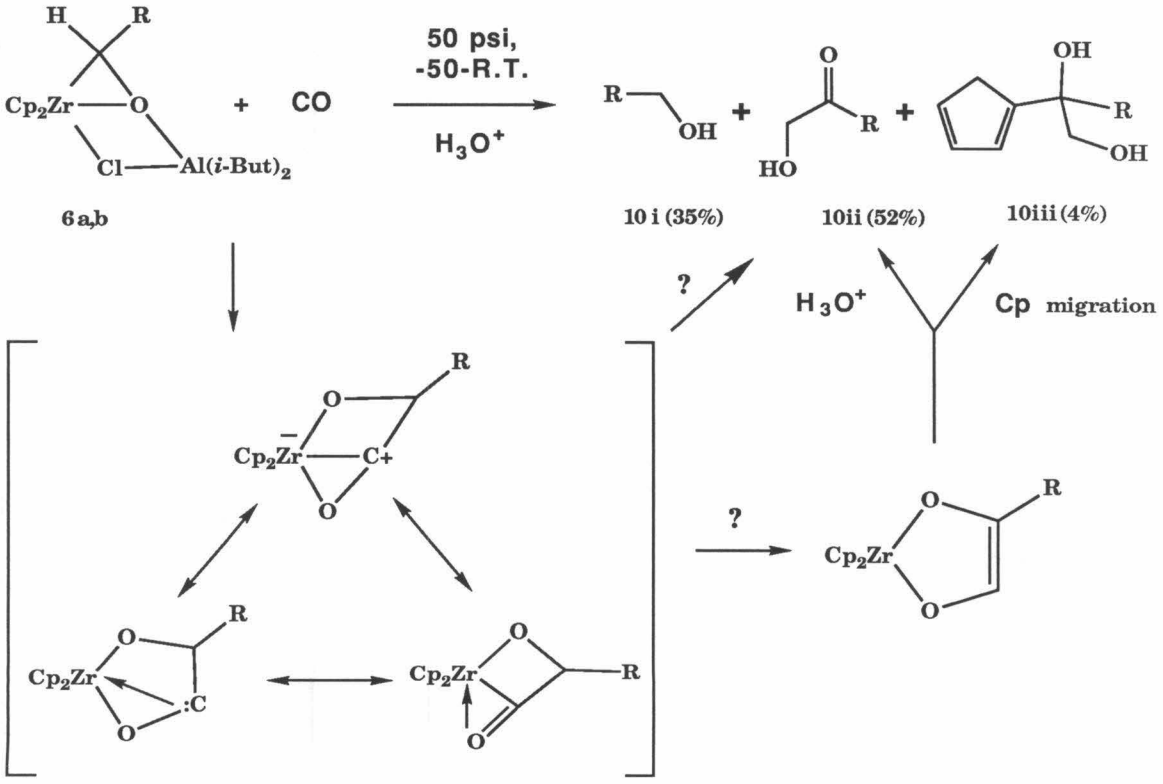


**Scheme 6. Possible intermediates for the insertion of CO into zirconium aldehyde complexes.**

This Cp displacement by carbon monoxide is not unusual and the postulated oxy-carbene nature of the CO insertion intermediate may provide an explanation for the unusual reactivity of these systems.[27] Also, studies of the interaction between CO and zirconocene dichloride-aluminum hydride adducts have demonstrated the ability of such systems to form insertion and reduction products.[28] Although Scheme 6 suggests the possible involvement of an ene-diolate intermediate similar to the type seen by Bercaw and co-workers in zirconium Cp* systems,[27] spectroscopic data fails to show any such complex in this system. In other studies,$^{14}$C labelled CO has been used for determining the number of active sites in similar types of transition-metal catalyzed polymerizations. These results are significant because they clearly demonstrate that two molecules of CO can be incorporated into one metal site thus invalidating the calculations for the number of active sites based on the uptake of one CO molecule.[29]

Although both polar and nonpolar solvents can be used for these reactions, no changes in diastereoselectivities are observed as a result of solvent effects. However, due to the instability of zirconium-hydrido chloride in chlorinated solvents, toluene is recommended for one-pot procedures. In addition, lower yields and longer reaction times are observed for coordinating solvents such as tetrahydrofuran.[26]

In an attempt to broaden the scope of the reaction, unsaturated zirconium acyls were treated with DIBAL to give the corresponding aldehyde complexes (eq 12).

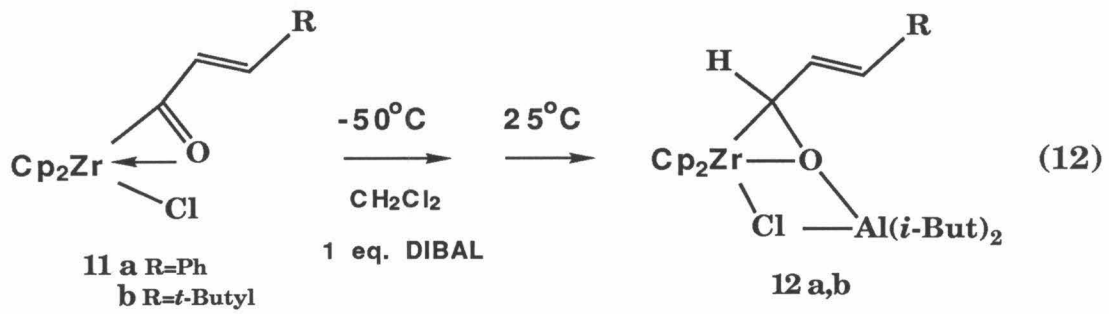


11 a R=Ph
b R=*t*-Butyl

12 a,b

(12)

The unsaturated zirconium aldehyde complexes proved to be more unstable than the saturated analogs and did not show useful reactivity with unsaturated substrates.[30] In addition, side reactions prevented the formation of pure complexes. The impure unsaturated complexes were characterized by $^{1}H$ and $^{13}C$ NMR and show similar spectroscopic properties in comparison to saturated aldehyde complexes (see experimental section).

As mentioned before, the zirconium aldehyde complexes are chiral and are formed as the racemate. As a result, attempts were made to react **6a** and **6b** with chiral aldehydes to explore possible enantioselective properties. Reaction of complex **6a** or **6b** with R-(-)-myrtenal yields two diastereomers, **13a** and **13b**, in a 1:1 mixture. Based on the Cp resonances, this mixture represents formation of the anti-diastereomer with differentiation resulting from the chiral ring structure. When one-half equivalent of R-(-)-myrtenal is added at low temperature, no diastereoselectivity was observed indicating a lack of kinetic resolution (eq 13).

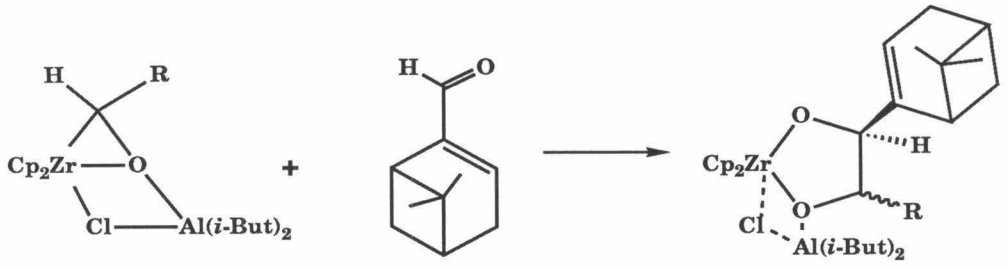


(13)

**6a,b (racemic)** **R-(-)-myrtenal** **13a,b**

**1:1 diastereomeric mixture**

Attempts were made to react the zirconium aldehyde complexes with the chiral aldehyde **14**, D-glyceraldehyde acetonide, however, the insertion was not very clean. This problem probably results from a combination of steric factors, the high activity of the aldehyde by sigma effects from adjacent oxygen atoms, and interference due to chelation by the acetal oxygens to the aluminum atom of the aldehyde complex.

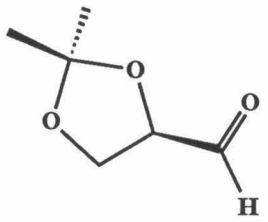


**14**

The zirconium aldehyde and ketone complexes also insert nitriles to yield intermediates such as **15** which after hydrolysis afford α–hydroxy ketones (eq 14).

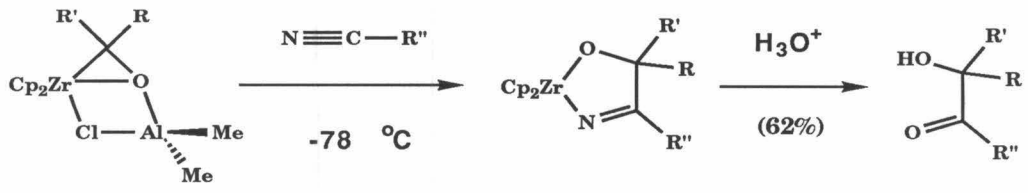


(14)

**5** **15** **16**

The insertion of acetylenes with either **6a** or **6b** yield zirconium oxymetallacyclopentenes which can be converted to allylic alcohols (eq 15).

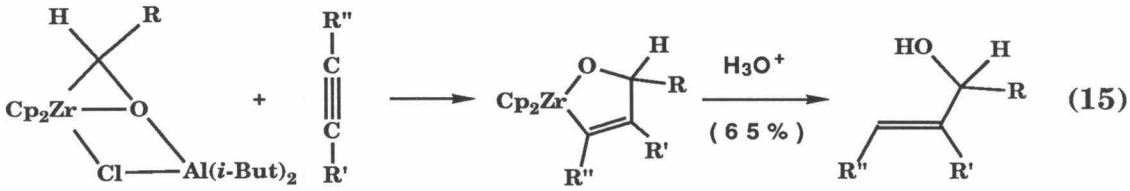


6a,b 17 18 (15)

When unsymmetrical acetylenes are used, the alkyl substituent is preferentially placed adjacent to the zirconium probably as a result of electronic effects.[31] This type of behavior was observed with the ketene complexes as well. Reaction of complex **6a** with dimethyl maleate and dimethyl fumarate does not give a clean reaction as compared with the Erker ketone complex (Figure 11).

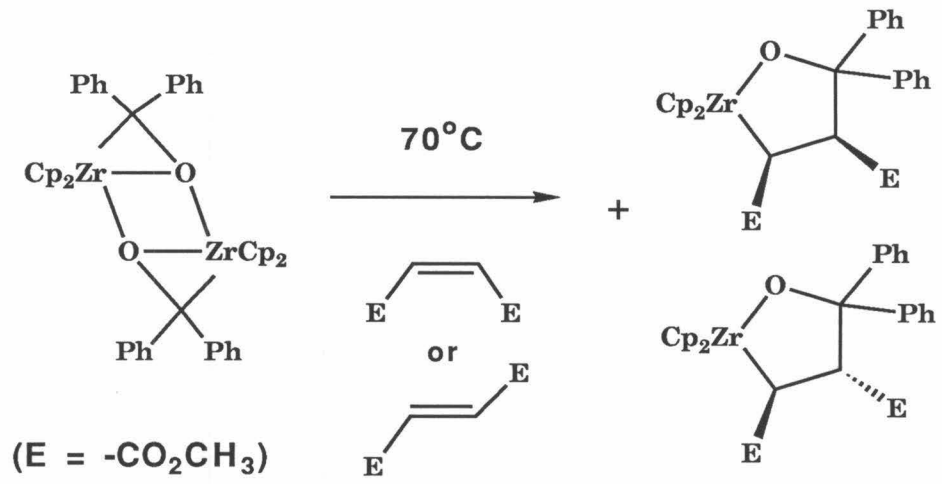


**Figure 11. Reactivity of Erker zirconium ketone complex.**

Both zirconium aldehyde complexes insert ethylene with **6a** giving an 80% yield of oxymetallacyclopentane **19a** in two hours and **6b** giving a 42% yield of **19b** after three days (eq 16).

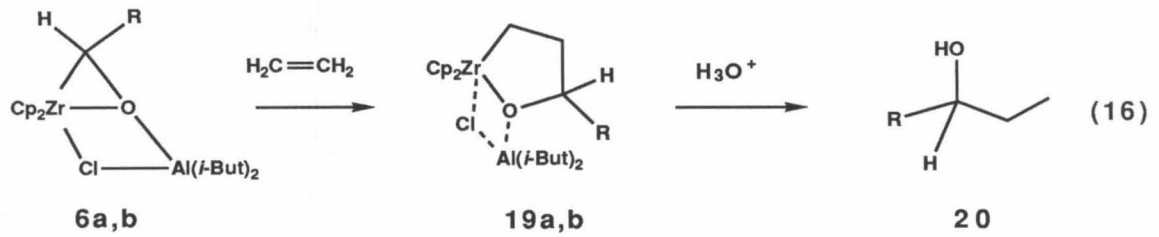


6a,b 19a,b 20 (16)

The zirconium aldehyde complexes do not insert unactivated olefins; however, a coordination complex without insertion was observed with styrene. In the case of allenes, 3,3-dimethylallene reacts in about three hours to give oxymetallacycle **21** which, after hydrolysis, affords the corresponding homoallylic alcohol (eq 17).

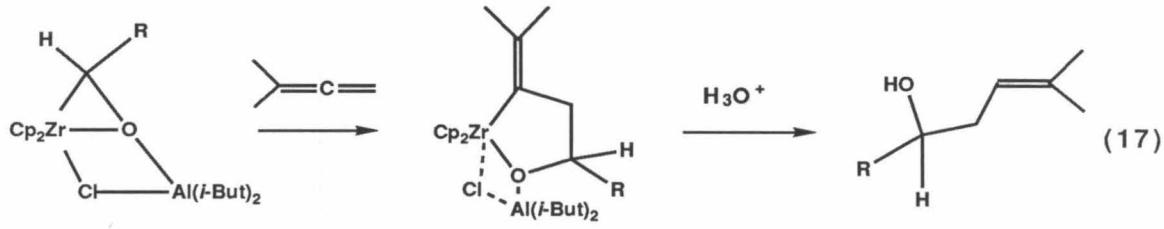


21 22 (17)

Beside aldehydes and ketones, zirconium aldehyde complexes insert ketenes, lactones, and acid chlorides as shown in (Figure 12).

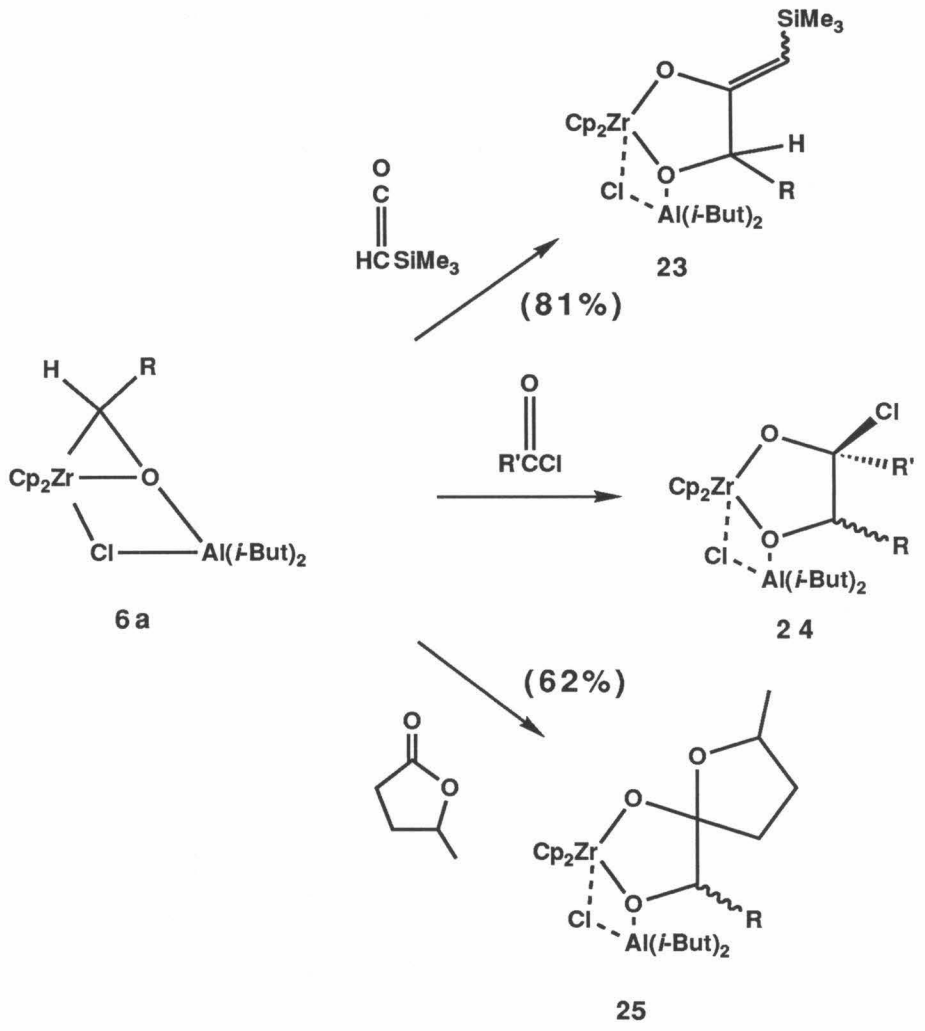


**Figure 12. Reaction of 6a with TMS ketene, acyl chlorides, and γ-lactones.**

When the reaction with acid chlorides was carried out in the presence of a trialkylamine, a 40% yield of a Cp migration product was obtained (eq 18).[26]

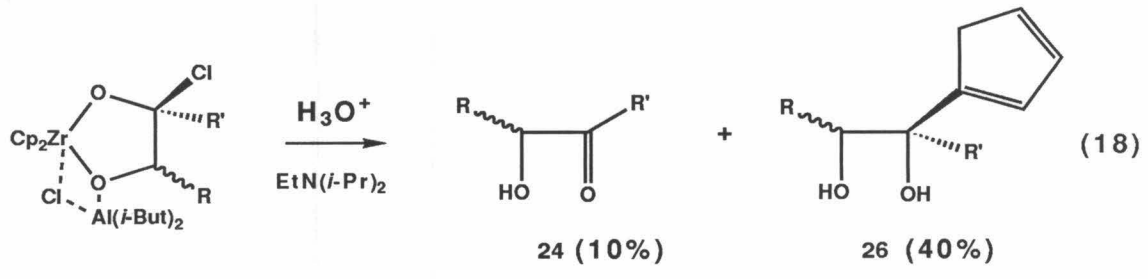

Apparently, the chloro substituted intermediate is susceptible to nucleophilic displacement by the cyclopentadienyl ligand. The zirconium aldehyde complexes do not insert unactivated esters which represents the activation requirement for these systems. Other oxygen containing substrates that show no reactivity are epoxides, ethers, and enol silanes.

**Summary.** Both zirconium aldehyde and ketone complexes stabilized by dialkylaluminum chloride ligands insert a number of unsaturated substrates. The more reactive aldehyde complexes can be formed *in situ* in excellent yields and show high diastereoselectivities during the insertion of aldehyde substrates. The insertion of ketones gives comparable yields with, however, little diastereoselectivity. A one-pot method was developed for the synthesis of unsymmetrical 1,2-diols which involves the coupling of an aldehyde or ketone substrate with a metal-bound aldehyde derived from an olefin and carbon monoxide. During the development of this method, the insertion of carbon monoxide was observed which constitutes the incorporation of two CO molecules per metal center. This result demonstrates a potential weakness in active site determination methods of similar metal systems using $^{14}$C labeled CO uptake. In addition, other carbonyl substrates such as ketenes, acid chlorides, and lactones gave insertion products with less sterically crowded zirconium aldehyde complexes. The zirconium aldehyde complexes also insert alkynes, ethylene, allenes, and nitriles to yield, after hydrolysis, allylic alcohols, saturated alcohols, homoallylic alcohols, and acyloins respectively. This pattern of reactivity is consistent with earlier results involving the closely related zirconium ketene complexes. The overall chemistry is limited, however, by the constraints of the initial hydrozirconation reaction, the

inability to control the chirality at the zirconium center, and the secondary reactivity of the aluminum ligands towards some functional groups. This concept of metal functional group activation by alkylaluminum reagents may one day play an important role in other related systems.

## Experimental Section

**General Considerations.** All air-sensitive manipulations were carried out under argon using standard Schlenk techniques or in a nitrogen-filled glove box (Vacuum Atmospheres DC-882) equipped with MO-40-1 purification train, DK-3E Dri-Kool conditioner, and Dri-Cold freezer. Flash chromatography was performed by the procedure of Still *et al.*,[32] using silica Woelm 32-63 (32-63 mm). Thin layer chromatography was performed on EM Reagents 0.25 mm silica gel 6-f plates and visualized with iodine vapor or *p*-anisaldehyde dip. Argon was purified by passage through columns of BASF RS-11 (Chemlog) catalyst and Linde 4Å molecular sieves. Benzene, diethyl ether, hexane, pentane (HPLC grade), THF, toluene, and NMR solvents were stirred over $CaH_2$ and transferred onto sodium benzophenone ketyl. All solvents were vacuum transferred and stored under argon in flasks equipped with teflon screw valves. Both perprotio- and deuterochloroform and methylene chloride were dried over $P_2O_5$, vacuum transferred, and degassed by successive freeze-thaw pump cycles. Trimethylaluminum was used as 2M solutions in toluene (Aldrich). Diisobutylaluminum hydride was obtained neat from Texas Alkyls and used without further purification. Mesitylene was dried over $CaH_2$, vacuum transferred, and stored in the drybox. Diethylaluminum hydride was obtained from Texas Alkyls as a 6% solution in heptane. Heptane was removed *in vacuo* to afford neat $Et_2AlH$ which was used without further purification. Carbon Monoxide (Matheson) and ethylene (Matheson) were used as received. NMR spectra were recorded on Varian EM-390 (90 MHz, $^1H$), Jeol FX-90Q (89.60 MHz, $^1H$), and Jeol 400GX (399.65 MHz, $^1H$; 100.4

MHz, $^{13}C$) spectrometers. Chemical shifts are reported versus residual protio-solvent signals ($^{1}H$: $C_6D_6$, δ 7.15; $CDCl_3$, δ 7.24; $C_7D_8$, δ 2.09; $^{13}C$: $C_6D_6$, δ 128.0; $CDCl_3$, δ 77.0; $C_7D_8$, δ 20.9;). Data are reported as follows: chemical shift, multiplicity (s=singlet, d=doublet, t=triplet, q=quartet, m=multiplet, br=broad), coupling constant (Hz), integration, and assignment. Elemental analyses were performed at the California Institute of Technology Analytical Facility. High resolution mass spectra were performed at the University of California, Riverside Mass Spectrometry Facility. Low resolution mass spectra were performed on Hewlett Packard Series 5970 mass selective detector in conjunction with a Series 5890 GC equipped with a 15 m SE-30 capillary column. Gas Chromatography was performed on a Shimadzu GC-mini 2 equipped with a Quadrex 50 m SE-30 capillary column. Infrared spectra were recorded as nujol mulls or in solution in $CDCl_3$ on a Perkin-Elmer 1600 instrument. The following reagents were used as received; zirconocene dichloride (Boulder Scientific), lithium tri-*tert*-butoxyaluminohydride (Aldrich), 3,3-dimethylallene (Aldrich), and phenylacetylene (Fluka). Benzonitrile was dried with $Na_2SO_4$, and distilled. All aldehydes were washed with aqueous bicarbonate and dilute mineral acid, dried with $MgSO_4$, distilled, degassed, and stored under nitrogen or purified by prep GC prior to use. Zirconocene-hydrido chloride, zirconocene-acyls, and trimethylsilylketene were prepared by literature methods.[11,31] D-glyceraldehyde acetonide **14** was a gift from Mike Lewis.

**[$Cp_2ZrCOMe.AlMe_2Cl$ (5)].** A 100 mL oven-dried Schlenk flask was charged with 0.518 g of zirconocene methyl acyl and 10 mL of a 1:1 benzene/pentane mixture under inert atmosphere. After cooling to 0 °C, the

mixture was treated with 1.1 mL of a 2M $Me_3Al$ solution in toluene to give a yellow solution. After solvent removal *in vacuo*, the pale yellow residue was washed with 2x5 mL of pentane to give a pale yellow powder (0.49g, 76%). $^1H$ NMR($C_6D_6$) δ 5.57 (s, 10H), 1.49 (s, 6H), -0.28 (s, 6H).

**[$Cp_2ZrCOR.Al(i\text{-}But)_2Cl$ {6a,b}].** An NMR tube was charged with 18 mg (0.49 mmol) of the zirconium-cyclohexyl acyl and dissolved in $CDCl_3$ in a $N_2$ filled glove box. The tube was cooled to -30 °C and 28 ml (0.50 mmol) of a 1.77 M DIBAL solution were added via syringe. After warming to room temperature, mesitylene standard was added. (**5b**) $^1H$ NMR (400MHz, $CDCl_3$) δ 5.96 (s, 5H, Cp), 5.93 (s, 5H, Cp), 2.97 (d, *J*=10Hz, 1H, aldehydic proton), 1.8 and 1.3 (m and m, 10H), 0.99 (m, 3H), 0.96 (dd, *J*=7Hz, *J*=2Hz, 6H), 0.93 (d, 6Hz, 6H), -0.04 (d, 7Hz, 2H), -0.10 (dd, *J*=7Hz, *J*=2Hz, 2H). Integration vs. mesitylene standard indicates 95% purity. $^{13}C$ NMR( 100.4 MHz, $CDCl_3$) δ 108.6, 108.5, 87.3, 45.6, 37.0, 29.5, 27.8, 27.6, 26.5, 26.0, 25.7, 25.4, 25.3. INEPT experiment gives a 146 Hz $J_{C\text{-}H}$ coupling constant for the aldehyde carbon. Selective decoupling of *iso*-butyl *ipso*-protons by irradiation at δ 2.08 results in 4 separate *iso*-butyl methyl shifts indicating a non-equilibrating diisobutylaluminum chloride ligand. IR(solution): 2955(m), 929, 903(vs), 800(s), 762,700(vs), 643(s) $cm^{-1}$. For the zirconium ethyl aldehyde complex (**5a**) $^1H$ NMR (400MHz, $CDCl_3$) δ 5.96 (s, 5H, Cp), 5.93 (s, 5H, Cp), 3.28 (dd, *J*=5Hz and 8Hz, 1H), 1.82 (m, 4H), 1.06 (t, *J*=7Hz, 3H), 0.95 (dd, *J*=5Hz and 6Hz, 12H), 0.03 (d, *J*=7Hz, 2H), 0.02 (dd, *J*=2Hz and 7Hz, 2H).

**General Procedure for the Reaction of (6a,b) with Aldehydes and Ketones.** A 100 mL oven-dried Schlenk flask was charged with 0.122 g (0.39 mmol) of zirconocene-ethyl acyl under inert atmosphere. The acyl was dissolved in 10 mL of methylene chloride and cooled to -30 °C. Into a

separate 50 mL Schlenk flask, 0.051 g (0.36 mmol) of DIBAL were dissolved in 5 mL of methylene chloride and cooled to -30 °C. The DIBAL solution was then cannulated into the acyl solution and stirred for 5 minutes before warming to room temperature slowly. The solution was then cooled to -78 °C and 22 μL (0.31 mmol) of propionaldehyde were added via syringe. The pale yellow solution was stirred for one hour before warming to 0 °C and adding 1 mL of saturated ammonium chloride solution (aq.). After 2 hours at room temperature, TLC indicated diol was present. The mixture was dried with $Na_2SO_4$ and eluted through a 5 cm silica gel plug with 150 mL of 1:1 ethyl acetate/ hexane. After concentration *in vacuo*, the crude product was flash chromatographed with a 20:80 ethyl acetate/ hexane solvent. All fractions containing product were combined to give 23.6 mg (65.6%) of 1,2 diol **8a**. $^1$H NMR(400MHz) ($CDCl_3$) (*anti*) δ , 3.31 (m, 2H), 2.64 (brs, 2H), 1.53 (m, 2H), 1.44 (m, 2H), 0.94 (t, *J*=7Hz, 3H). (*syn*) 3.48 (m, 2H), 2.64 (brs, 2H), 1.53 (m, 2H), 1.44 (m, 2H), 0.95 (t, *J*=8Hz, 3H). Comparison with authentic syn sample, carbinyl proton δ 3.47, indicates anti isomer is the major product.

**8b** (colorless crystals) m.p. 69.0-70.0 °C. $^1$H NMR (400MHz, $CDCl_3$) (*anti*) δ 3.35 (m, 2H), 3.12 (m, 2H), 2.16 (brs, 2H), 1.8-1.1 (m, 13H), 0.94 (t, *J*=7Hz, 3H). (*syn*) δ 3.34 (m, 2H), 3.12 (m, 2H), 2.16 (brs, 2H), 1.8-1.1 (m, 13H), 0.94 (t, *J*=7Hz, 3H). IR(nujol): 3370cm$^{-1}$. An exact mass determination gave *m/e* 172.1464 (calcd for $C_{10}H_{20}O_2$, 172.269).

**8c** (NMR Rxn) $^1$H NMR (400MHz, $CDCl_3$) of diolate complex (*anti*) δ 6.212 (s, 5H, Cp), 6.207 (s, 5H, Cp), 3.92 (m, 1H), 3.56 (m, 1H), 1.87 (m, 2H, *i*-But), 1.63 (m, 2H, Et-$CH_2$), 0.99-0.89 (m, 21H), 0.04 (m, 4H, *i*-But). (*syn*) δ 6.25 (s, 5H, Cp), 6.21 (s, 5H, Cp), 4.20 (m, 1H), 3.56 (m, 1H), 1.87 (m, 2H, *i*-

But), 1.63 (m, 2H, Et-$CH_2$), 0.99-0.89 (m, 21H), 0.04 (m, 4H, *i*-But). $^1$H NMR (400MHz, $CDCl_3$) of Diol δ (*anti*) 3.49 (m, 1H), 3.28 (m, 1H), 1.79 (m, 1H, CH), 1.6-1.22 (brm, 4H, $CH_2$), 0.98-0.82 (m, 9H). (*syn*) δ 3.68 (m, 1H), 3.49 (m, 1H), 1.79 (m, 1H, CH), 1.6-1.22 (brm, 4H, $CH_2$), 0.98-0.82 (m, 9H).

**8d.** (NMR Rxn) $^1$H NMR (400MHz, $CDCl_3$) of diolate complex (*anti*) δ 6.20 (s,10H, Cp), 4.04 (m, 1H), 3.48 (d, *J*=8.4Hz, 1H), 1.86 (m, 2H, *i*-Bu), 1.8-1.05 (brm, 11H, Cyclohexyl), 0.97 (m, 18H), -0.88 (m, 4H, *i*-Bu). $^1$H NMR (400MHz, $CDCl_3$) of Diol δ (*anti*) 3.70 (m, 1H), 3.19 (m, 1H), 2.0-1.06 (brm, 16H, $CH_2$), 0.89 (t, *J*=6.6Hz, 6H). (*syn*) 3.76 (m, 1H), 3.45 (m, 1H), 2.0-1.06 (brm, 16H, $CH_2$), 0.89 (t, *J*=6.6Hz, 6H).

**8e.** Same as **8b**.

**8f.** (Colorless crystals), $^1$H NMR (400MHz, $CDCl_3$) (*anti*) δ 3.33 (dd, *J*=5Hz, 2H ), 1.8-1.0 (m, 24H). IR: 3390$cm^{-1}$.

**8g.** (Colorless crystals, m.p. 80.0-81.0 °C), $^1$H NMR (400MHz, $CDCl_3$) (*anti*) δ 3.65 (dd, *J*=6Hz,7Hz, 1H), 3.04 (d, *J*=7Hz, 1H), 2.34 (d, *J*=7Hz, 1H), 1.91 (d, *J*=6Hz, 1H), 1.53 (m, 2H), 0.93 (t, *J*=8Hz, 3H), 0.92 (s, 9H). $^{13}$C NMR( 100.4 MHz, $CDCl_3$) δ 79.4, 70.8, 34.9, 29.7, 26.2, 10.1. IR: 3745, 3600 $cm^{-1}$. An exact mass determination gave *m/e* 146.1311 (calcd for $C_8H_{18}O_2$, 146.231).

**8h.** $^1$H NMR (400MHz, $CDCl_3$) (*anti*) δ 5.70 (m, 1H), 5.52 (dd, *J*=15Hz,8Hz, 1H), 3.98 (dd, *J*=3Hz,7Hz, 1H), 3.53 (m, 1H), 2.46 (brs, 2H), 1.68 (d, *J*=5Hz, 3H), 1.37 (m, 2H), 0.93 (t, *J*=8Hz, 3H). (*syn*) δ 5.70 (m, 1H), 5.43 (dd, *J*=15Hz,7Hz, 1H), 3.81 (t, *J*=7Hz, 1H), 3.32 (m, 1H), 2.46 (brs, 2H), 1.67 (d, *J*=3Hz, 3H), 1.37 (m, 2H), 0.94 (t, *J*=8Hz, 3H). $^{13}$C NMR( 100.4 MHz, $CDCl_3$) δ (130.5, 129.8), (129.0, 128.8), (76.0, 75.9), (75.7,75.6), 25.8, 25.1, (17.9, 17.8),

(10.2, 9.90). IR: 3616, 3583, 3457cm$^{-1}$.

**8i**. $^{1}$H NMR (400MHz, $CDCl_3$) (*anti*) δ 5.74 (m, 1H), 5.48 (dd, *J*=7Hz,16Hz, 1H), 4.04 (m, 1H), 3.18 (m, 1H), 1.71 (d, *J*=6Hz, 1H), 1.65-1.0 (m, 11H). (*syn*) δ 5.74 (m, 1H), 5.57 (dd, *J*=7Hz,15Hz, 1H), 4.13 (m, 1H), 3.36 (m, 1H), 1.69 (d, *J*=7Hz, 0.27H), 1.65-1.0 (m, 11H). $^{13}$C NMR( 100.4 MHz, $CDCl_3$) δ (131.0, 129.8), 128.8, (78.7, 78.1), 73.4, 73.0), (39.7, 39.6), (30.3, 28.8), 27.1, (26.4, 26.3), 26.1,(25.9, 25.8), (17.9, 17.8). IR: 3609, 3569, 3444, 1672(w) cm$^{-1}$. An exact mass determination gave *m/e* 184.1474 (calcd for $C_{11}H_{20}O_2$, 184.1463).

**8j**. $^{1}$H NMR (400MHz, $CDCl_3$) (*anti*) δ 7.32 (s, 5H), 4.64 (d, *J*=4Hz, 1H), 3.70 (m, 1H), 2.66 (brs, 1H), 2.02 (brs, 1H), 1.43 (m, 2H), 0.92 (t, J=7Hz, 3H). (*syn*) δ 7.33 (s, 5H), 4.40 (d, *J*=7Hz, 1H), 3.56 (m, 1H), 2.66 (brs, 1H), 2.02 (brs, 1H), 1.43(m, 2H), 0.86 (t, J=6Hz, 3H). $^{13}$C NMR( 100.4 MHz, $CDCl_3$) δ 140.4, 128.3, 127.8, 126.8, 76.9, 76.6, (26.0, 24.6), (10.2, 10.0). IR: 3684 cm$^{-1}$.

**Reaction of (6b) with Carbon Monoxide.** In a 10 mL Schlenk tube, (0.25 mmol) of compound **6b** were prepared by the previously described procedure and transferred to a Fischer-Porter bottle. After cooling to -40 °C, the bottle was pressurized to 60 psi with carbon monoxide. The solution turned deep yellow within one minute. The cold bath was removed and the solution was stirred at room temperature for 4 hours before hydrolysis with 1 mL of a saturated ammonium chloride solution (aq.). $^{1}$H NMR indicated three major products corresponding to cyclohexyl methanol (35%), a carbon monoxide insertion product **10ii** (52%), and a carbon monoxide insertion product **10iii** with a substituted cyclopentadiene group (4%). $^{1}$H NMR (400MHz, $CDCl_3$) of **10ii** δ 4.27 (d, *J*=4.6Hz, 2H, $CH_2$), 3.14 (brs, 1H), 2.35 (m,

1H), 1.8-1.1 (brm, 10H, Cyclohexyl). IR: 3320 and 1710 $cm^{-1}$. $^1H$ NMR (400MHz, $CDCl_3$) of **10iii** δ 6.5-6.2 (brm, 4H), 3.71 (m, 2H), 3.01 (dd, *J*=1.2Hz, *J*=18.5Hz, 2H), 2.41 (d, *J*=16.6Hz, 1H, OH), 1.8-0.95 (brm, 11H). IR: 3400 $cm^{-1}$. Low resolution mass spectra does not give parent ion of 208, however, the strong primary fragment of 177 corresponds to a loss of $CH_2OH$. Also, the peak at 65 suggests a $Cp^+$ fragment. When two equivalents of DIBAL are used, the yield of **10iii** increases to 12 %.

**[$Cp_2Zr$(C, O-η²-O(H)CHCH($C_6H_5$)·Al(*i*-But)$_2$Cl{12a}].** An NMR tube was charged with 21 mg (0.051 mmol) of compound **11a** and dissolved in $CDCl_3$. After cooling to -50 °C, 7.3 mg (0.051 mmol) of DIBAL were added via syringe, mixed thoroughly, and characterized by $^1H$ NMR at -45 °C. $^1H$ NMR shows 70% aldehyde product was formed which decomposes at 25 °C within minutes. $^1H$ NMR (400MHz, $CDCl_3$) δ 6.99 (brs, 5H), 5.65 (s, 5H), 5.54 (s, 5H), 3.74 (d, 1H), 1.53 (m, 2H), 0.597 (brs, 12H), -0.31 (dd, 4H).

**[$Cp_2Zr$(C, O-η²-O(H)CHCH($CH_3$)$_3$)·Al(*i*-But)$_2$Cl{12b}].** An NMR tube was charged with 13 mg (0.035 mmol) of compound **11b** and dissolved in $CDCl_3$. After cooling to -50 °C, 5.0 mg (0.035 mmol) of DIBAL were added via syringe, mixed thoroughly, and characterized by $^1H$ NMR. $^1H$ NMR shows 60% aldehyde product was formed which slowly decomposes at 25 °C. $^1H$ NMR (400MHz, $CDCl_3$) δ 5.61 (s, 10H), 3.87(dd, *J*=1.7Hz, *J*=2.4Hz, 1H), 2.10 (m, 2H), 1.23 (d, *J*=6Hz, 6H), 1.18 (d, *J*=6Hz, 6H), 1.13 (s, 9H), 0.46 (m, 4H). $^{13}C$ NMR(100.4 MHz, $C_7D_8$) δ 129.5, 128.5, 109.8, 108.9, 77.0, 32.7, 30.7, 28.6, 28.4, 28.3, 228.2, 26.4, 26.3. $J_{CH}$ =159Hz for the aldehydic proton.

**Reaction of (6a) with R-(-)-Myrtenal.** An NMR tube was charged with 12.2 mg (0.039 mmol) of compound **4a** and dissolved in $CDCl_3$. After cooling

to -30 °C, 6.8 mg (0.039 mmol) of DIBAL were added via syringe, mixed thoroughly, and characterized by $^1$H NMR which indicated 85% purity. The tube was cooled to -60 °C and 5.9 mg (0.039 mmol) of R-(-)-myrtenal were added via syringe. The tube was warmed to 25 °C and characterized by $^1$H NMR which indicated 75% conversion to a 1:1 mixture of diastereomeric insertion products. $^1$H NMR (400MHz, $CDCl_3$) δ 6.27 (s, 2.5H), 6.25 (s, 2.5H), 6.24 (s, 2.5H), 6.22 (s, 2.5H), 5.41 (brs, 1H), 4.34 (d, *J*=9.5Hz, 0.5H), 4.24 (d, *J*=9.2Hz, 0.5H), 2.14 (m, 2H), 1.93(m, 2H), 1.66 (m, 1H), 1.38 (s, 1.5H), 1.36 (s, 1.5H), 1.02 (m, 16H), 0.90 (s, 1.5H), 0.81 (s, 1.5H), 0.11 (m, 4H).

**Reaction of (6b) with R-(-)-Myrtenal.** An NMR tube was charged with 17.4 mg (0.048 mmol) of compound **6b** and dissolved in $CDCl_3$. After cooling to -30 °C, 6.8 mg (0.048 mmol) of DIBAL were added via syringe, mixed thoroughly, and characterized by $^1$H NMR which indicated 95% purity. The tube was cooled to -60 °C and 7.2 mg (0.048 mmol) of R-(-)-myrtenal were added via syringe. The tube was warmed to 25 °C and characterized by $^1$H NMR which indicated 90% conversion to a 1:1 mixture of diastereomeric insertion products. $^1$H NMR (400MHz, $CDCl_3$) δ 6.26 (s, 2.5H), 6.23 (s, 2.5H), 6.22 (s, 2.5H), 6.21 (s, 2.5H), 5.42 (brs, 1H), 4.45 (d, *J*=9.2Hz, 0.5H), 4.43 (d, *J*=9.5Hz, 0.5H), 3.73 (d, *J*=9.5Hz, 0.5H), 3.69 (d, *J*=9.5Hz, 0.5H), 2.53 (m, 0.5H), 2.40 (m, 0.5H), 2.30 (m, 2H), 2.14 (m, 1H), 1.94 (m, 2H), 1.85-1.60 (brm, 6H), 1.40 (s, 1.5H), 1.37 (s, 1.5H), 1.36-1.05 (m, 12H), 0.91 (s, 1.5H), 0.85 (s, 1.5H), 0.11 (m, 4H).

**2-Hydroxy-2-Methyl-1-Phenylpropanone (16).** Into a 20 ml Schlenk tube, 95 mg (62.6 mmol) of ketone-complex **5** were added and dissolved in 5 ml of methylene chloride. After cooling to -50 °C, 30 µl (0.29 mmol) of benzonitrile were added via syringe. The pale yellow solution became deep

yellow upon addition of the nitrile. The color faded while warming to room temperature. After 30 min., 1 ml of saturated $NH_4Cl$(aq) was added and the solution was allowed to stir for 2 hr. The white, zirconium μ-oxo-polymer appeared after 5 min. of hydrolysis. TLC indicated product was present after 2 hr. The solution was separated and the aqueous layer washed with diethyl ether, dried with $Na_2SO_4$ (anhyd), and eluted through a pad of silica gel. Chromatography, 30:70 THF/cyclohexane, yielded 26 mg (62%) of pure product. $^1$H NMR (90MHz, $CDCl_3$) δ 8.0 (m, 2H), 7.48 (m, 3H), 4.06 (s, 1H), 1.63 (s, 6H). IR(neat): 3440, 1672cm$^{-1}$. The results are consistent with those reported in the literature.

**Reaction of (6a) with Phenylacetylene.** (See general procedure for aldehydes and ketones section for experimental.) Product **18a** 38.7 mg (65%), $^1$H NMR (400MHz, $CDCl_3$) δ 7.30 (s, 5H), 6.50 (d, *J*=15.9Hz, 1H), 6.14 (dd, *J*=15.9Hz,*J*=6.8Hz, 1H), 4.13 (m, 1H),1.59 (m, 2H), 0.90 (t, *J*=7.6Hz, 3H). The results are consistent with those reported in the literature. Product **18b** 1.8 mg (6%), $^1$H NMR (400MHz, $CDCl_3$) δ 7.25 (s, 5H), 5. (d, *J*=15.9Hz, 1H), 4.57 (m, 1H),1.51 (m, 2H), 0.90 (t, *J*=7.3Hz, 3H).

**Reaction of (6a) with Ethylene.** An NMR tube was charged with 16.0 mg (0.051 mmol) of compound **6a** and dissolved in $CDCl_3$. After cooling to -30 °C, 7.1 mg (0.051 mmol) of DIBAL were added via syringe, mixed thoroughly, and characterized by $^1$H NMR which indicated 87% purity. The tube was cooled to -60 °C and an excess of ethylene was added via syringe. After 2 hr at room temperature, $^1$H NMR indicated an 80% yield of insertion product. $^1$H NMR (400MHz, $CDCl_3$) δ 6.032 (s, 5H), 6.030 (s, 5H), 3.78 (m, 1H), 2.13 (m, 1H), 1.84 (m, 1H), 1.82 (m, 2H, *i*-But-CH), 1.54 (m, 2H, Et-$CH_2$), 1.53 (m, 1H), 1.15 (m, 1H), 0.92 (m, 12H, *i*-But), 0.79 (t, *J*=7.6Hz, 3H, Et-$CH_3$),

-0.04 (m, 4H, *i*-But-$CH_2$). $^1H$ NMR (400MHz, $CDCl_3$) of hydrolysis product δ 3.43 (m, 1H), 1.42 (m, 4H), 0.89 (t, *J*=7.6Hz, 6H).

**Reaction of (6b) with Ethylene.** An NMR tube was charged with 21.9 mg (0.06 mmol) of compound **6b** and dissolved in $CDCl_3$. After cooling to -30 °C, 8.5 mg (0.06 mmol) of DIBAL were added via syringe, mixed thoroughly, and characterized by $^1H$ NMR which indicated 85% purity. The tube was cooled to -60 °C and an excess of ethylene was added via syringe. After 2h at room temperature, $^1H$ NMR indicated a 42% yield of insertion product. $^1H$ NMR (400MHz, $CDCl_3$) δ 6.01 (s, 5H), 6.00 (s, 5H), 3.74 (m, 1H), 2.0-1.0 (brm, 13H), 0.90 (m, 12H, *i*-But), -0.01 (m, 4H, *i*-But-$CH_2$).

**Reaction of (6a) with Dimethylallene.** An NMR tube was charged with 15.4 mg (0.049 mmol) of compound **6a** and dissolved in $CDCl_3$. After cooling to -30 °C, 7.0 mg (0.049 mmol) of DIBAL were added via syringe, mixed thoroughly, and characterized by $^1H$ NMR which indicated 85% purity. The tube was cooled to -60 °C and 5.0 mg (0.049 mmol) of dimethylallene were added via syringe. The tube was warmed to 25 °C and characterized by $^1H$ NMR which indicated 77% conversion to insertion product after 3 hr. $^1H$ NMR (400MHz, $CDCl_3$) δ 6.27 (s, 5H), 6.22 (s, 5H), 3.83 (m, 1H), 2.59 (m, 2H), 1.88 (m, 2H), 1.69 (s, 3H), 1.55 (s, 3H), 0.98 (m, 12H), 0.85 (t, *J*=7.3Hz, 3H), 0.05 (m, 4H).

**Reaction of (6a) with Trimethylsilylketene.** An NMR tube was charged with 13.2 mg (0.042 mmol) of compound and dissolved in $CDCl_3$. After cooling to -30 °C, 6.0 mg (0.042 mmol) of DIBAL were added via syringe, mixed thoroughly, and characterized by $^1H$ NMR which indicated 84% purity. The tube was cooled to -60 °C and 6.6 mg (0.058 mmol) of

trimethylsilylketene were added via syringe. The tube was warmed to 25 °C and characterized by $^1$H NMR which indicated 81% conversion to insertion product **23** $^1$H NMR (400MHz, $CDCl_3$) δ 6.28 (s, 5H), 6.27 (s, 5H), 4.66 (m, 1H), 3.58 (s, 1H), 1.92 (m, 2H), 1.67 (m, 2H), 0.99 (m, 12H), 0.92 (t, *J*=7.3Hz, 3H), 0.10 (m, 4H).

**Reaction of (6a) with δ–Valerolactone.** An NMR tube was charged with 14.2 mg (0.045 mmol) of compound and dissolved in $CDCl_3$. After cooling to -30 °C, 6.4 mg (0.045 mmol) of DIBAL were added via syringe, mixed thoroughly, and characterized by $^1$H NMR which indicated 85% purity. The tube was cooled to -60 °C and 4.5 mg (0.045 mmol) of δ–valerolactone were added via syringe. The tube was warmed to 25 °C and characterized by $^1$H NMR which indicated 62% conversion to insertion product after 1 day. $^1$H NMR (400MHz, $CDCl_3$) δ 6.32 (s, 5H), 6.28 (s, 5H), 4.63 (m, 1H), 2.55 (m, 1H), 1.84 (m, 2H), 1.70 (m, 2H), 1.42 (d, *J*=6.1Hz, 3H), 0.92 (m, 14H), -0.06 (m, 4H).

## References and Notes

1. a) Herrman, W.A.; Plank, J. *Angew. Chem. Int. Ed. Engl.* **1978**, *17*, 525. b) Grubbs, R.H.; Miyashito, A. *Tetrahedron Lett.* **1981**, 1255. c) Herrman, W.A.; Gimeno, J.; Weicmann, J.; Ziegler, M.L.; Balbach, B. *J. Organomet. Chem.* **1981**, *213*, C2. d) Takenchi, A.; Katzer, J.R. *J. Phys. Chem.* **1980**, *86*, 2438. e) Blyholder, G.; Emmett, P.H. *J. Phys. Chem.* **1960**, *64*, 470. f) Morrison, E.P.; Steinmetz, G.R.; Geoffroy, G.L.; Fultz, W.C.; Rheingold, A.L. *J. Am. Chem. Soc.* **1984**, *106*, 4783.

2. a) Herrman, W.A. *Angew. Chem. Int. Ed. Engl.* **1974**, *13*, 335. b) Schorpp, K.; Beck, W. *Z. Naturforsch, B.* **1973**, *28*, 738. c) Herrman, W.A.; Plank, J.; Ziegler, M.L.; Weidenhammer, K. *J. Am. Chem. Soc.* **1979**, *101*, 3133. d) Bristow, G.S.; Hitchcock, P.B.; Lappert, M.F. *J. Chem. Soc., Chem. Commun.* **1982**, 462. e) Gambarotta, S.; Pasquali, M.; Floriani, C.; Chiesi-Villa, A.; Guastini, C. *Inorg. Chem.* **1981**, *20*, 1173.

3. Straus, D.A., Ph.D. Thesis, California Institute of Technology, 1983.

4. Ho, S.C., Ph.D. Thesis, California Institute of Technology, 1985.

5. a) Sinn, H.; Kaminsky, W. *Adv. Organomet. Chem.* **1980**, *18*, 99-149. b) Pino, P.; Mulhaupt, R. *Angew. Chem. Int. Ed. Engl.* **1980**, *19*, 857-875. c) Chien, J.W.; Wu, J.C. *J. Pol. Sci., Chem. Ed.* **1985**, *20*, 2445.

6. a) Ivin, K.J. "Olefin Metathesis;" Academic Press: London; **1983**. b) Grubbs, R.H. "Comprehensive Organometallic Chemistry;" Wilkinson, G.; Stone, F.G.A.; Abel, E.W.; Eds. Pergamon Press: Oxford, **1982**, Vol. 9, 499.

7. Waymouth, R.M., Ph.D. Thesis, California Institute of Technology, 1986.

8. Waymouth, R.M.; Santarsiero, B.D.; Grubbs, R.H. *J. Am. Chem. Soc.* **1984**, *106*, 4050.

9. Erker, G.; *et al,Organometallics* **1986**, *5*, 668.

10. a) Schwartz, J. *J. Organometal. Chem. Library* **1976**, *1*, 461. b) Schwartz, J. Labinger, J.A. *Angew. Chem. Int. Ed. Engl.* **1976**, *15*, 333. c) Yoshida, T.; Negishi, E. *J. Am. Chem. Soc.* **1981**, *103*, 1276. d) Negishi, E.; Takahashi, T. *Aldrichimica Acta* **1985**, *18*, No. 2.

11. Bertelo, C.A.; Schwartz, J. *J. Am. Chem. Soc.* **1975**, *97(1)*, 228-230.

12. a) Erker, G.; Rosenfeldt, F. *J. Organometal. Chem.* **1982**, *224*, 29. b) Erker, G. *Acc. Chem. Res.* **1984**, *17*, 103. c) Erker, G.; Kropp, K. *Chem. Ber.* **1982**, *115*, 2437. d) Erker, G.; Kropp, K.; Skibbe, V. *J. Am. Chem. Soc.* **1983**, *105*, 3353. e) Skibbe, V.; Erker, G. *J. Organometal. Chem.* **1983**, *241*, 15.

13. Gray, D.R.; Brubaker, C.H. *Inorganic Chem.* **1971**, *Vol. 10*, No. 10, 2143.

14. The Cp shifts of both the decomposition product and the aluminum adduct of the zirconocene alkoxide match exactly, however, the methylene protons are not clearly defined due to possible oligomeric complexation of aluminum decomposition products. Complex multiplet peaks at around 3.7 ppm occur in both samples which correspond to the methylene protons adjacent to the oxygen atom of the alkoxide.

15. a) Wolczanski, P.T.; Bercaw, J.E. *J. Am. Chem. Soc* **1979**, *101*, 218. b) Threlkel, R.S.; Bercaw, J.E. *J. Am. Chem. Soc.* **1981**, *103*, 2650.

16. Negishi, E.; Takahashi, T. *Tetrahedron Lett.* **1980**, *21* , 1501.

17. Reaction of the zirconium aldehyde hydride complex with propionaldehyde results in the formation of isobutylene and Al-bound alkoxides which yield propanol upon hydrolysis.

18. Meinhart, J. D.; Anslyn, E.V.; Grubbs, R.H. *Organometallics* **1989**, *8(3)*, 583-9.

19. Reaction of the titanacene methylidene trimethylphosphine adduct with 1 equivalent of DIBAL results in a new titanium complex that resembles a hydride analog of Tebbe's reagent. $^{1}H$ NMR showed the characteristic bridging methylene peak at 9.10 ppm (s, 2H), Cp's at 5.66 ppm (s, 10H), and hydride shift at -3.81 ppm. $^{13}C$ NMR showed bridging methylene peak at 213.9 ppm with a $J_{CH}$=127 Hz.

20. Hydride shifts (δ) for compounds (a) 0.19, (b) -3.03, (c) -0.70.

21. a) Browning, J.; Empsall, H.D.; Green, M.; Stone, F.G.A. *J. Chem. Soc., Dalton Trans.* **1973,** *381*, and refs. therein. b) Hunt, M.M.; Kemmitt, R.D.; Russel, D.R.; Tucker, P.A. *J. Chem. Soc., Dalton Trans.* **1979**, 287. c) Fachinetti, G.; Biran, C.; Floriani, C.; Chiesi-Villa, A.; Guastin, C. *J. Am. Chem. Soc.* **1978**, *100*, 1921-1922. d) Fachinetti, G.; et al *Inorg. Chem.* **1978**, *17*, 2995-3002.

22. a) Masamune, S.; Choy, W. *Aldrichimica Acta* **1982**, *Vol. 15*, No. 3. b) Fuson, R.C. *Rec. Chem. Prog.* **1951**, *12*, 1. c) Tsuge, O.; *et al. Chem. Lett.* **1984**, 1803-6.

23. a) Corey, E.J. ; Danheiser, R. L.; Chandrasekaran, S. *J. Org. Chem.* **1976**, *41*, 260. b) Molander, G.A.; Kenny, C. *J. Org. Chem.* **1988**, *53*, 2132-2134. c) Nakayama, J.; Yamaoka, S.; Hoshino, M. *Tett. Lett.* **1987**, *No. 16*, 1799-1802.

24. Cardin, D.J.; Lappert, M.F.; Raston, C.L. "Chemistry of Organo-Zirconium and Hafnium Compounds;" Halstead Press, New York, **1986**.

25. An authentic sample was prepared of diol **7a** and compared by $^1$H NMR and VPC to verify the diastereomeric assignment.

26. Wysong, E.B.; Mori, M.; Grubbs, R.H., unpublished results.

27. a) Roddick, D.M.; Bercaw, J.E. *Chem. Ber.* **1989**, *122*, 1579-1587. b) Manriquez, J.M.; Fagan. P.J.; Marks, T.J.; Day, V.; Day, C.S. *J. Am. Chem. Soc.* **1978**, *100*, 7112.

28. a) Shoer, L.I.; Schwartz, J. *J. Am. Chem. Soc.* **1977**, *99*, 5831-5832. b) Shoer, L.I.; Gell, K.I.; Schwartz, J. *J. Organometal. Chem.* **1977**, *136*, C19-C22.

29. a) Caunt, A.D. *British Polymer Journal* **1981**, 22-26. b) Warzelhan, V.; Burger, T.F.; Stien, D.J. *Makromol. Chem.* **1982**, *183*, 489-504. c) Burfield, D.R. *ibid.*, 2709-2717. d) Bukatov, G.D.; Shepelev, S.H.; Zakharov, V.A. *ibid.*, 2657-2665. e) Bukatov, G.D.; Goncharov, V.S.; Zakharov, V.A. *Makromol. Chem.* **1986**, *187*, 1041-1051.

30. Attempts to react either complex with aldehydes gave poor yields of insertion products.

31. Ruden, R.A. *J. Org. Chem.* **1974**, *39*, 3607.

32. Still, W.C.; Kahn, M.; Mitra, A. *J. Org. Chem.* **1978**, *43*, 2923-2925.

# CHAPTER 2

## Reaction of Titanacyclobutanes with Aryl Epoxides via Catalytic Trimethylphosphine Addition: Synthesis of Titanium Oxymetallacyclopentanes and γ-Lactones

## Introduction

The chemistry of titanacyclobutanes has been the focus of considerable research within the Grubbs group during the past few years. The starting material for these titanium compounds is the well-known Tebbe reagent **2**. This complex was discovered and developed by F.N. Tebbe at Du Pont Central Research during olefin metathesis investigations and has been shown to behave as essentially a dimethylaluminum chloride protected titanocene methylidene.[1] The formation of Tebbe's reagent proceeds through α-hydrogen abstraction from an intermediate chlorotitanium complex **1**, which is formed through initial transmetallation (Figure 1).

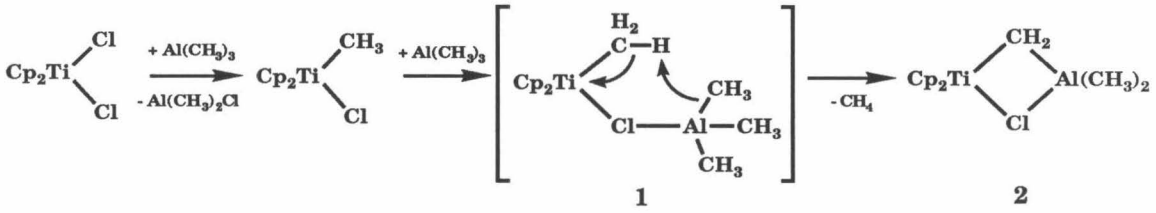


**Figure 1. Tebbe's reagent synthesis.**

An important breakthrough concerning the chemistry of Tebbe's reagent was made by Howard *et al.*,[2] who discovered that it reacted with alkenes in the presence of a Lewis base such as pyridine or vinylpyridine-styrene copolymer to produce isolable *bis*(cyclopentadienyl) titanacyclobutanes (eq 1).

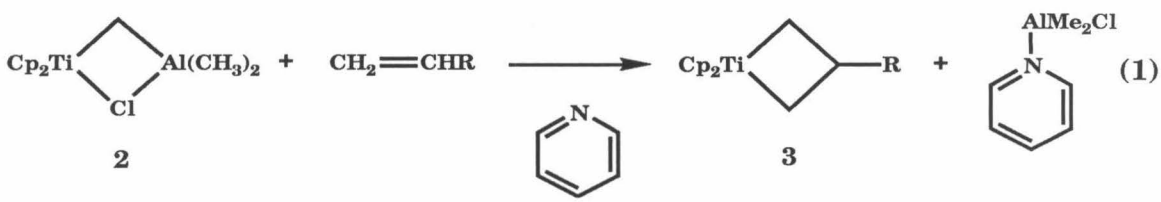


(1)

Studies using various alkenes with **2** in the presence of pyridine bases provided the first direct evidence for the involvement of metallacyclic intermediates in olefin metathesis. The structure, reactivity, and reaction mechanisms for many titanacyclobutanes have been extensively studied in this group. Spectroscopic and x-ray techniques indicate a planar, fairly symmetrical, four-member metallacyclic ring structure **A** for these complexes as opposed to an equilibrating carbene-olefin complex **B** (Figure 2).[3]

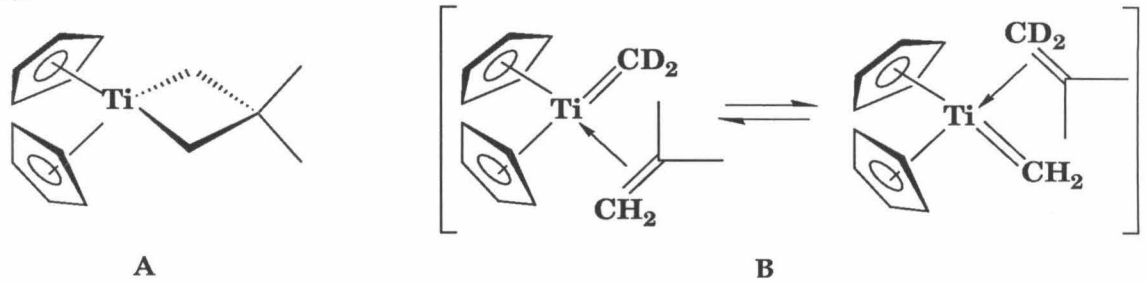


**Figure 2. Titanacyclobutane structures: (A) metallacyclic ring, (B) equilibrating carbene-olefin complex.**

The titanacyclobutanes exhibit a wide range of reactivity. Scheme 1 illustrates some of the many reactions which include: (a) reaction with alkynes to produce titanacyclobutenes, (b and c) methylene transfer to organic carbonyls such as ketones and esters, (d and e) photochemical and thermal reductive elimination, (f and g) electrophilic cleavage of the Ti-C bonds by halogens or acids ($H^+$), and (h) formation of enolates from acid chlorides.[4]

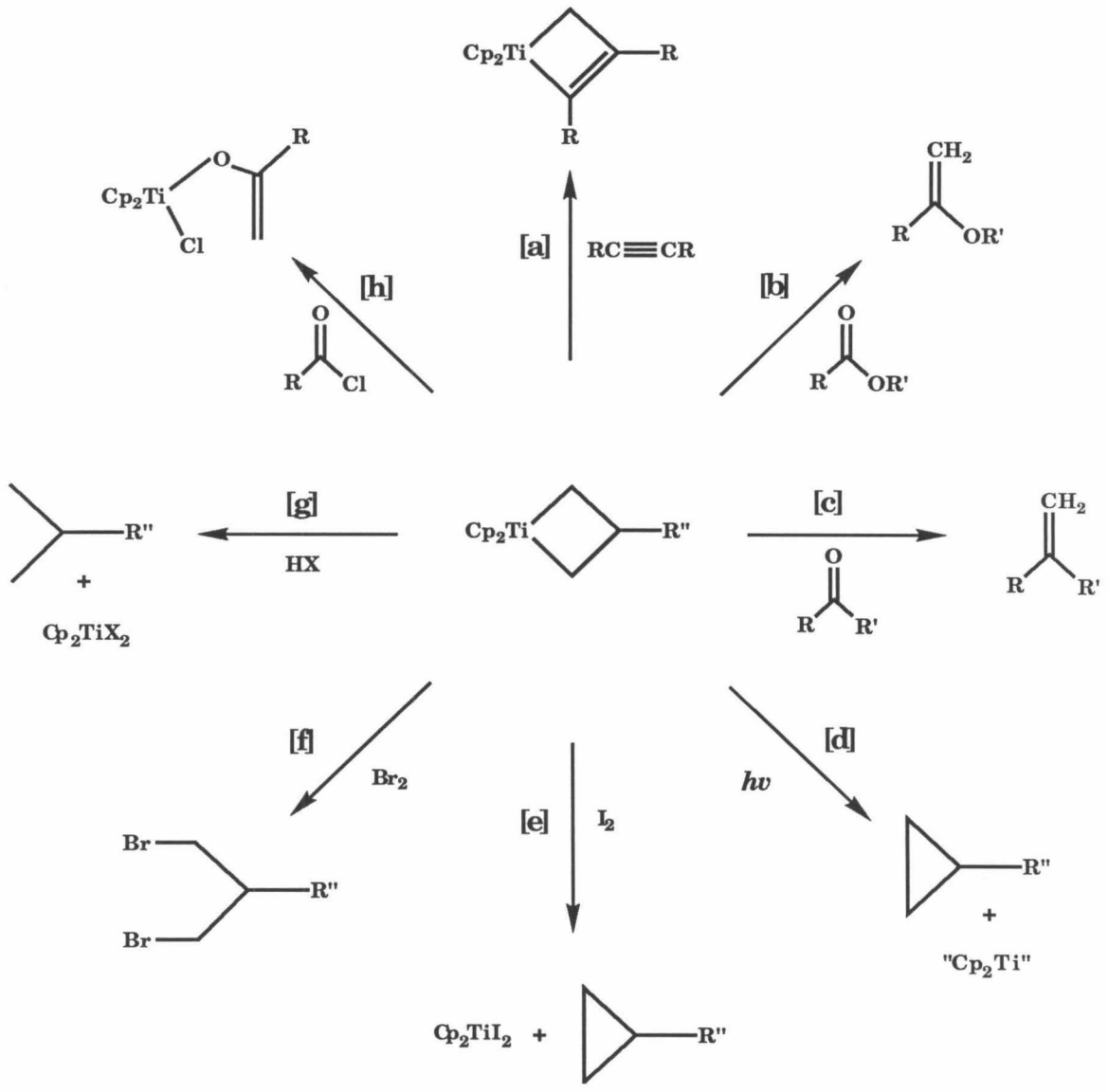


**Scheme 1. Titanocyclobutane reactivity.**

Most of the reaction chemistry of titanacyclobutanes can best be understood in terms of a reactive titanocene methylidene intermediate generated by retro 2+2 cycloaddition. In the case of methylene transfer to carbonyl compounds, the reaction of the methylidene intermediate with

carbonyl compounds is believed to yield metallaoxetanes which cleave to form the corresponding olefin and titanium oxide (Figure 3).[4]

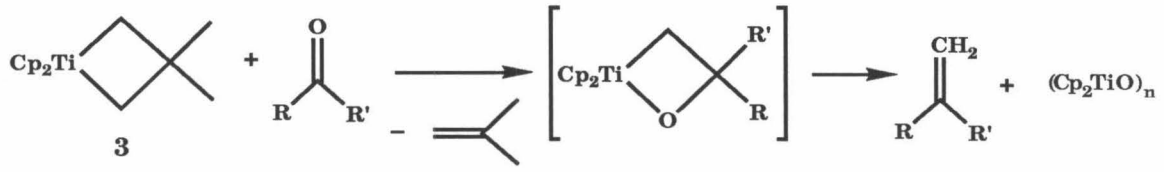


**Figure 3. Reaction of titanacyclobutane (3) with carbonyl substrates.**

This entire process is driven by the formation of extremely strong metal-oxygen bonds in the titanium by-product. By reacting efficiently and selectively with carbonyl substrates such as ketones, esters, and amides, these titanium reagents have become standard reagents in organic synthesis.

Ring opening metathesis polymerization represents another important use for titanacyclobutanes. Strain energy of cyclic olefin monomers provide the driving force for ring opening and subsequent alkylidene formation that continues the polymerization (Figure 4).[5]

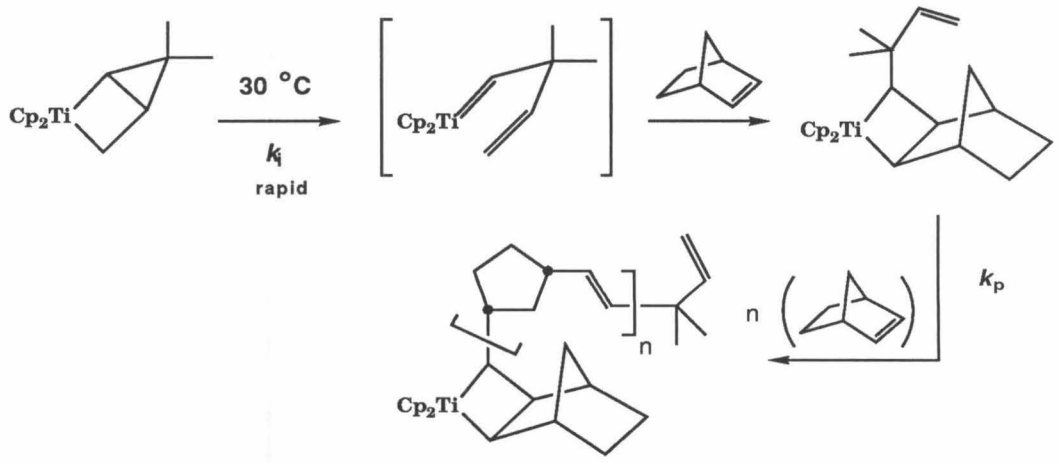


**Figure 4. Ring opening metathesis polymerization of norbornene via titanacyclobutane catalysis.**

The stability of the terminal titanacyclobutane imparts a living behavior to these polymerizations and enables the synthesis of monodisperse, di-block, and tri-block polymers.[6]

The titanocene methylidene intermediates can be trapped by phosphine ligands.[7] These adducts show similar reactivity toward alkenes and alkynes as titanacyclobutanes.[7] In addition, J.W. Park[8] demonstrated the reactivity of the trimethyl phosphine adduct **4** towards epoxides (eq 2).

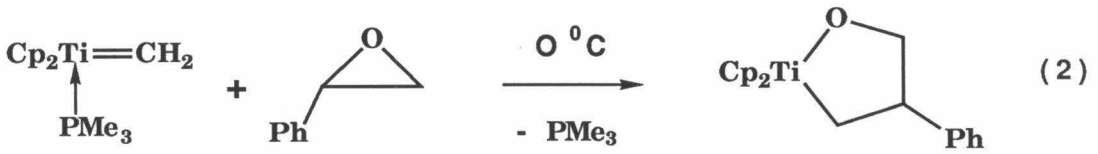


**4** **5** (2)

The formation of titanocene oxymetallacycle **5** contrasts strongly with the reactivity of complex **4** towards styrene sulfide to form **6** (eq 3).[9]


**4** **6** (3)

This difference of reactivity between epoxides and episulfides may imply that the formation of $Cp_2Ti(\eta^2\text{-}CH_2O)\cdot PMe_3$ is thermodynamically less favorable than that of $Cp_2Ti(\eta^2\text{-}CH_2S)\cdot PMe_3$. Deuterium labeling experiments, as well as substituent effect studies on substituted styrene oxides, suggest a stepwise mechanism involving a biradical intermediate is operating with aryl epoxides (Scheme 2).[8]

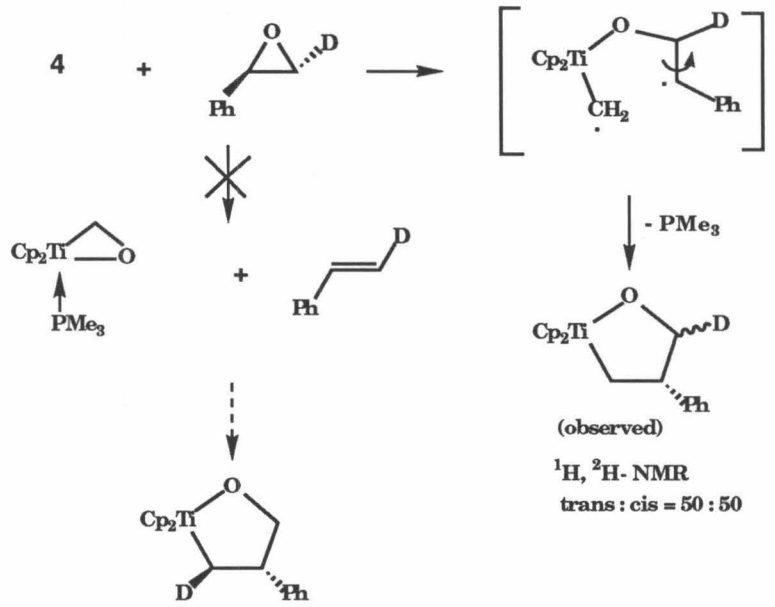


**Scheme 2. Reaction of titanium methylidene phosphine adduct (4) with deuterium labeled styrene oxide.**

An interesting application of this reaction involves a new carbon-carbon bond formation which has synthetic potential in producing γ-lactones (eq 4).

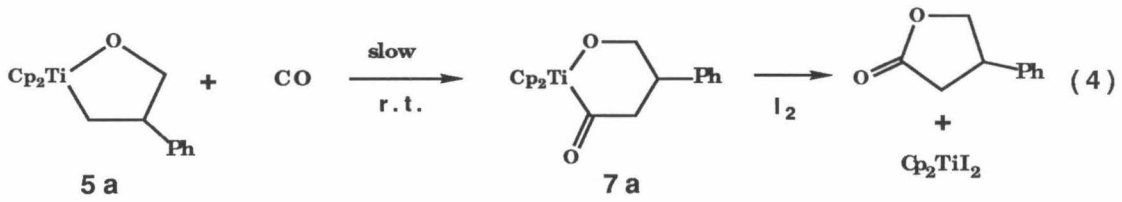


There are few literature examples of transformations converting an epoxide into a γ-lactone, however, Figure 5 illustrates some methods involving alkenes.[10]

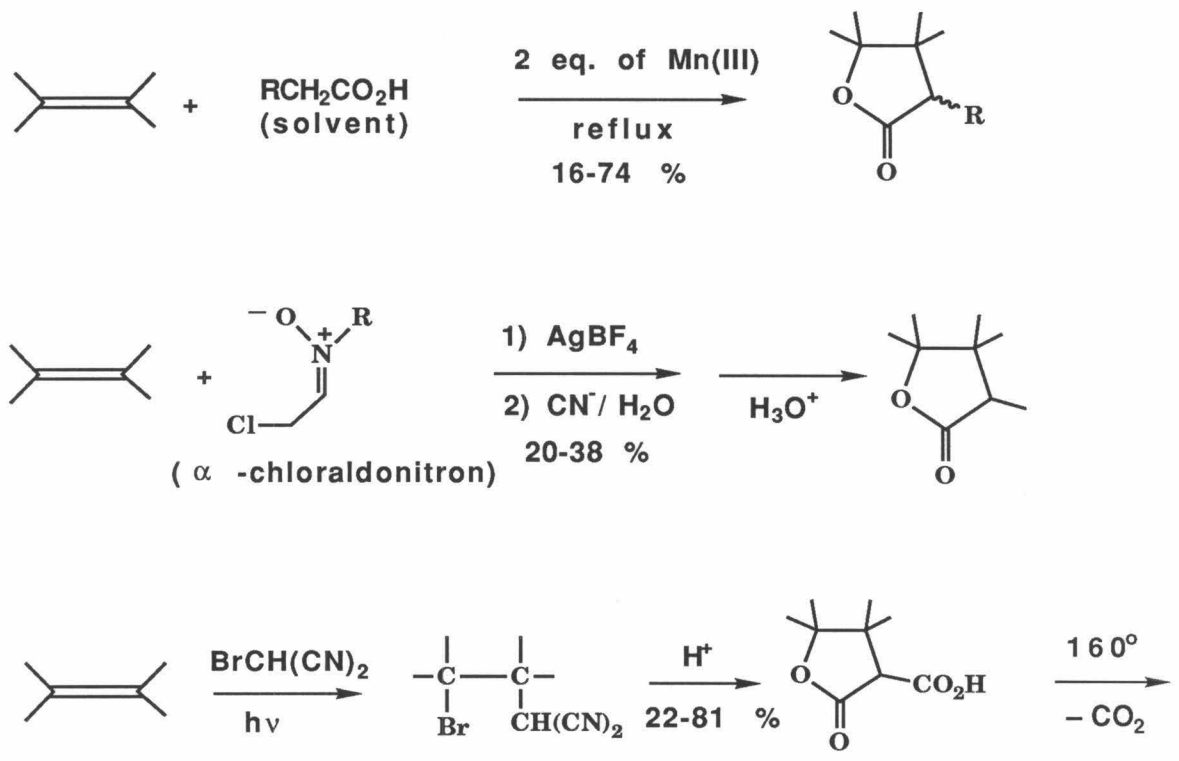


**Figure 5.** γ-Lactones syntheses from alkenes.

A significant problem with using adducts such as **4** involves their difficult synthesis and thermal instability. This chapter describes efforts to overcome this problem and to determine the scope of this new carbon-carbon bond forming reaction.

## Results and Discussion

**Catalytic Phosphine Methodology.** Due to the difficult syntheses of titanium alkylidene phosphine adducts, as well as their thermal instability in solution, a catalytic phosphine method was considered that would eliminate the need for phosphine adduct isolation and minimize the amount of the expensive, highly toxic phosphine ligand required for insertion reactions.

Before exploring epoxide insertion methodology with phosphines, control experiments were performed. The reaction of complex **3a** with styrene oxide in the absence of trimethylphosphine yielded no insertion product. This suggests that the epoxide is not a suitable ligand for stabilizing the titanium methylidene and that the ligated methylidene moiety is necessary for the insertion to occur. This is consistent with the observations of E. Ansyln which demonstrated the greater reactivity of phosphine and DMAP ligated titanium methylidenes in comparison to free titanium methylidenes.[11]

Based on the order of stability for various phosphine ligands determined by Meinhart *et al.,* (figure 6)[7], as well as earlier attempts to trap the titanocene methylidene with ligands such as DMAP, pyridine, trimethylphosphite[7], triphenylphosphine, and triflurophosphine[7], trimethylphosphine was chosen as the catalytic ligand for further studies.

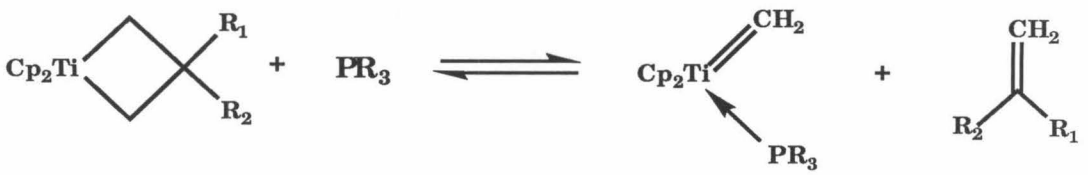


**3. a)** $R_1=R_2=CH_3$
**b)** $R_1=CH_3$, $R_2=C_3H_7$

**4. a)** $PR_3=PMe_3$
**b)** $PR_3=PMe_2Ph$
**c)** $PR_3=PEt_3$

**Order of Stability: $PMe_3 > PMe_2Ph >> PEt_3$.**

**Figure 6. Stability of titanocene methylidene phosphine adduct complexes.**

By reacting a solution of metallacycle **3a** with 0.1 equivalents of trimethylphosphine prior to epoxide addition, a high yield of insertion product was obtained (eq 5).

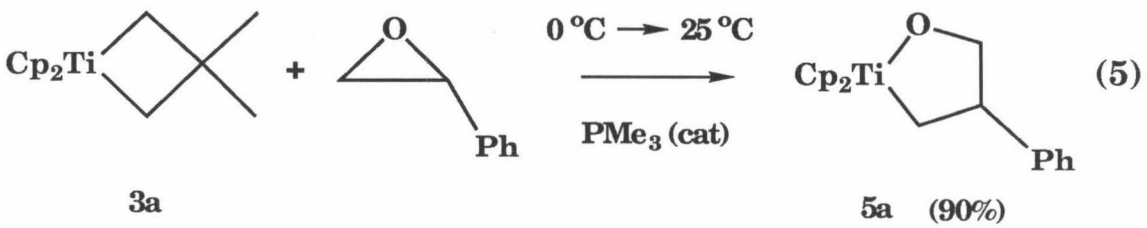


**3a** **5a (90%)** **(5)**

The success of this catalytic reaction is consistent with the mechanism proposed by Meinhart *et al.*, [7] for trimethylphosphine adduct formation and reactivity. It has been shown that the rate limiting step in the formation of **4a** involves the dissociation of alkene followed by rapid complexation by a phosphine ligand (Figure 7).[11]

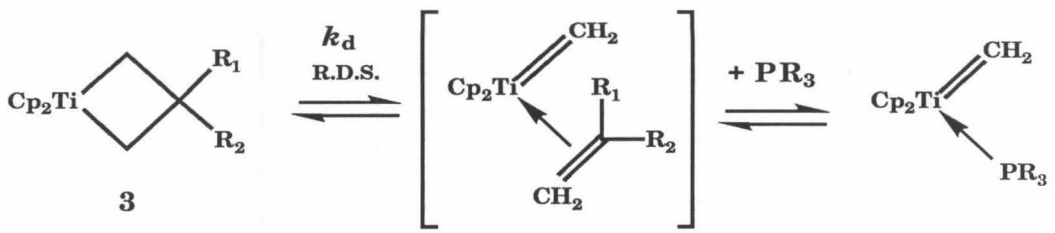


**3**

**Figure 7. Formation of titanocene methylidene phosphine adducts.**

The rate of methylidene trapping by alkynes was shown to be one-tenth the rate of trapping by phosphine.[7] As a result, the addition of a small amount of trimethylphosphine to the metallacycle **3a** yields a corresponding amount of adduct **4a** in solution in the presence of displaced olefin (as observed by $^1$H NMR). The phosphine adducts have been previously characterized and are best described by a true methylidene phosphine complex rather than an ylide complex (Figure 8).[7]

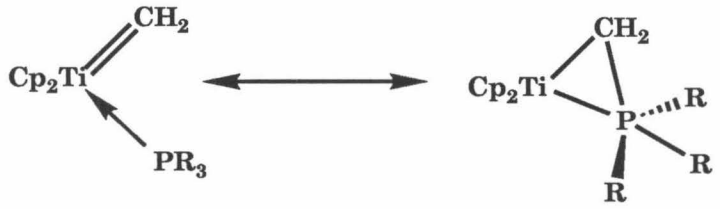


**Figure 8. Titanocene methylidene trimethylphosphine adduct structure.**

Attempts made to go back one step further to the Tebbe reagent using an excess of DMAP proved unsuccessful due to aluminum catalyzed ring opening polymerization of the styrene oxide.

**Catalytic Phosphine Reactivity.** Using the catalytic trimethylphosphine method with titanacyclobutane **3a**, a number of epoxides were screened for insertion reactivity (Table 1).

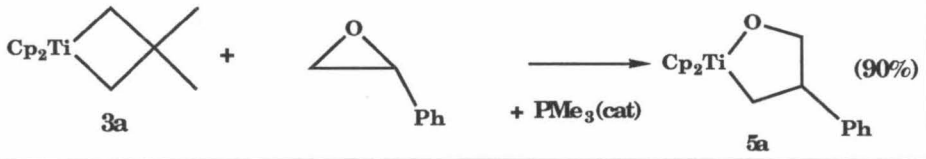


| Metallacycle | Epoxide | Product |
|---|---|---|
| 3a | 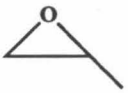 | N.R. |
| 3a |  | N.R. |
| 3a | 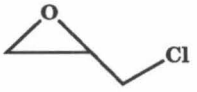 | 40% reacted (not clean) |
| 3a |  | N.R. |
| 3a | 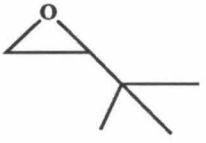 | N.R. |
| 3a | 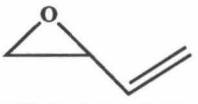 | 100% reacted (Not clean) |

**Table 1. Reaction of titanacyclobutane 3a with epoxides.**

The results clearly show that aliphatic substituted epoxides are not as reactive as vinyl and aryl substituted epoxides. In the case of epichlorohydrin, it is difficult to determine whether electron transfer reactions with the halogen functionality are competing with epoxide insertion. These results are quite different from the Gibson *bis*-Cp* titanium methylidene chemistry in which aliphatic substituted epoxides react to give titanium enolates (Figure 9).[12]

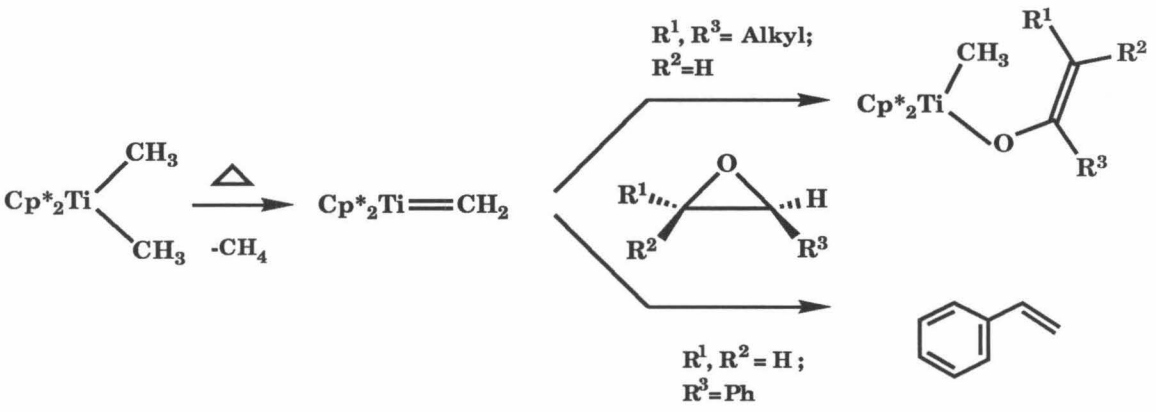


**Figure 9. Reaction of thermally generated $Cp^*_2$ titanium methylidene with aliphatic and aryl substituted epoxides.**

In contrast, butadiene monoxide reacted completely, however, yielding little desired product. This may be a consequence of the reactive nature of the biradical allyl intermediate or interference by the double bond with the titanium methylidene.

In order to explore the effect of temperature on epoxide insertion and possibly enhance the reactivity of the methylidenes, additional titanacyclobutanes with higher activation temperatures were examined (Figure 10).

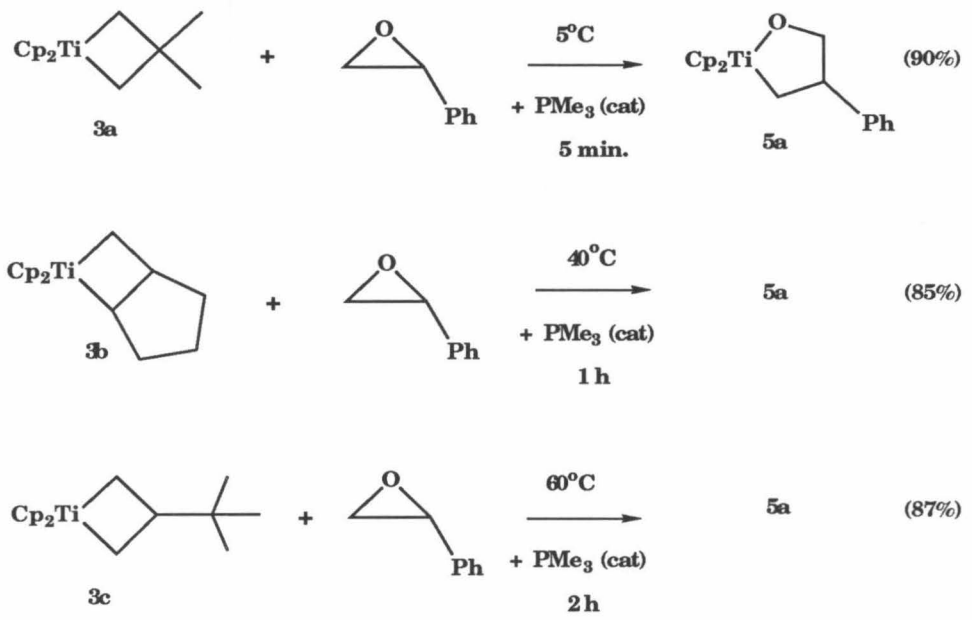


**Figure 10. Reaction of styrene oxide with β-substituted titanacyclobutanes.**

Although styrene oxide undergoes insertion with titanium methylidenes at higher temperatures with comparable yields, no insertion with aliphatic alkyl substituted epoxides was observed. At 60 °C, the characteristic titanocene methylidene proton shift at 12 ppm was observed indicating the presence of the titanocene methylidene trimethylphosphine adduct in solution at high temperatures. This is significant in that this methodology enables the use of phosphine adducts in solution at temperatures well above the decomposition temperature for isolated phosphine adducts.

A series of aliphatic and aryl substituted styrene oxides were examined in order to probe steric and electronic effects on insertion yield and the determine the extent of isomerization (Table 2).

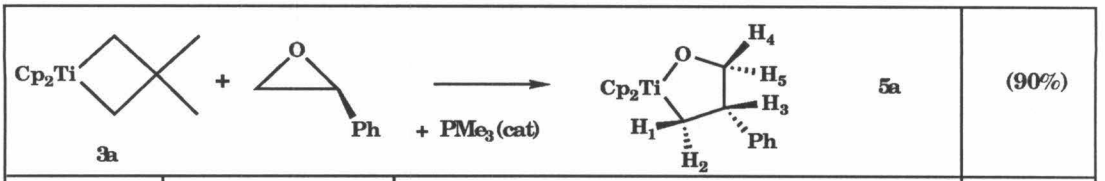


| Metallacycle | Epoxide | Products | Yield [anti:syn] |
|---|---|---|---|
| 3a | 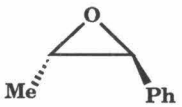 | 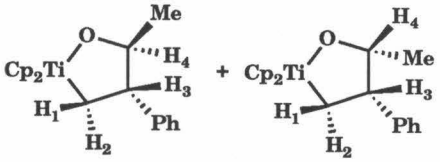 5b | (62%) [4:1] |
| 3a | 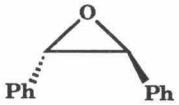 | 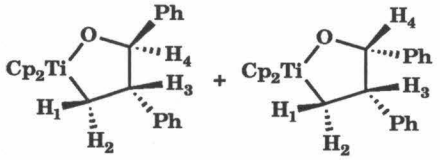 5c | (13%) [9:1] |
| 3a |  | 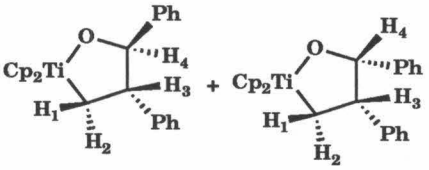 5d | (45%) [9:1] |
| 3a | 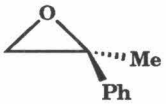 | 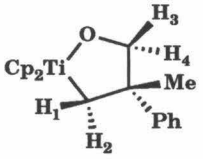 5e | (55%) |
| 3a | 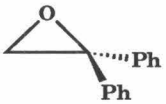 | 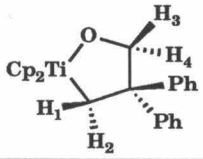 5f | (31%) |

**Table 2. Reaction of titanacyclobutane (3a) with aliphatic and aryl substituted epoxides.**

Overall, the yields diminished as the steric bulk of the epoxides increased. The *trans*-1-phenylpropene oxide example shows a 4:1 anti:syn ratio that is close to the 5.2:1 ratio observed by Groves for the ruthenium(II) porphyrin catalyzed isomerization of the same substrate (Figure 11).[13]

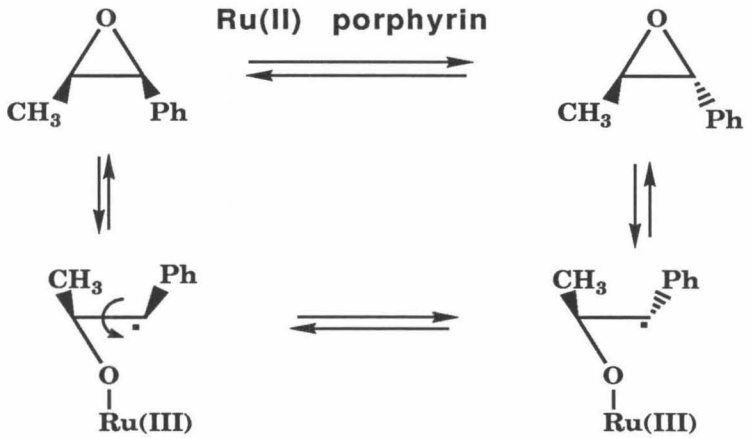


**Figure 11. Ruthenium(II) catalyzed epoxide isomerization mechanism.**

This result provides additional support for the biradical transition state intermediate proposed by Park which has sufficient time to undergo bond rotation before closing. The lower anti-to-syn ratio of insertion products for *trans*-1-phenylpropene oxide in comparison to the stilbene oxides is probably due to less steric interactions between the methyl and phenyl substituents. As a result, the diastereomers are closer in energy. As shown in Table 2, both *cis*-and *trans*-stilbene oxide yielded essentially the same ratio of diastereomers favoring the more thermodynamically stable anti insertion product. The results are also consistent with the 8% retention of *E*-stilbene obtained during deoxygenation of *cis*-stilbene oxide using a tungsten system that is postulated to proceed via a similar biradical intermediate.[14] The lower yield of the *trans*-stilbene oxide insertion product probably reflects the greater steric requirements involved for the substrate entering the *bis*(cyclopentadienyl) metal cavity. Both stilbene oxides were much more sensitive to the batch of metallacycle used than the other oxides and easily polymerized if trace aluminum compounds were present.

In the case of 1,1 diphenylethylene oxide, the absence of olefin shifts in the $^1H$ NMR indicates no deoxygenation occurred. This is significant in that this substrate with two geminal aryl groups should impart the greatest stability to a radical intermediate and thereby enhance additional types of reactivity such as deoxygenation. As shown in Figure 9, the Gibson *bis*-Cp*titanium methylidene deoxygenates styrene oxide, however, the resulting titanium product (presumably a titanium formaldehyde complex) was not characterized.[12] In the case of styrene sulfide, Park found that desulfurization occurs yielding styrene and a titanium thioaldehyde complex.[8] These results support the assumption that formation of a *bis*-Cp titanium formaldehyde complex is thermodynamically unfavorable which results in the observed insertion behavior (Scheme 3).

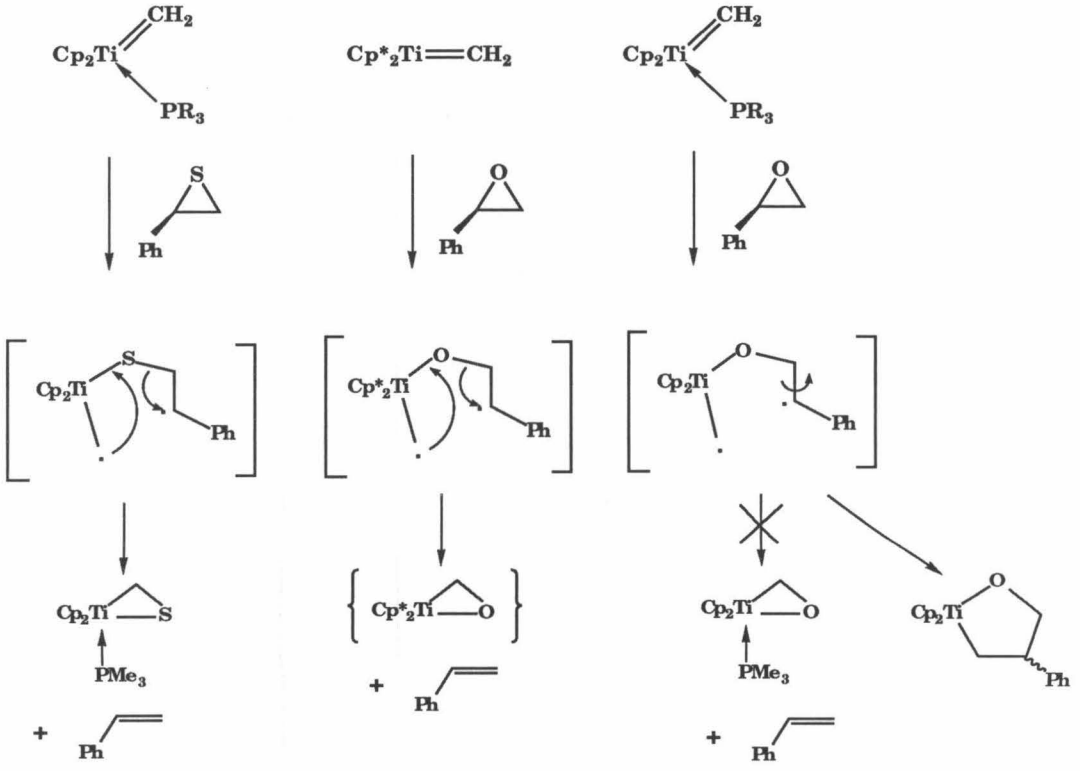


**Scheme 3. Comparison of titanium methylidene reactivity.**

**Possible Mechanism of Epoxide Insertion.** Based on all of the results observed thus far, a possible mechanism for the insertion of epoxides with titanium methylidene phosphine adducts involves a disrotatory ring opening of a titanium-epoxide adduct A to give a homoallylic conformation B (Figure 12).[13]

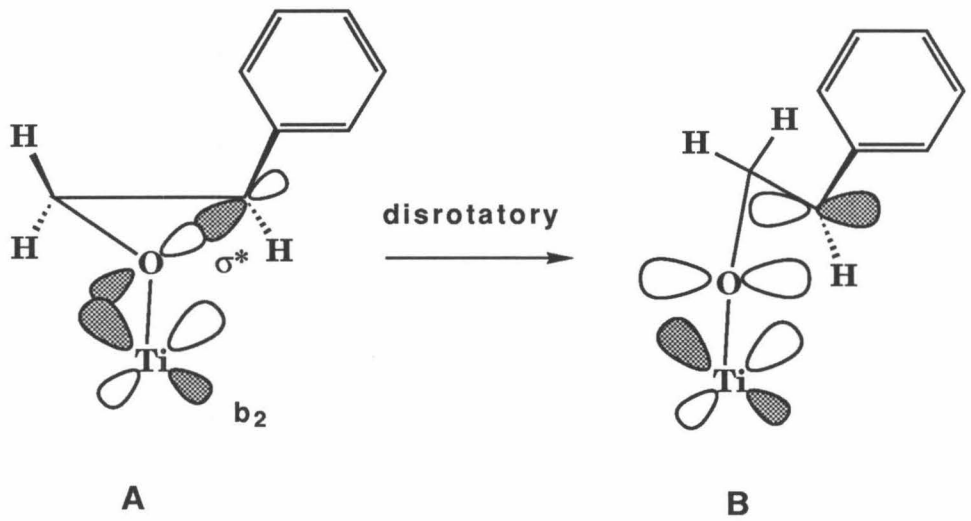


**Figure 12. Idealized orbital diagram for the disrotatory opening of titanium-epoxide adduct (A) to a homoallylic conformation (B). The oxygen p-orbital has been drawn without indicating phase inorder to emphasize nodal character.**

According to a similar mechanism proposed by Groves for the isomerization of epoxides by ruthenium(II), the epoxide oxygen of conformer B occupies a nodal position thus accommodating a biradical transition state intermediate.[13] In the orbital diagram of Figure 12, the $b_2$-orbital is suggested as interacting with the oxygen σ*-orbital, however, it is not clear which orbital would actually participate in this reaction. Assuming that the titanium atom is $d^1$, the entire process can be

considered as a metal-centered cyclopropyl carbinyl rearrangement (Figure 13)

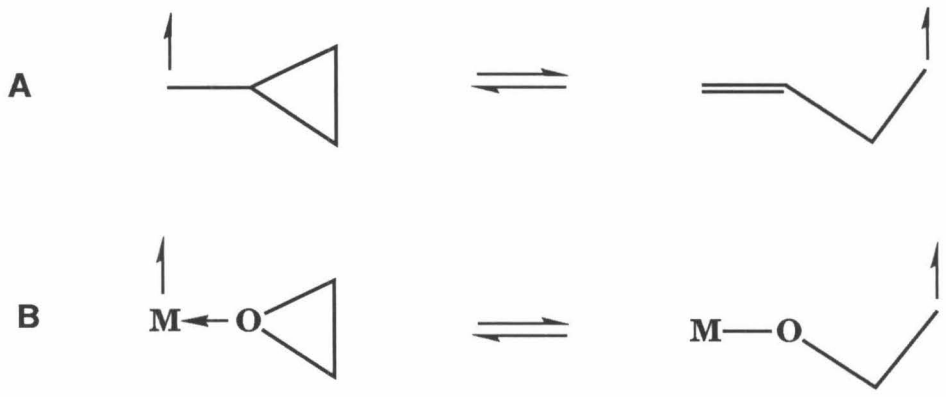


**Figure 13. Comparison of cyclopropyl carbinyl rearrangement (A) to metal-centered cyclopropyl carbinyl rearrangement (B).**

Although the titanium is usually considered to be $d^0$ in these systems, experiments reported by E. Ansyln that clearly demonstrated electron-transfer behavior suggest that the $d^1$ oxidation state is accessible with these ligated methylidene complexes.[11] Similar reactivity of titanium(III) metallocenes with epoxides has recently been reported by Nugent which involved hexenyl radical cyclizations (Figure 14).[15]

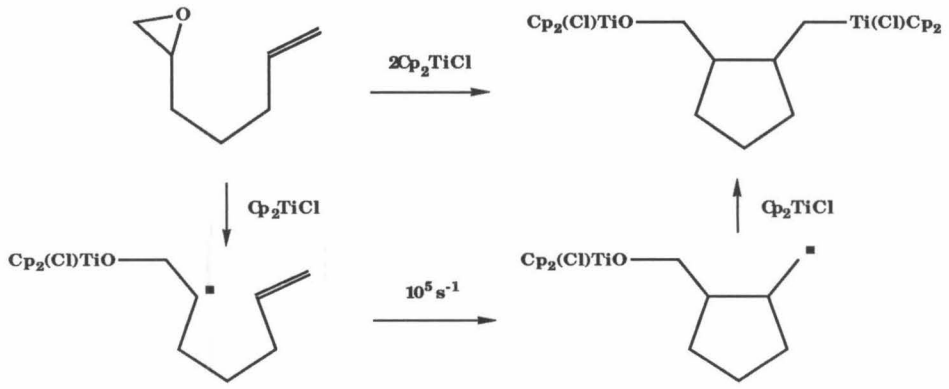


**Figure 14. Titanium(III) induced cyclization of epoxyolefins.**

**One-Pot γ-Lactone Synthesis.** In order to form γ-lactones, carbonylation of **5a** at mild pressure yields the corresponding CO insertion complexes with high conversion (eq 6).

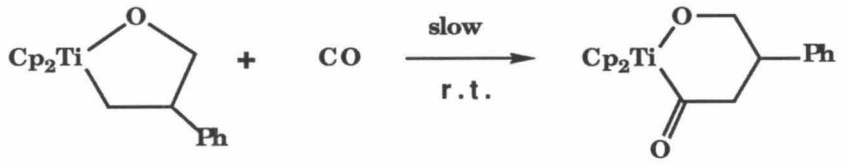


**5a** **7a** (6)

The iodine treatment method of complex **7a** reported by Park[8] to give the γ-lactone **8a** provided unsatisfactory yields on larger scales. This is probably a result of the readily accessible +3 oxidation state of titanium, which in the presence iodine, results in radical by-products. Two superior methods of oxidative cleavage were treatment of complex **7a** with DDQ or dioxygen, the latter giving the cleanest workup (eq 7).

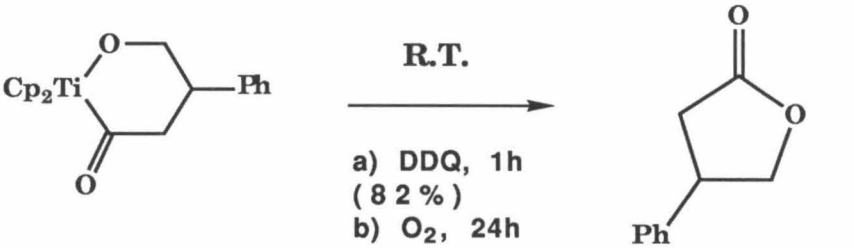


**7a** **8a** (7)

After purification via flash chromatography, the γ-lactone **8a** was fully characterized and displays a highly symmetric $^1$H NMR spectrum (Figure 15).

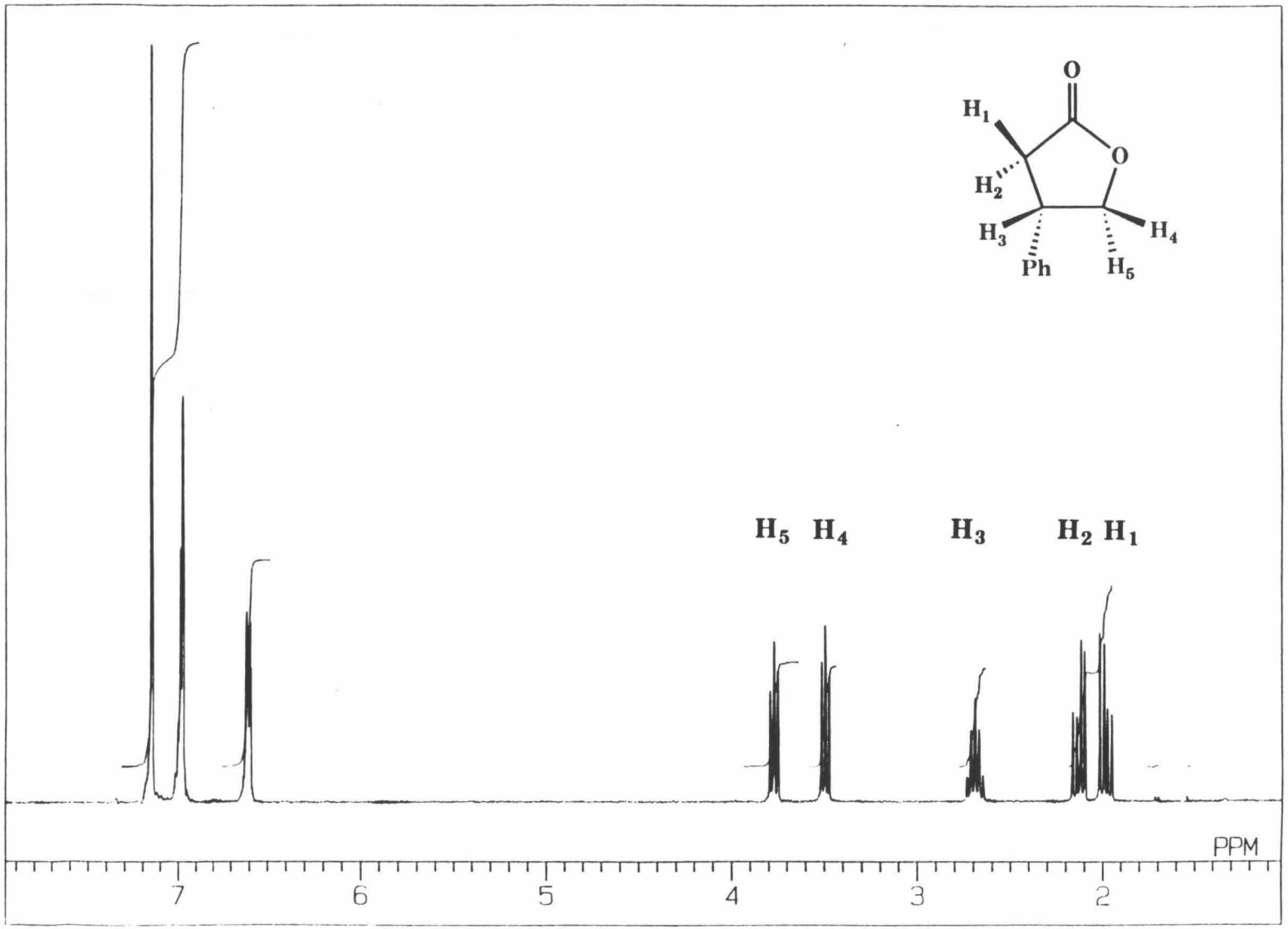


Figure 15. $^{1}H$ NMR spectrum of γ-lactone (8a).

In an attempt to broaden the scope of the method, various titanocene-alkylidenes were screened for reactivity. However, none of these provided epoxide insertion products (Figure 16).

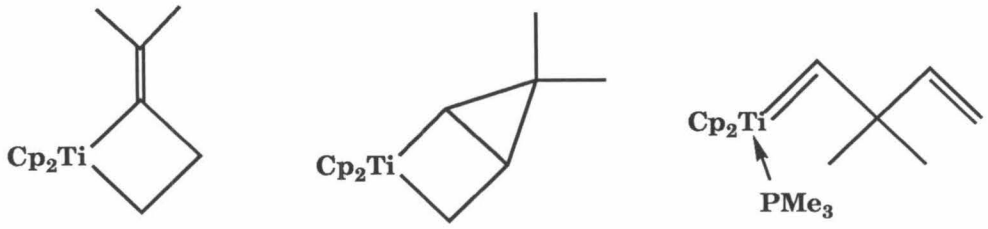


3d 3e 9

**Figure 16. Sources of substituted titanium alkylidenes.**

**Summary.** In summary, titanacyclobutanes, in the presence of catalytic amounts of trimethylphosphine, undergo facile insertion of aryl substituted epoxides. The diastereoselectivity, as well as deuterium labeling studies, support a biradical transition state intermediate as part of a metal-centered cyclopropyl carbinyl rearrangement mechanism. As a result of the radical intermediate, epoxides without radical stabilizing functional groups do not give insertion products. Carbonylation of epoxide insertion products followed by oxidative cleavage using dioxygen affords the corresponding γ-lactone in moderate to good yield. The method works with various β-substituted titanacyclobutanes at temperatures from 0 °C to 60 °C, however, no insertion is observed with α-substituted titanacyclobutanes. These results demonstrate a new facet of titanium methylidene chemistry.

## Experimental Section

**General Considerations.** All air-sensitive manipulations were carried out under argon using standard Schlenk techniques or in a nitrogen filled glove box (Vacuum Atmospheres DC-882) equipped with MO-40-1 purification train, DK-3E Dri-Kool conditioner, and Dri-Cold freezer. Flash chromatography was performed by the procedure of Still *et al.*,[16] using silica Woelm 32-63 (32-63 mm). Thin layer chromatography was performed on EM Reagents 0.25 mm silica gel 6-f plates and visualized with iodine vapor or *p*-anisaldehyde dip. Argon was purified by passage through columns of BASF RS-11 (Chemlog) catalyst and Linde 4Å molecular sieves. Benzene, diethyl ether, hexane, pentane (HPLC grade), THF, toluene, and NMR solvents were stirred over $CaH_2$ and transferred onto sodium benzophenone ketyl. All solvents were vacuum transferred and stored under argon in flasks equipped with teflon screw valves. Methylene chloride was dried over $P_2O_5$, vacuum transferred, and degassed by successive freeze-thaw pump cycles. Mesitylene was dried over $CaH_2$, vacuum transferred, and stored in the drybox. Carbon Monoxide (Matheson) was used as received. NMR spectra were recorded on Varian EM-390 (90 MHz, $^1H$), Jeol FX-90Q (89.60 MHz, $^1H$), and Jeol 400GX (399.65 MHz, $^1H$; 100.4 MHz, $^{13}C$) spectrometers. Chemical shifts are reported versus residual solvent signals ($^1H$: $C_6D_6$, δ 7.15; $CDCl_3$, δ 7.24; $C_7D_8$, δ 2.09; $^{13}C$: $C_6D_6$, δ 128.0; $CDCl_3$, δ 77.0; $C_7D_8$, δ 20.9;). Data are reported as follows: chemical shift, multiplicity (s=singlet, d=doublet, t=triplet, q=quartet, m=multiplet, br=broad), coupling constant (Hz), integration, and assignment. Measurement of weight was conducted after minimizing

static interference through the use of Staticmaster ionizing unit (Nuclear Products Company). All reaction temperatures were measured externally. Elemental analysis were performed at the California Institute of Technology Analytical Facility. High resolution mass spectra were performed at the University of California, Riverside Mass Spectrometry Facility. Gas Chromatography were performed on a Shimadzu GC-mini 2 equipped with a Quadrex 50m SE-30 capillary column. Infrared spectra were recorded as nujol mulls or in solution in $CDCl_3$ on a Perkin-Elmer 1600 instrument. Styrene oxide, cyclohexene oxide, butadiene monoxide, *m*-chloroperbenzoic acid, $\alpha$-methylstyrene, trimethylsulfonium iodide, iodine, *cis*- and *trans*-stilbene oxide, (1R, 2R) (+) phenylpropene oxide, and 3,3-dimethylallene (Aldrich) were used as received. $\beta$-$\beta$-Dimethyl-titanacyclobutane, diphenylethylene oxide[17a], $\alpha$-methylstyrene oxide[17b], dimethylallenemetallacycle **3d**, and Tebbe's reagent **2** were prepared using known methods. $\beta$-*t*-butyltitanacyclobutane **3c**, dimethyl-cyclopropenemetallacycle **3e**, phosphine adduct **9**, and cyclopentanemetallacycle **3b** were gifts of T. Swager and D. Wheeler.

**General Procedure for NMR Tube Reactions.** An NMR tube was first weighed under static-free conditions in a nitrogen atmosphere. Solids were loaded into the tube, static was removed, and weight was recorded. Solvent (400 µl) was added and a latex septum was fitted onto the NMR tube and sealed with parafilm. The tube was cooled to -20 °C and trimethylphosphine and integration standards were added via syringe. The reaction vessel was then warmed to the required temperature before the appropriate epoxide was added via syringe.

**Reaction of Complex (4a) with Styrene Oxide.** $^1$H NMR analysis with internal standard indicated an 80% yield of **5a**. $^1$H NMR ($C_7D_8$) δ 7.25–7.09 (m, 5H, Ph), 5.89 (s, 5H, Cp), 5.87 (s, 5H, Cp), 4.66 (m, 1H, $H_3$), 4.45 (dd, $J_{H5H4}$ = 9.0 Hz, $J_{H5H3}$ = 11.0 Hz, 1H, $H_5$), 4.23 (ddd, $J_{H4H3}$ = 6.6 Hz, $J_{H4H5}$ = 9.0 Hz, $J_{H4H1}$ = 2.2 Hz, 1H, $H_4$), 3.10 (dd, $J_{H2H1}$ = 10.5 Hz, $J_{H2H3}$ = 12.5 Hz, 1H, $H_2$), 1.30 (ddd, $J_{H1H2}$ = 5.3 Hz, 1H, $H_1$). $^{13}$C NMR ($C_6D_6$) δ 147.8, 128.4, 127.0, 126.0, 114.5, 114.2, 81.1, 66.2, 57.2 . $^1$H NMR ($C_7D_8$) of hydrolysis product δ 7.32-7.24 (m, 5H, Ph), 3.69 (t, $J$ = 6.2Hz, 1H, $H_1$), 2.93 (m, 1H, $H_2$), 1.30 (m, 1H, $H_2$), 1.26 (d, $J$ = 6.8Hz, 3H, $H_3$), 0.89 (m, 1H, $H_4$), 0.85 (d, $J$ = 6.2 Hz, 3H, Me). $^{13}$C NMR ($C_7D_8$) δ 143.7, 128.6, 127.5, 126.7, 68.7, 42.5, 17.6.

**Reaction of Complex (4a) with (1R, 2R)-(+)-Phenylpropene Oxide.** $^1$H NMR analysis with internal standard indicated a 62% yield of **5b** with a 4:1 (anti:syn) mixture of diastereomers. $^1$H NMR ($C_7D_8$) Major isomer (*anti*) δ 7.14 (m, 5H, Ph), 5.88 (s, 5H, Cp), 5.84 (s, 5H, Cp), 5.03 (m, 1H, $H_3$), 4.73 (m, 1H, $H_4$), 3.44 (dd, $J$ = 10.3 Hz, $J$ = 13.6 Hz, 1H, $H_2$), 0.89 (m, 1H, $H_1$), 0.85 (d, $J$ = 6.2 Hz, 3H, Me). $^1$H NMR ($C_7D_8$) Minor isomer (*syn*) δ 7.14 (m, 5H, Ph), 5.90 (s, 5H, Cp), 5.88 (s, 5H, Cp), 4.60 (m, 1H, $H_3$), 4.06 (m, 1H, $H_4$), 2.96 (m, 1H, $H_2$), 1.18 (m, 1H, $H_1$), 1.08 (d, $J$ = 5.1 Hz, 3H, Me). $^1$H NMR ($C_7D_8$) of hydrolysis product (*anti*) δ 7.06 (m, 5H, Ph), 3.57 (m, 1H), 2.43 (m, 1H), 1.08 (d, $J$ = 7.1Hz, 3H, Me ), 1.01 (d, $J$ = 6.1Hz, 3H, Me). $^1$H NMR ($C_7D_8$) of hydrolysis product (*syn*) δ 7.06 (m, 5H, Ph), 3.25 (m, 1H), 2.43 (m, 1H), 1.20 (d, $J$ = 6.8Hz, 3H, Me ), 0.87 (d, $J$ = 6.4Hz, 3H, Me).

**Reaction of Complex (4a) with *trans*-Stilbene Oxide.** $^1$H NMR analysis with internal standard indicated a 13% yield of **5c** in a 9:1

(anti:syn) mixture of diastereomers. $^1$H NMR ($C_7D_8$) Major isomer (*anti*) δ 6.96 (m, 10H, Ph), 5.97 (s, 5H, Cp), 5.92 (s, 5H, Cp), 6.06 (m, 1H, $H_3$), 5.23 (m, 1H, $H_4$), 3.37 (dd, $J$ = 10.5 Hz, $J$ = 12.5 Hz, 1H, $H_2$), 0.93 (dd, $J$ = 10.5 Hz, $J$ = 5.3 Hz, 1H, $H_1$). $^1$H NMR ($C_7D_8$) Minor isomer (*syn*) δ 6.96 (m, 10H, Ph), 6.00 (s, 5H, Cp), 5.95 (s, 5H, Cp), 4.34 (m, 1H, $H_3$), 3.11 (m, 1H, $H_2$), 1.26 (m, 1H, $H_1$). $^1$H NMR ($C_7D_8$) of hydrolysis product (*anti*) δ 7.13 (m, 5H, Ph), 4.30 (d, $J$ = 7.8 Hz, 3H), 2.85 (m, 1H), 0.99 (d, $J$ = 7.1Hz, 3H, Me ). $^1$H NMR ($C_7D_8$) of hydrolysis product (*syn*) δ 7.13 (m, 5H, Ph), 4.30 (d, $J$ = 7.8 Hz, 1H), 2.85 (m, 1H), 1.24 (d, $J$ = 7.1Hz, 3H, Me ).

**Reaction of Complex (4a) with *cis*-Stilbene Oxide.** $^1$H NMR analysis with internal standard indicated a 45% yield of **5c** in a 9:1 (anti:syn) mixture of diastereomers. $^1$H NMR ($C_7D_8$) Major isomer (*anti*) δ 6.96 (m, 10H, Ph), 5.97 (s, 5H, Cp), 5.92 (s, 5H, Cp), 6.06 (m, 1H, $H_3$), 5.23 (m, 1H, $H_4$), 3.37 (dd, $J$ = 10.5 Hz, $J$ = 12.5 Hz, 1H, $H_2$), 0.93 (dd, $J$ = 10.5 Hz, $J$ = 5.3 Hz, 1H, $H_1$). $^1$H NMR ($C_7D_8$) Minor isomer (*syn*) δ 6.96 (m, 10H, Ph), 6.00 (s, 5H, Cp), 5.95 (s, 5H, Cp), 4.34 (m, 1H, $H_3$), 3.11 (m, 1H, $H_2$), 1.26 (m, 1H, $H_1$). $^1$H NMR ($C_7D_8$) of hydrolysis product (*anti*) δ 7.13 (m, 5H, Ph), 4.30 (d, $J$ = 7.8 Hz, 3H), 2.85 (m, 1H), 0.99 (d, $J$ = 7.1Hz, 3H, Me ). $^1$H NMR ($C_7D_8$) of hydrolysis product (*syn*) δ 7.13 (m, 5H, Ph), 4.30 (d, $J$ = 7.8 Hz, 1H), 2.85 (m, 1H), 1.24 (d, $J$ = 7.1Hz, 3H, Me ).

**Reaction of Complex (4a) with α-Methylstyrene Oxide.** $^1$H NMR analysis with internal standard indicated a 55% yield of **5d**. $^1$H NMR ($C_7D_8$) δ 7.28 (m, 5H, Ph), 5.91 (s, 5H, Cp), 5.67 (s, 5H, Cp), 4.63 (d, $J$ = 9.5Hz, 1H, $H_4$), 4.35 (d, $J$ = 9.5Hz, 1H, $H_3$), 2.25 (d, $J$ = 10.7Hz, 1H, $H_1$), 2.02 (d, $J$ = 11.0Hz, 1H, $H_2$), 1.44 (s, 3H, Me). $^1$H NMR ($C_7D_8$) of hydrolysis product δ 7.14 (m, 5H, Ph), 3.31 (s, 2H), 1.15 (s, 2H).

**Reaction of Complex (4a) with Diphenylethylene Oxide.** $^1$H NMR analysis with internal standard indicated a 31% yield of **5e**. $^1$H NMR ($C_7D_8$) δ 7.20 (m, 10H, Ph), 5.74 (s, 10H, Cp), 4.72 (s, 2H, $H_3$,$H_4$), 2.57 (s, 2H, $H_1$,$H_2$). $^1$H NMR ($C_7D_8$) of hydrolysis product δ 7.14 (m, 10H, Ph), 3.31 (s, 2H), 1.15 (s, 6H, 2Me).

**Carbon Monoxide Insertion of Complex (5a).** When complex **5a** was allowed to react with excess carbon monoxide overnight, color of the solution changed to purple. The insertion product **7a** is not susceptible to decarbonylation under vacuum. $^1$H NMR ($C_6D_6$) δ 7.24–7.08 (m, 5H, Ph), 5.83 (s, 5H, Cp), 5.73 (s, 5H, Cp), 4.57 (dd, 1H), 4.28 (t, 1H), 2.97 (m, 1H), 2.7–2.5 (m, 2H). $^{13}$C NMR ($CD_2Cl_2$) δ 248, 141.3, 128.2, 127.3, 126.3, 113.0, 112.0, 83.1, 56.3, 46.3.

**One-Pot Synthesis of γ-Lactone (8a).** A 10 ml Schlenk flask was charged with 0.116 mg (0.47mmol) of titanocene metallacycle **3a** under a nitrogen atmosphere. After cooling to -20 °C, 10 ml of dry toluene and 4.5 μl (0.047 mmol) of trimethylphosphine were added via syringe. The temperature was raised to 0 °C and 56 μl (0.47 mmol) of styrene oxide were slowly added. After warming to room temperature and stirring 2 hours, the deep-red solution was transferred to a Fischer-Porter bottle and pressurized with CO ( 50psi). After stirring 12 hours, the purple-brown solution was exposed to an atmosphere of oxygen for an additional 24 hours at 25 °C. The solution was passed through a pad of silica gel and, after careful concentration *in vacuo*, yielded 40 mg (57%) of essentially pure product . The product was purified by prep GC and analyzed by $^1$H NMR, $^{13}$C NMR, IR, and High Resolution Mass Spectroscopy. $^1$H NMR ($CDCl_3$) δ:

7.16 (m, 5H, Ph), 4.54 (dd, $J_{H5H4}$=9.0Hz, $J_{H4H3}$=8.0Hz, 1H, H5), 4.14 (dd, $J_{H4H5}$=9.0Hz, $J_{H4H3}$=8.0Hz, 1H, H4), 3.66 (m, 1H, H3), 2.79 (dd, $J_{H2H1}$=17.5Hz, $J_{H2H3}$=8.8Hz, 1H, H2), 2.55(dd, $J_{H1H2}$=17.5Hz, $J_{H1H3}$=8.6Hz, 1H, H1), $^{13}$C NMR ($CDCl_3$) δ: 176.4, 139.4, 129.1, 127.7, 126.7, 74.0, 41.1, 35.7. IR: ($CDCl_3$) 1775 $cm^{-1}$ ( C=O stretch, γ-lactone). An exact mass determination gave m/e=162.0672 (calcd for $C_{10}H_{10}O_2$, 162.0681).

## References and Notes

1. (a) Tebbe, F. N.; Parshall, G. W.; Ovenall, D. W. *J. Am. Chem. Soc.* **1979**, *101*, 5074-5075. (b) Klabunde, U.; Tebbe, F. N.; Parshall, G. W.; Harlow, R. L. *J. Mol. Catal.* **1980**, *8*, 37-51.

2. Howard, T. R.; Lee, J. B.; Grubbs, R. H. *J. Am. Chem. Soc.* **1980**, *102*, 6876-6878.

3. Lee, J.B. Gajda, G.J.; Schaefer, W.P.; Howard, T.R.; Ikariya, T.; Straus, D.A.; Grubbs, R.H. *ibid.* , **1981**, *103*, 7358.

4. (a) For review, see Brown-Wensley, K. A.; Buchwald, S. L.; Cannizzo, L. F.; Clawson, L. E.; Ho, S.; Meinhart, J. D.; Stille, J. R.; Straus, D. A.; Grubbs, R. H. *Pure Appl. Chem.* **1983**, *55*, 1733-1744. (b) Lee, J. B.; Ott, K. C.; Grubbs, R. H. *J. Am. Chem. Soc.* **1982**, *104*, 7491-7496. (c) Ansyln, E. V.; Grubbs, R. H. *ibid.* **1987**, *109*, 4880-4890. (d) Mackenzie, P. B.; Ott, K. C.; Grubbs, R. H. *Pure Appl. Chem.* **1984**, *56*, 59-61. (e) Buchwald, S. L.; Ansyln, E. V. ; Grubbs, R. H. *J. Am. Chem. Soc.* **1985**, *107*, 1766-1768. (f) Ho, S. C.; Strauss, D. A.; Grubbs, R. H. *ibid.*. **1984**, *106*, 1533-1534.

5. Gilliom, L. R.; Grubbs, R. H. *ibid.*. **1986**, *108*, 733-742.

6. (a) Cannizzo, L.F.; Grubbs, R.H. *Macromolecules* **1987**, *20*, 1488. (b) Wheeler, D.R.; Risse, W.K.; Grubbs, R.H. *Macromolecules*, **1989**, *22*, 3205-3210.

7. Meinhart, .J D.; Anslyn, E.V.; Grubbs, R.H. *Organometallics* **1989**, *8(3)*, 583-9.

8. Park, J. W., Ph. D. Thesis, California Institute of Technology, Pasadena, California, 1989.

9. For examples of early transition-metal formaldehyde complexes, see (a) Green, M. L. H.; Parkin, G. *J. Chem. Soc., Chem. Commun.* **1986**, 90-91. (b) Gambarotta, S.; Floriani, C.; Chiesi-Villa, A.; Guastini, C. *J. Am. Chem. Soc.* **1982**, *104*, 2019-2020. (c) Threlkel, R. S.; Bercaw, J. E. *ibid.* **1981**, *103*, 2650-2659.

10. For conventional methods for the preparation of γ-lactones from alkenes, see (a) Heiba, E. I.; Dessau, R. M., Rodewald, P. G. *J. Am. Chem. Soc.* **1974**, *96*, 7977-1981. (b) Das Gupta, T. K.; Felix, D.; Kempe, U. M.; Eschenmoser, A. *Helv. Chim. Acta* **1972**, *55*, 2198-2205. (c) Boldt, P.; Thielecke, W.; Etzemüler, J. *Chem. Ber.* **1969**, *102*, 4157-4163.

11. Anslyn, E.V., Ph. D. Thesis, California Institute of Technology, Pasadena, California, 1987.

12. Gibson, C. P.; Dabbagh, G.; Bertz, S. H. *J. Chem. Soc., Chem. Commun.* **1988**, 603-605.

13. Groves, J. T.; Ahn, K.H.; Quinn, R. *J. Am. Chem. Soc.* **1988**, *110*, 4217-4220.

14. a) Sharpless, K.B.; Umbreit, M.A.; Neih, M.T.; Flood, T.C. *J. Am. Chem. Soc.* **1972**, *94*, 6538. b) McMurry, J.E.; Silvestri, M.G.; Flemming, M.P.; Holtz, T.; Grayston, M.W. *J. Org. Chem.* **1978**, *43*, 3249. c) Hayasi, Y.; Schwartz, J. *Inorg. Chem.* **1981**, *20*, 3473-3476. d) Sato, M.; Oshima, K. *Chem. Lett.* **1982**, 157.

15. Nugent, W.A.; RajanBabu, T.V. *J. Am. Chem. Soc.* **1989**, *110*, 8561-8562.

16. Still, W.C.; Kahn, M.; Mitra, A. *J. Org. Chem.* **1978**, *43*, 2923-2925.

17. a) Corey, E.J.; Chaykovsky, M. *J. Am. Chem. Soc.* **1965**, *87*, 1353. b) Camps, F.; Coll, J.; Messeguer, A.; Pericas, M.A. *Tetrahedron Lett.* **1981**, *22*, 3895-3896.

# CHAPTER 3

## New Applications of Magnesium Chloride Supported Titanium Catalysts : Catalytic Lewis Acid Condensation of Enol Silanes with Aldehydes

## Introduction

Since its discovery, the Lewis acid mediated reaction of enol silanes with aldehydes (Mukaiyama reaction) has attracted the interest of synthetic organic chemists and has provoked considerable research and interpretation (eq 1).[1]

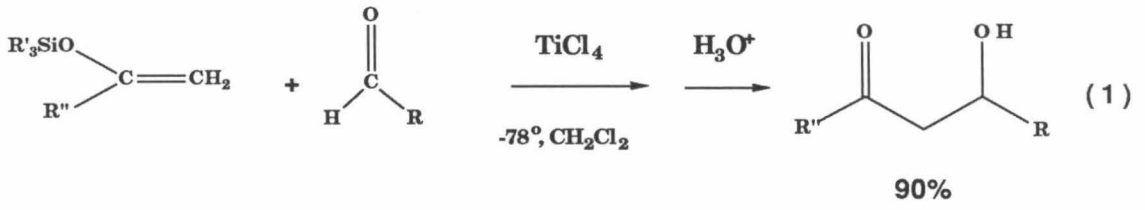


(1)

The basic method uses titanium tetrachloride as the Lewis acid and affords high yields of aldol product upon hydrolysis.[1] This method, however, generally shows little diastereoselectivity with prochiral aldehydes and prochiral enol silanes.[2] The mechanism of the Mukaiyama reaction has been the subject of much debate with cyclic 6 member, cyclic 8 member, and open transition states being proposed (Figure 1).[1,2,3]

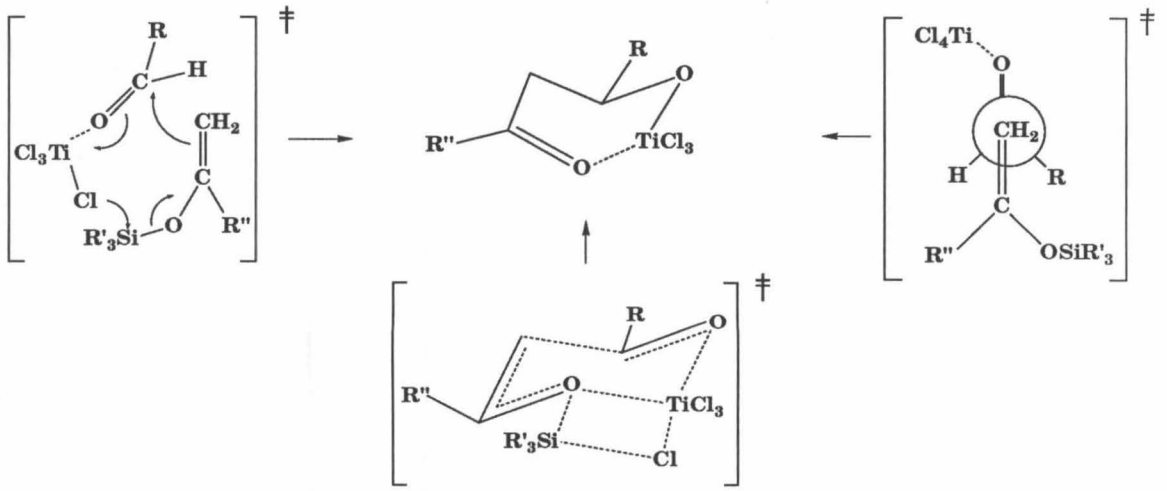


**Figure 1. Mukaiyama reaction transition states.**

Experimental evidence has been reported which support both cyclic chair transition states[4] as well as open transition states.[2,5] The reaction can be catalyzed with other Lewis acids such as boron trifluoride etherate, tin tetrachloride, and dialkylaluminum chlorides, however, titanium tetrachloride consistently gives the best yields.[1] The condensation of enol silanes with carbonyl compounds can also be anionically catalyzed by fluoride ion with varying degrees of diastereoselection (Figure 2).[6]

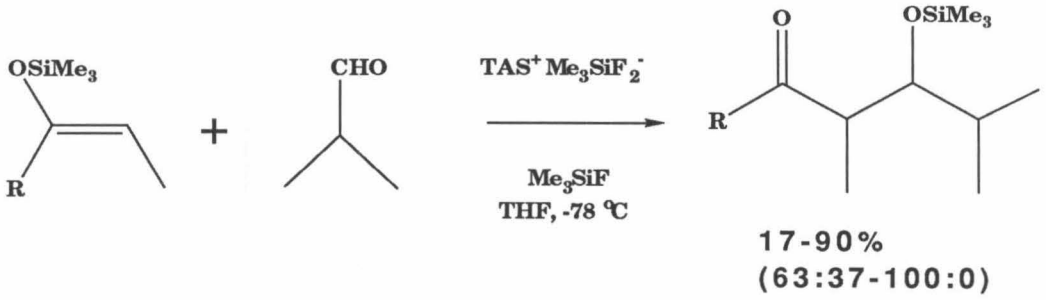


**Mechanism**

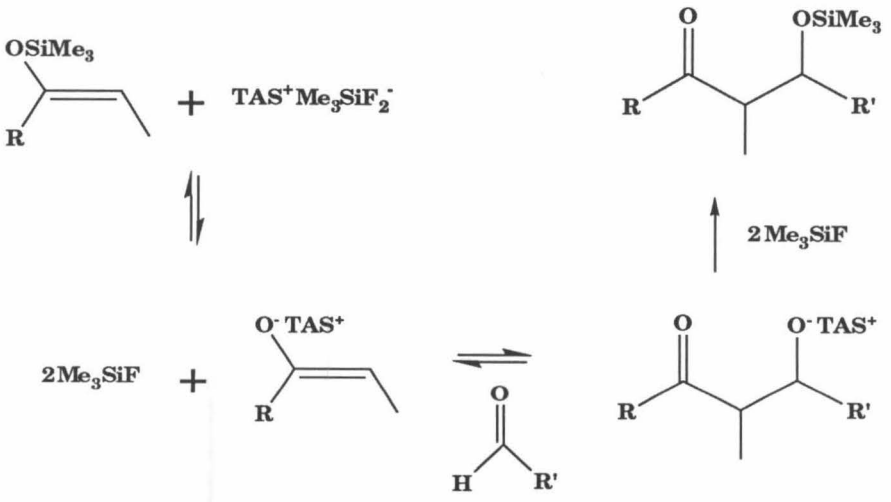


TAS =tris(diethylamino)sulfonium

**Figure 2. Fluoride catalyzed Mukaiyama reaction.**

In order to enhance the diastereoselectivity and enantioselectivity of the Lewis acid catalyzed Mukaiyama reaction, researchers have exploited the chelation ability of certain bifunctional substrates with titanium.[7] Figure 3 illustrates some examples of chelation controlled selectivities.

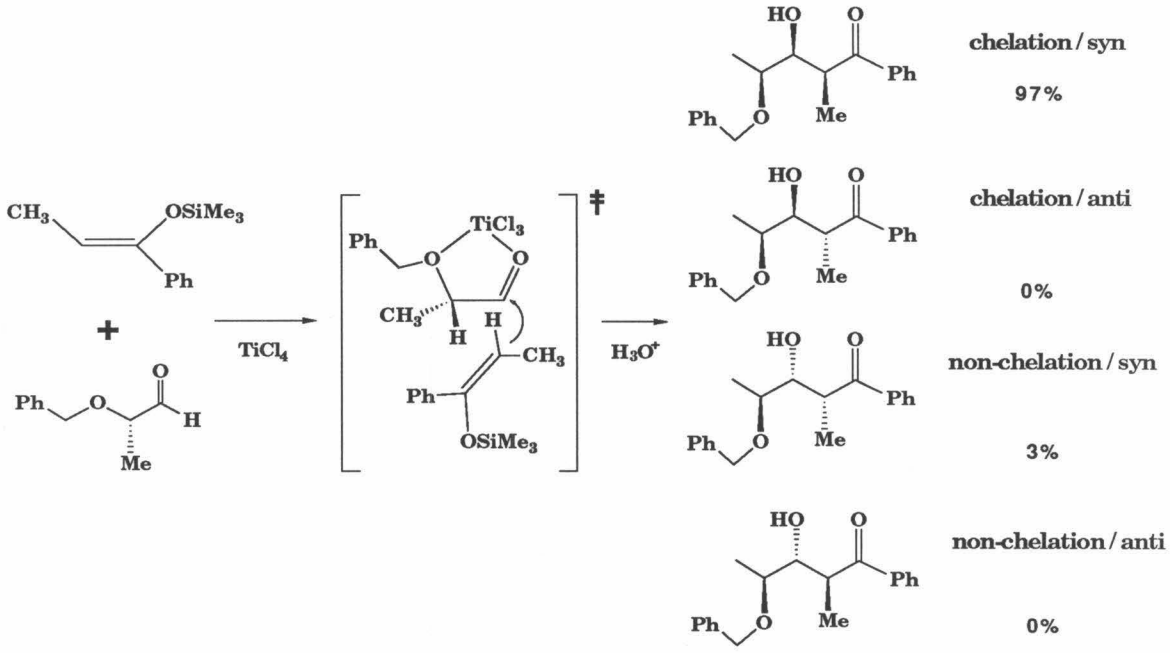


**Figure 3 . Chelation controlled Mukaiyama reaction.**

The basic Mukaiyama reaction is stoichiometric in titanium tetrachloride and is believed to form titanium enolates which are ultimately hydrolyzed.[1] Enolate formation is driven by the high oxophilicity of titanium with the generation of by-product chlorotrimethylsilane. By using less oxophilic Lewis acids, group transfer of the silyl group between oxygen atoms is facilitated with the formation of silylated aldol products and regeneration of the catalyst. Based on this concept, some researchers have explored catalytic condensations using chiral Lewis acid catalysts (Figure 4).[8]

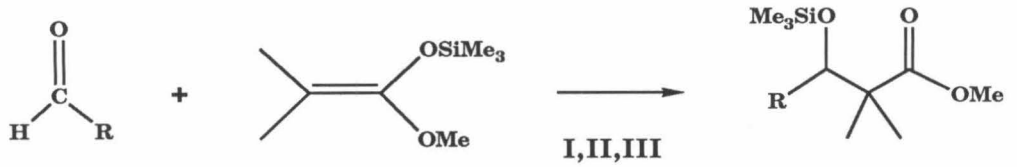


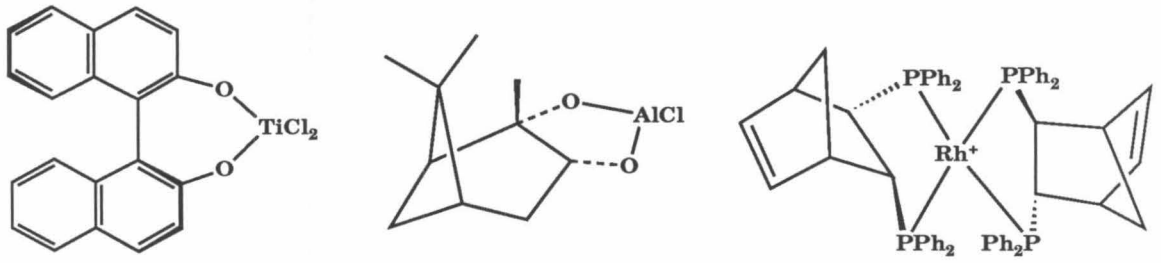


I II III

| Catalyst | Yield | ee |
|---|---|---|
| I | 60 % (R=*i*-pr) | 8 % |
| II | 15 % (R=*i*-pr) | 66 % |
| III | 75 % (R=Ph) | 12 % |

**Figure 4. Chiral Lewis acid Mukaiyama catalysts.**

Although the selectivities are low, the reactions demonstrate some degree of catalytic activity.[8] Expanding on this concept, chemists at Du Pont Central Research have developed a polymerization method for methylmethacrylate that exhibits living behavior.[9] Both Lewis acid and bifluoride catalysis have been used with the latter giving the best results (eq 2).[9]

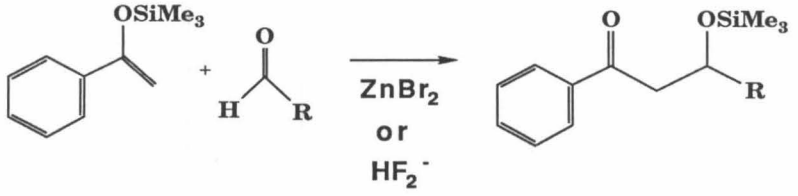


(2)

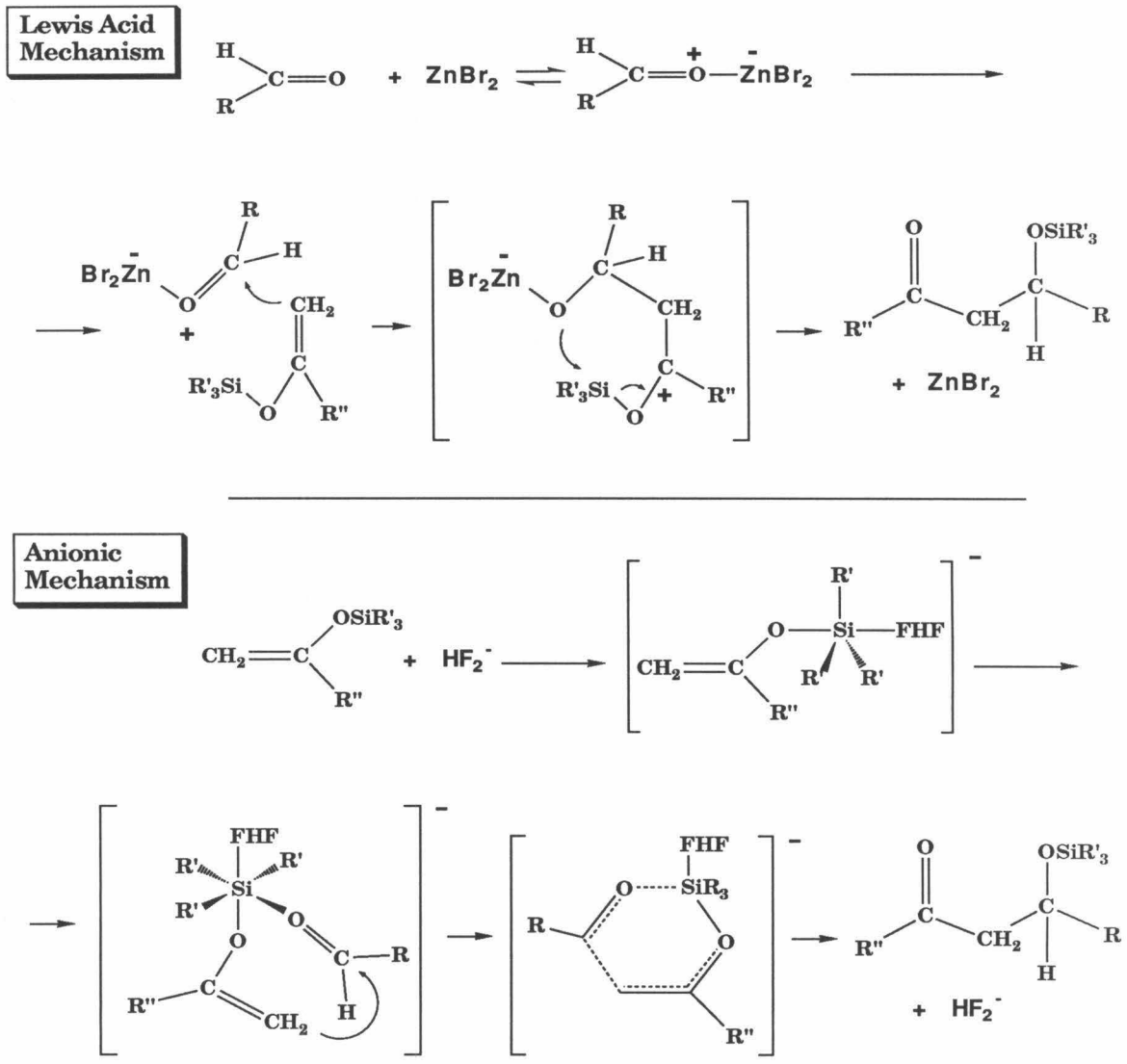


**Scheme 1. Lewis acid and anionic catalyzed group transfer aldol condensations.**

Supported Lewis acids that have been developed for Ziegler-Natta polymerization catalysts may provide alternative catalysts for group transfer aldol chemistry.[10] The interaction of titanium tetrachloride with a magnesium chloride support may offer a way of preventing enolate formation while still retaining sufficient Lewis acidity for catalytic group

tranfer aldol condensations. In addition, based on the ability of supported catalyst systems to impart tacticity to polymers such as polypropylene through active site geometry, stereoselectivity with the aldol reaction may be possible.[10]

Magnesium chloride supported titanium catalysts have been developed over the last 15 years with current examples affording polypropylene in high yield and with low molar mass molecular weights.[10] It is believed that the ability of such catalysts to give mostly isotactic polymer results from the structure of the magnesium chloride crystallite (Figure 5).[11]

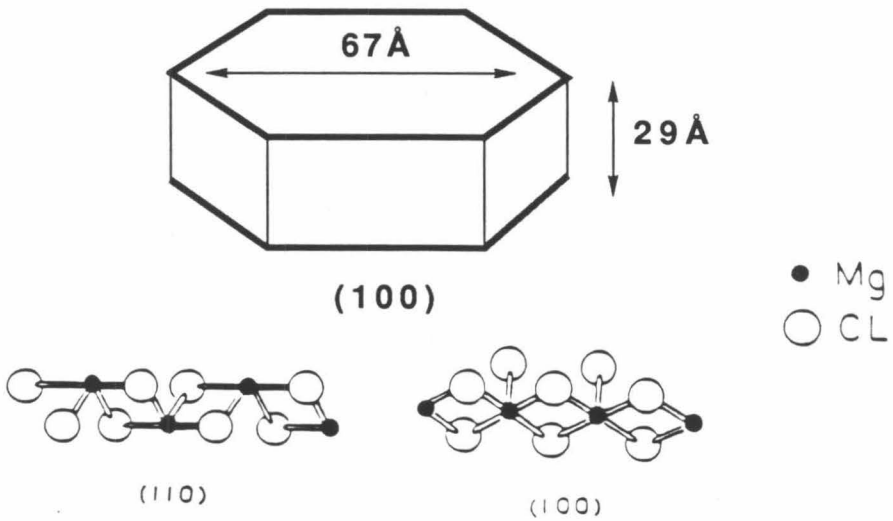


**Figure 5. Magnesium chloride crystallite structure with detail of edge defects.**

Magnesium atoms with both one and two open coordination sites are present in a 1:1 mixture on the edges of the crystallite.[11] In order to obtain a high concentration of such defects, a highly disordered magnesium chloride is required. Both physical methods, such as intensive ball milling, and chemical methods, such as addition of silicon tetrachloride (a chlorinating reagent) to magnesium Grignard compounds, are used to

obtain highly disordered magnesium chloride.[11] Treatment of the magnesium chloride support with titanium tetrachloride results in attachment of titanium chloride molecules onto the open sites of edge magnesium atoms (Figure 6).[11]

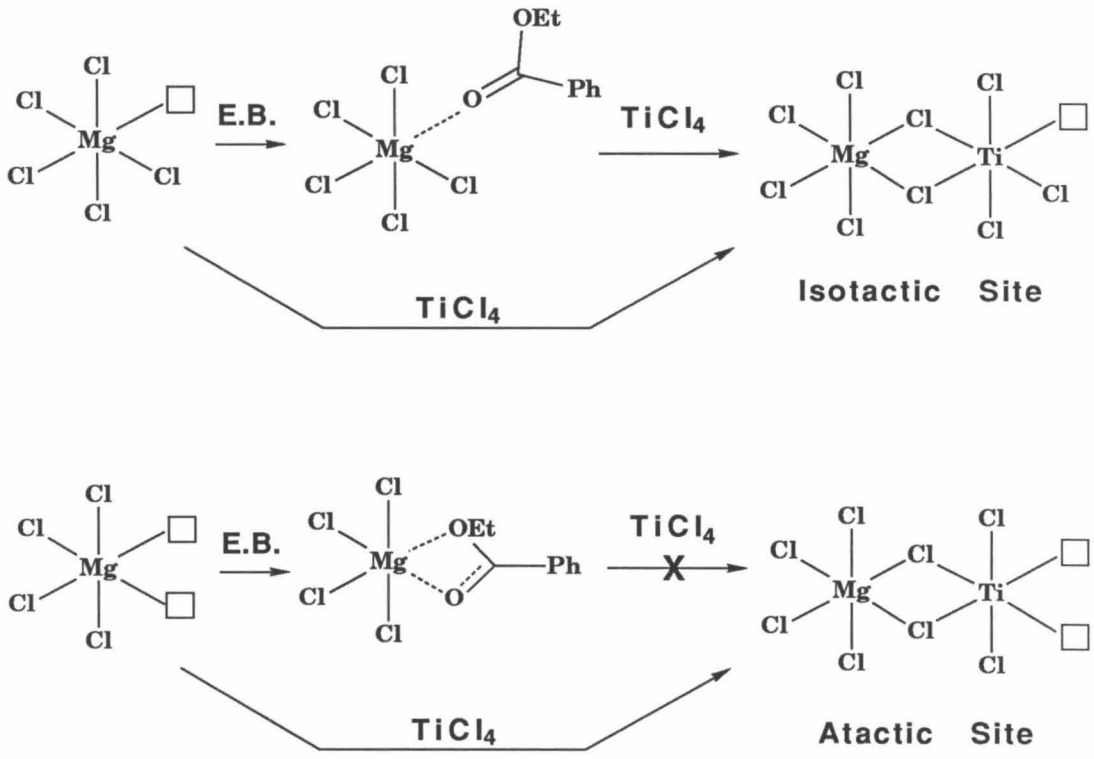


**Figure 6. Preparation of isotactic catalysts via ethyl benzoate (E.B.) selective poisoning.**

It has been postulated that titanium atoms with two coordination sites are responsible for atactic polymerization while single site atoms result in isotactic polymerization.[11] Introduction of internal modifiers, usually a Lewis base such as ethyl benzoate, before titanium tetrachloride treatment results in the formation of isotactic catalysts.[10,11] Researchers have shown that the Lewis base coordinates weakly with single open-site magnesium atoms, but binds strongly to the two-site atoms via bidentate ligation.[12]

In addition to internal modifiers, cocatalysts such as alkyl aluminums and Lewis bases are added during later phases of catalyst preparation.[10] Although some evidence supports the basic ideas about the function of modifiers, other results clearly indicate a more complicated interaction between the catalyst components.[10]

This chapter describes efforts to catalyze silyl group transfer aldol condensations with magnesium supported titanium tetrachloride polypropylene catalysts and assess the potential for diastereo- and enantioselection with various catalyst modifications.

## Results And Discussion

Initially, magnesium supported titanium catalysts were screened for catalytic activity of the Mukaiyama reaction. The condensation of propiophenone derived enol silane **1** with various aldehydes (Figure 7) was chosen as the model reaction because of the documentation of its reactivity and selectivity[13] and the facile characterization of the resulting diastereomeric products.

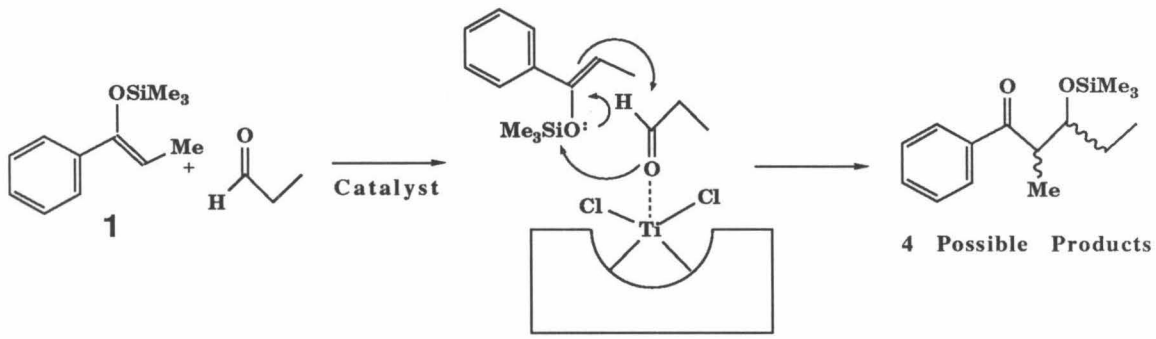


**Figure 7. Supported catalyst model reaction.**

Due to the difficulty in preparing supported catalysts with reproducible properties, a number of isotactic polypropylene catalysts were generously supplied by the Sumitomo Chemical Company.[14] As a result of the confidential nature of catalyst composition, only the titanium content was reported to us. Because the Mukaiyama reaction gives optimum yields and selectivities at -78 °C in methylene chloride[1a] and due to the compatibility of the supported catalysts with this solvent, these conditions were used for catalyst screening with the model reaction. Table 1 summarizes the results of adding a 15 fold excess of reactants to the various catalysts.

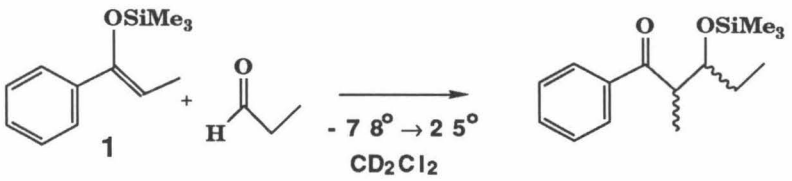


| Catalyst | #Turnovers |
|---|---|
| (A) $TiCl_3$ A.A. | 13 |
| (B) $TiCl_3(AlCl_3)_x(R_2O)_y$ | 8 |
| (C) $TiCl_4$ + EB + $MgCl_2$ | 4 |
| (D) $TiCl_4$ + DiBP + $MgCl_2$ | 1.6 |
| (E) $TiCl_2OR(R_2O)_x(MgCl_2)_y$ | 1 |
| (F) $TiCl_3H$ | 0 |
| (G) $TiCl_4$ | 0 |
| (H) $MgCl_2$ | 0 |

A.A.: active aluminum, EB: ethyl benzoate, DiBP: dibutyl phthalate

**Table 1. Magnesium chloride supported titanium catalyst screening using enol silane (1) and propionaldehyde.**

The reactions were monitored by $^1H$ NMR after warming to room temperature. The number of turnovers were determined by comparing the yield of products to the concentration of theoretical active sites.[15] In all cases, the reactions were complete at room temperature with inactivation of the catalyst. The catalyst based on titanium tetrachloride reduced by active aluminum showed the highest number of turnovers. A similar catalyst

with added alkyl ether also showed catalytic activity. The simplest supported catalyst using ethyl benzoate as the internal modifier demonstrated 4 catalytic turnovers. The same type of catalyst with dibutyl phthalate as the internal modifier gave only 2 turnovers. An alkoxide catalyst showed low activity, whereas titanium tetrachloride reduced by hydrogen, titanium tetrachloride, and the magnesium support as catalysts showed no catalytic activity. These results are significant in that they clearly demonstrate that the titanium-magnesium-ethyl benzoate interaction retards the normal mechanism of enolate formation in the Mukaiyama reaction and allows silyl group transfer to occur. The catalysts, however, eventually lose activity with the production of chlorotrimethylsilane in about a one to one ratio to the calculated number of active sites.[15] This may indicate that titanium enolate formation is a major pathway of catalyst deactivation either from starting material or from the group transfer product. This result also supports the calculation of the number of titanium sites on the surface of the catalyst.[15]

Before further investigations could be carried out, a selection of the most suitable catalyst was needed. Although the screening results show that the titanium trichloride (A.A.) catalyst gave the highest number of turnovers, certain problems were discovered with this system. Because the selectivity of these catalysts stems from their physical structure, a truly heterogeneous system is required.[10] Addition of 1 equivalent of dimethylaminopyridine (DMAP), a strong binding titanium ligand, to the titanium trichloride (A.A.) catalyst in methylene chloride resulted in the formation of at least two soluble titanium species as observed by $^{1}H$ NMR. In addition, the catalyst contains 30% aluminum, an excellent Lewis acid,

thus, it would be difficult to ascertain whether titanium or aluminum or both are responsible for catalysis in this system. In contrast, the $MgCl_2 \cdot TiCl_4$·E.B. system displayed no soluble titanium species with DMAP and contains only one type of Lewis acid. As a result, this system was selected as the initial catalyst for further experiments.

A number of control reactions and experiments were carried out in order to learn more about the basic system. As with the original Mukaiyama reaction, methylene chloride gives the highest yields. The diastereoselectivity is, however, opposite that of the original reaction with the anti isomer being the preferred product. This may be a result of the catalyst surface inhibiting the cyclic chair transition state which is believed responsible for the syn selectivity with titanium tetrachloride.[1] The diastereoselectivity was insensitive to temperatue and reaction time. In addition, the overall diastereoselectivity is marginal which may indicate that the pre-coordination of the aldehyde occurs with the carbonyl carbon positioned away from the catalytic site. In polypropylene polymerization, the alkene is bound in an $\eta^2$-coordination mode before insertion thus maintaining a close proximity to the catalytic site (Figure 8).[10]


**Figure 8. Suggested substrate binding modes for aldehydes (A) versus olefins (B).**

$^1$H NMR also reveals information about the effects of the reactants on the catalyst. Aldehydes are stronger $\eta^1$ binding titanium ligands than esters. The $^1$H NMR of the reaction mixture after aldehyde addition shows ethyl benzoate in solution. However, due to the complexity of the catalyst, it cannot be absolutely determined whether the ethyl benzoate was displaced from a titanium site or from a magnesium site. Also, after the reaction is complete, propiophenone is formed. This is most likely a result of desilylation of the enol silane starting material by the catalyst, however, it is unclear what the proton source is in this reaction. Addition of a large excess (>100 mol %) of either aldehyde or enol silane to the catalyst results in deactivation. In the case of aldehydes, deactivation is probably a result of dissolution of the catalyst surface by excess polar substrate. With enol silanes, trace impurities such as water or titanium enolate formation may contribute to catalyst deactivation. As a result of these observations, a series of enol silanes and aldehydes were examined at a 10 fold excess in order to optimize the number of turnovers and diastereoselectivity. These are illustrated in Table 2.

| Enol Silane | Aldehyde | Product | #Turn/anti:syn |
|---|---|---|---|
| 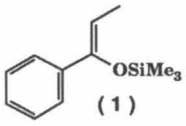 (1) | 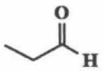 | 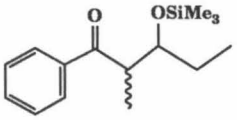 3a | 3.8 (2:1) |
| 1 | 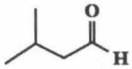 | 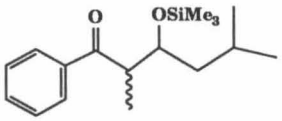 3b | 4.0 (2:1) |
| 1 | 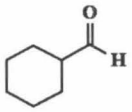 | 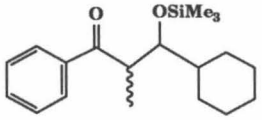 3c | 6.0 (3:1) |
| 1 | 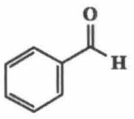 | 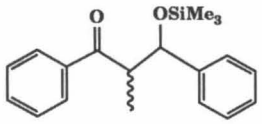 3d | 6.6 (1.5:1) |
| 1 | 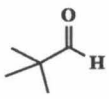 | | N.R. |
| 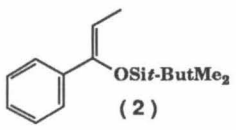 (2) | 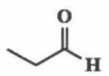 | 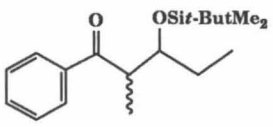 3e | 8.0 (1:1) |
| 2 | 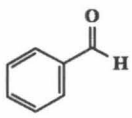 | 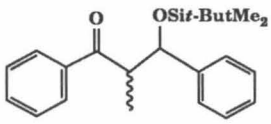 3f | 9.2 (1:1.7) |

**Table 2. Reaction of enol silanes (1) and (2) with aldehydes using catalyst (C).**

It appears that increasing the size of the aldehyde alkyl substituent group results in only a slight increase in diastereoselectivity. In the case of benzaldehyde, the trend is reversed, possibly because of favorable π-stacking interactions between phenyl rings. The number of turnovers is greater with benzaldehyde than with some of the alkyl aldehydes. This may reflect the higher reactivity of benzaldehyde. Based on the assumption that

titanium enolate formation is a dominant pathway for catalyst deactivation, substitution of a less labile silyl group, such as *t*-butyldimethylsilyl, should reduce side reactions and increase the number of turnovers. This proved to be the case with the *t*-butyldimethylsilyl enol ether of propiophenone giving the highest number of turnovers with either propionaldehyde or benzaldehyde. This enol silane, though, gives the opposite diastereoselectivity than the trimethylsilyl enol ether in the reaction of benzaldehyde. One possible explanation involves considering the staggered, open transition states for this reaction (Scheme 2).[2]

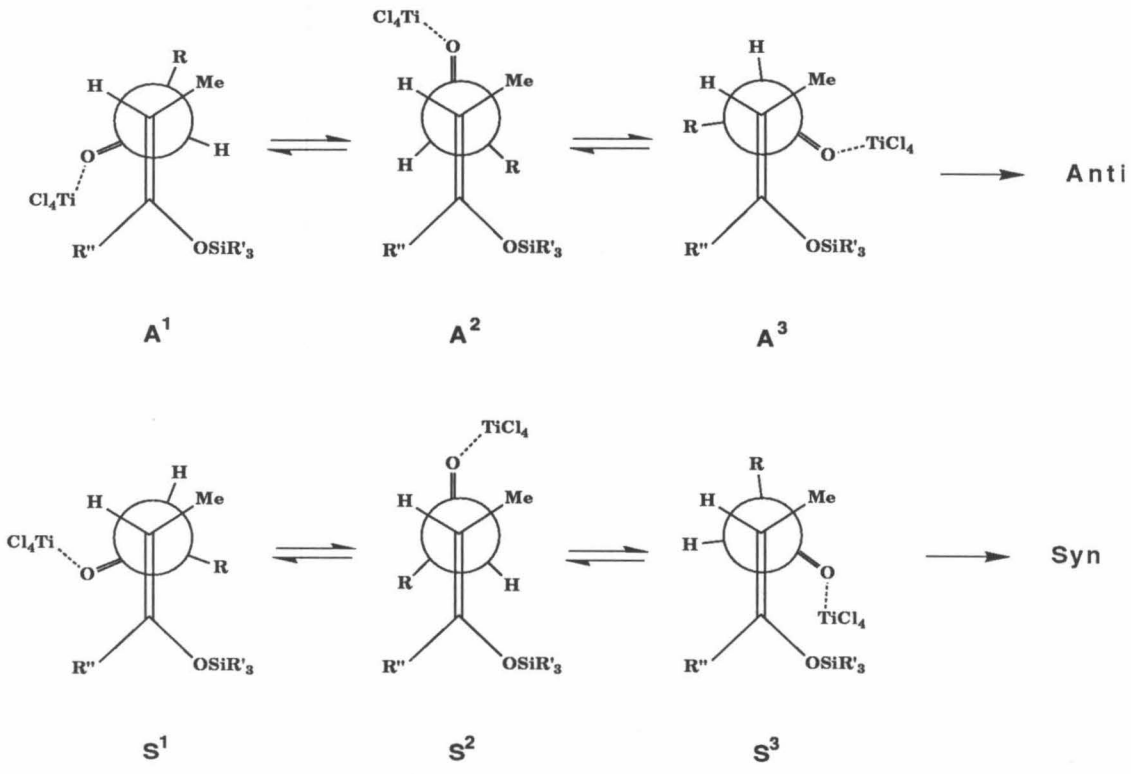


**Scheme 2. Staggered transition states for the reaction of enol silanes with aldehydes.**

In this scheme, it is assumed, as a result of sterics, that the titanium tetrachloride occupies a coordination site on the oxygen that is cis to the aldehyde hydrogen.[2] Transition states **A3** and **S3** should be *disfavored* by

the unfavorable dipole-dipole interactions of the two carbon-oxygen bonds.[16] Transition state **A**[1] is probably not important due to the steric interaction between the phenyl group of the enol silane and the titanium tetrachloride and **S**[1] is also probably not important because of the phenyl:OTMS nonbonded interactions.[2] Of the two remaining transition states **A**[2] and **S**[2], substitution of the trimethylsilyl group with the more sterically bulky *t*-butyldimethylsilyl group should disfavor the anti **A**[2] transition state and adopt the syn **S**[2] transition state. Due to the magnitude of the diastereomer ratios, the energy differences must be small between these transition states.

Because of low diastereoselectivity, it seemed possible that the silylated aldol products were equilibrating under the reaction conditions to yield a thermodynamic mixture of diastereomers. In order to this test hypothesis, pure diastereomers were isolated and subjected to the reaction conditions (Figure 9). The results showed no change in diastereomer ratios under the reaction conditions.

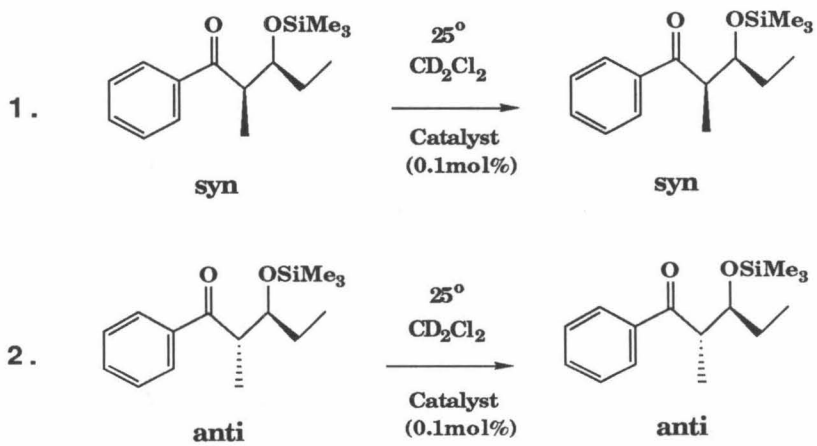


**Figure 9. Diastereomer equilibration control experiment.**

In addition, a deuterium double-label crossover experiment was carried out in order to determine the fate of the silyl groups (Figure 10). A mixture of 8 diastereomers corresponding to a 2:1 ratio of the four possible products was obtained. Based on the equilibration experiment, these results indicate that the silyl groups are rapidly exchanging between the aldol products under the reaction conditions.

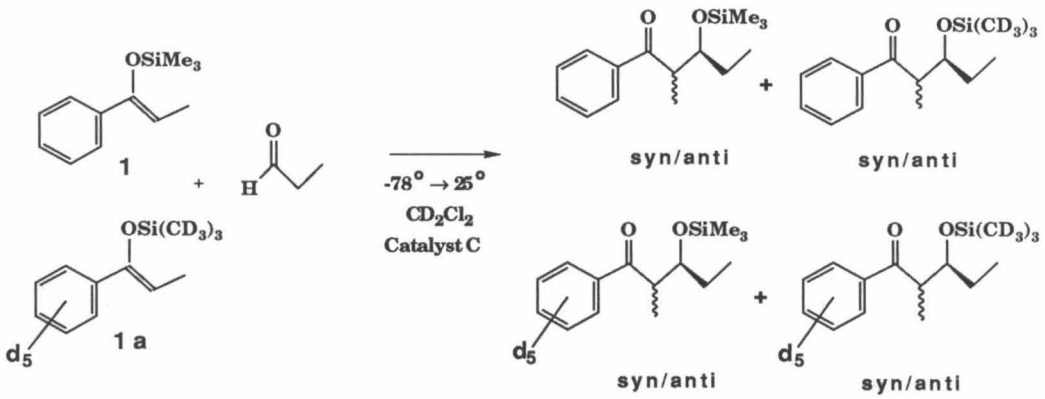


**Figure 10. Deuterium double-label crossover experiment.**

Another possible cause of poor diastereoselectivity involved the dissolution of the catalyst under the reaction conditions. X-ray powder diffraction spectra of catalyst samples before and after the reaction indicated no gross change in physical structure, however, the technique is not sensitive enough to determine changes that may occur on the surface of the magnesium chloride crystallites.

The *Z*-isomers of the enol silanes were used during the initial experiments due to the facile synthesis of this isomer in high purity. In the Mukaiyama reaction, *Z*-enol silanes generally favor the syn diastereomer while the *E*-enol silanes favor the anti isomers. With this catalyst system, the *E*-isomer of the trimethylsilyl enol ether of cyclohexanone gives a 1.3 : 1

(anti:syn) ratio while the Mukaiyama conditions yield a 3.3 : 1 (anti:syn) ratio (eq 3).[1]

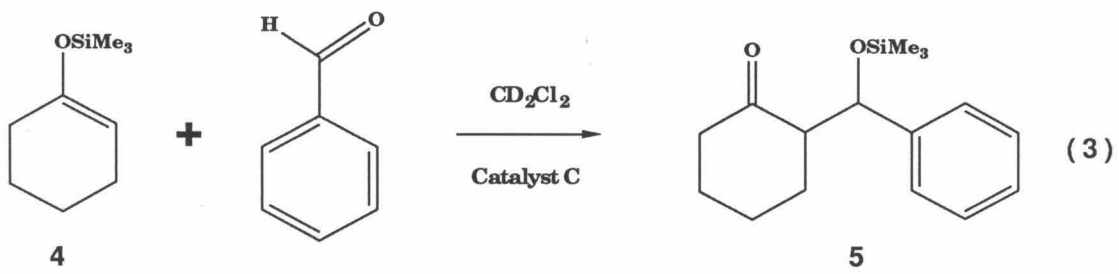


4 5 (3)

In order to increase the number of turnovers, the *t*-butyldimethylsilyl enol ether derived from acetophenone was prepared and condensed with benzaldehyde (eq 4).


6 7 (4)

**140 Turnovers**

Using supported catalyst **C**, the reaction proceeded with 140 turnovers. However, control reactions revealed that the reaction is also slowly catalyzed by the magnesium chloride support. Based on the difference of reaction rates between the titanium catalyst and the magnesium chloride support, seconds versus days, it is assumed that the number of turnovers for the above reaction are mainly a result of the titanium sites. This result also demonstrates the large difference in reactivity that methyl substitution at C-2 makes with these substrates.

Silyl ketene acetals are commonly used with the Mukaiyama reaction to increase the scope of synthetic applications. The condensation reaction of benzaldehyde with the silyl ketene acetal **8** was examined with catalyst **C**

(eq 5). The reaction was very clean giving 8 turnovers with a 10-fold excess of reactants.

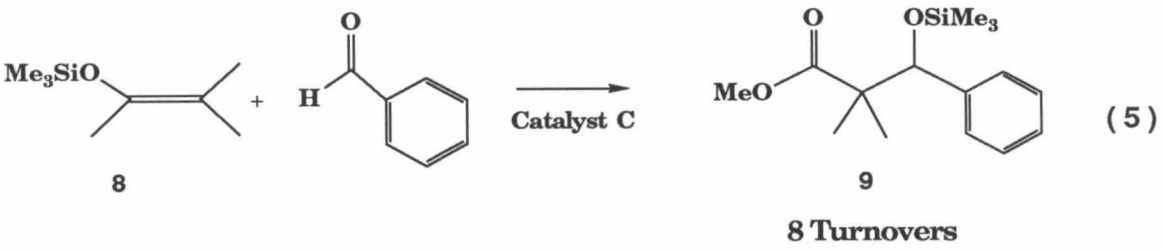


8 9 (5)

**8 Turnovers**

**Catalyst Modification.** In an attempt to increase the diastereoselectivity and probe the enantioselectivity of this catalyst system, two approaches were chosen. The first approach involved the selective poisoning of potentially chiral titanium sites with chiral ligands. The second method consisted of chemical modification of the catalyst sites.

Addition of 1 equivalent of either amine or phosphine ligands effectively poisoned the condensation reaction. This is consistent with the titanium sites being more active than the surrounding magnesium sites. In an attempt to determine the effect of chiral ligands, one-half equivalent of R-(+)-α-methylbenzylamine and (2S,3S)-(-)-bis-(diphenylphosphino)-butane were added to separate portions of supported catalyst before the addition of reactants. No change in diastereoselection was observed for the reaction of benzaldehyde with enol silane **1** and no enantioselectivity was observed for the reaction of benzaldehyde with ketene acetal **8**.

The second approach to selectivity control involved the direct modification of the titanium active site. One way to accomplish this consisted of the formation of a titanium alkoxide on the catalyst surface that possessed a large alkyl group that would extend away from the catalytic site and, perhaps, direct the approach of the incoming enol silane (Figure 11).

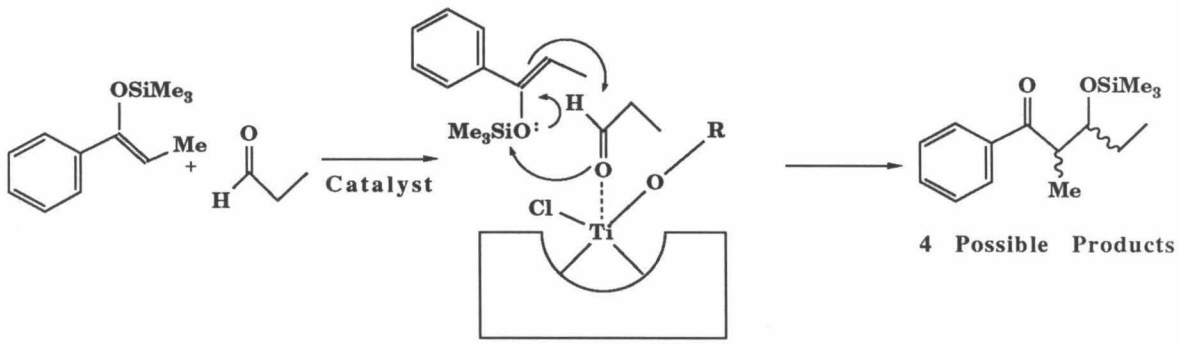


**Figure 11. Alkoxide catalyst scheme.**

The first attempt to accomplish this used a catalyst formed by treating the ethyl benzoate-magnesium chloride support with trichlorotitanium phenoxide. This catalyst did not perform well in methylene chloride but gave 5 turnovers and a 1.3:1 anti:syn selectivity with the reaction of **1** with benzaldehyde and 9 turnovers and a 1:1.5 anti:syn selectivity with the reaction of **2** and benzaldehyde in toluene (eq 6).

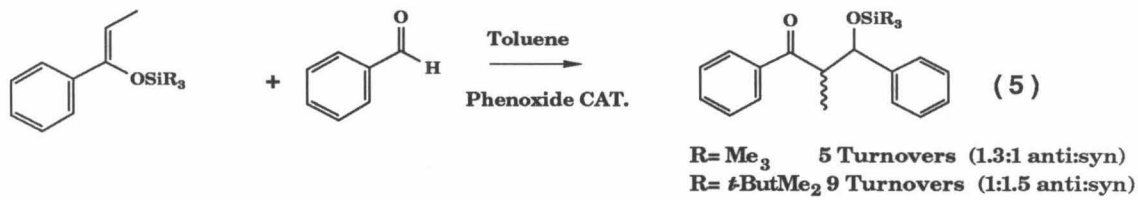


This diastereoselectivity ratio represents a very small change from the regular catalyst with 1.5:1 and 1:1.7 for the same reactions, respectively. This method of forming titanium alkoxides on the catalyst surface may be plagued by disproportionation reactions between the trichlorotitanium phenoxide and the support itself or titanium atoms on the surface. As a result, more than one kind of catalyst site can be formed with non-alkoxide sites possibly catalyzing the reaction. A second method relied on brute force with direct treatment of the catalyst with potassium *t*-butoxide. This catalyst, however, showed no catalytic activity. This was probably a result

of the alkoxide lowering the Lewis acidity of the titanium, multiple alkoxide formation which could prevent approach of the reactants, or general destruction of the active site. A more subtle method was chosen which took advantage of the ability of titanium to form alkoxides via reaction with silylated alcohols. Trimethylsilyl protected *l*-menthol was synthesized and added to the catalyst in a four-fold excess. $^1$H NMR indicated one-quarter of the silyl-alcohol reacted to form chlorotrimethylsilane as the expected by-product. This new alkoxide catalyst gave 9 turnovers of product in a 1.2:1 anti:syn ratio (eq 6).

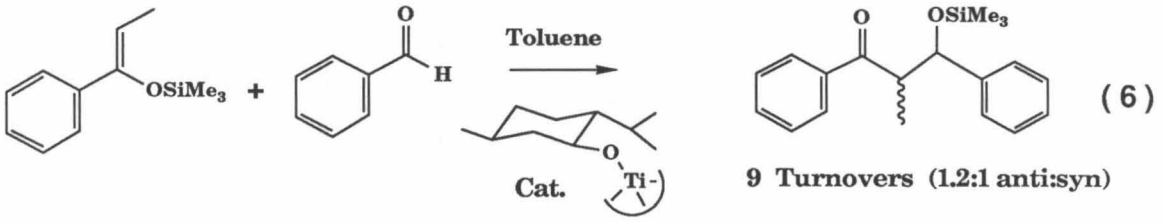


(6)

Apparently, modification of the catalysts based on a simple level of theory concerning site geometry is not adequate for this type of reaction. In addition to alkoxide catalysts, a catalyst based on tin tetrachloride was examined. This catalyst, however, showed very low catalytic activity.

**Polymerizations.** As mentioned in the introduction of Chapter III, a major application of group transfer technology involves the polymerization of monomers such as methylmethacrylate and the *t*-butyldimethylsilyl enol ether of acetaldehyde. Little information is given in the literature about the tacticities of such polymerizations probably due to the lack of stereocontrol in simple Lewis acid catalysis. As a result, the supported catalysts were screened for polymerization activity. Using the ketene acetal **8** as an initiator, the polymerization of methylmethacrylate was attempted (Figure 12). The reaction, however, was too slow for any polymerization to occur.

In addition, the polymerization of ethylacrylate was also unsuccessful. These results are consistent with earlier experiments in which higher temperatures are required for condensations to occur than with titanium tetrachloride by itself. This probably reflects the lower Lewis acidity of the titanium bound to the support surface.

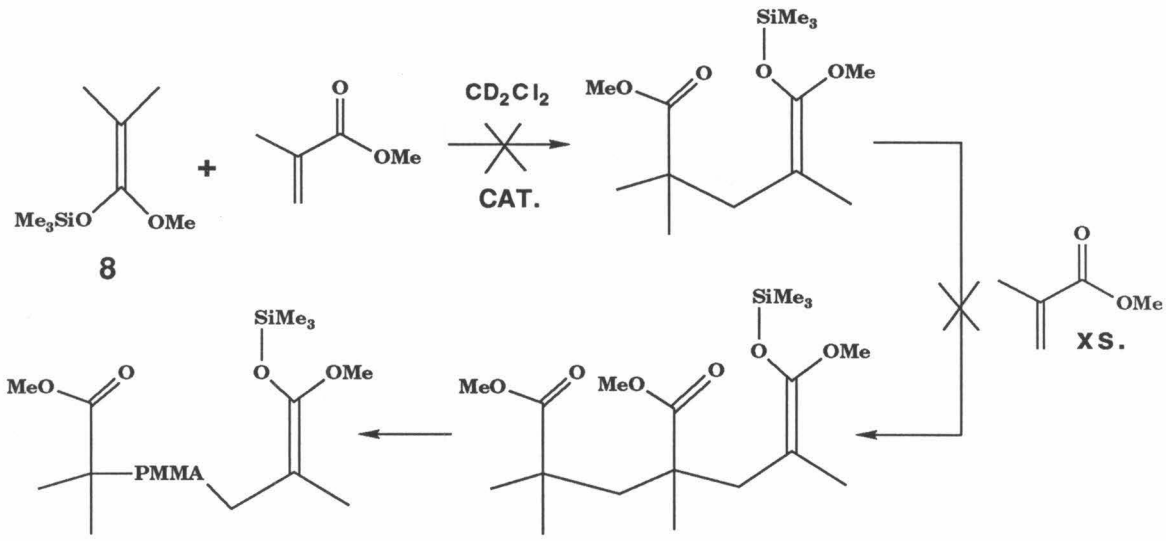


**Figure 12. Attempted methylmethacrylate polymerization.**

The methylmethacrylate GTP polymerization relies on the transfer of the silyl group from the initiator to the monomer. Another type of polymerization, the aldol polymerization, involves the transfer of the silyl group from the monomer to initiator. The polymerization of the *t*-butyldimethylsilyl enol ether of acetaldehyde was attempted and proved to be much more successful. Initiation with benzaldehyde resulted in polymers with molecular weights up to 10,000 (with respect to styrene standards) and molar mass dispersities of about 1.5 (Figure 13).

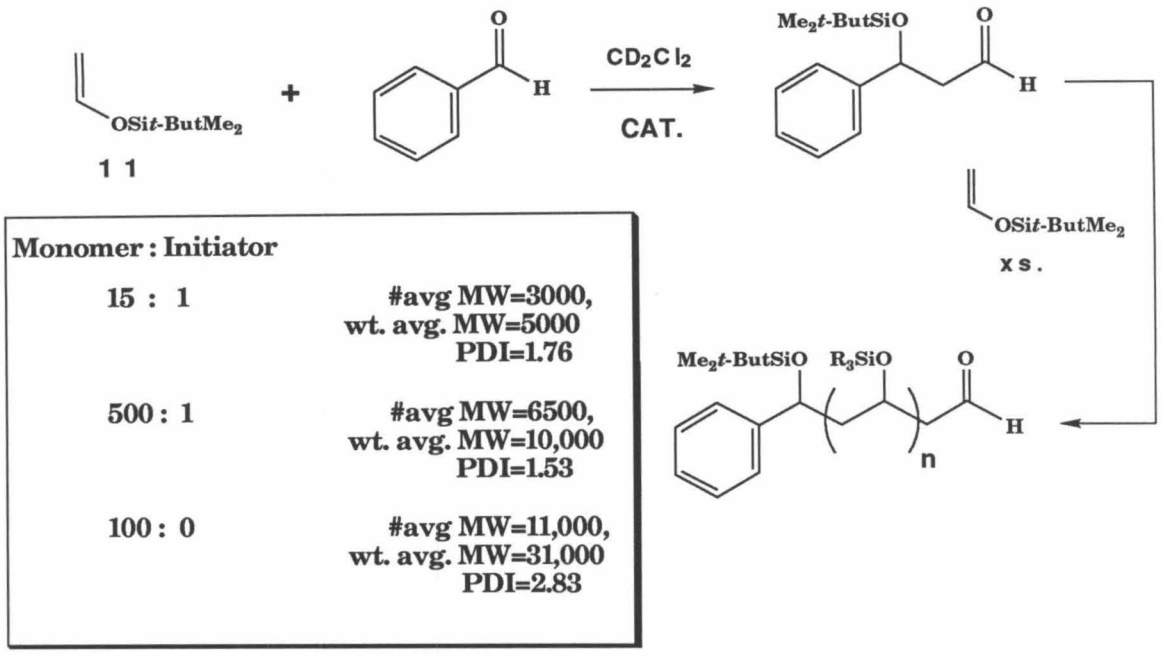


**Figure 13. Polymerization of *t*-butyldimethylsilyloxyethene.**

The resulting silylated polyols were colorless, tacky solids that could be drawn into fibers easily. Comparison with zinc chloride catalysis, however, indicated a molecular weight barrier existed in the supported catalyst system of about 25,000. A control experiment with monomer and catalyst without benzaldehdye showed that the catalyst was converting monomer into acetaldehyde which is an initiator for this type of polymerization. As a result, the extent of monomer deprotection establishes the maximum molecular weight of polymer in this system. A control reaction between the monomer and the magnesium chloride support indicated no polymerization occurs, thus side reactions with the titanium catalysts contribute to the desilylation of monomer. Attempts to determine the tacticity of the polysilylated alcohols via $^{13}C$ NMR analysis have proven unsuccessful due to broad methine signals.

A similar monomer was examined which was derived from propionaldehyde. With the added methyl group, this monomer had the potential for forming a polymer with an easier to define tacticity. Reaction of both the E and Z isomers of the monomer with benzaldehyde resulted in only the basic Mukaiyama addition (Figure 14).

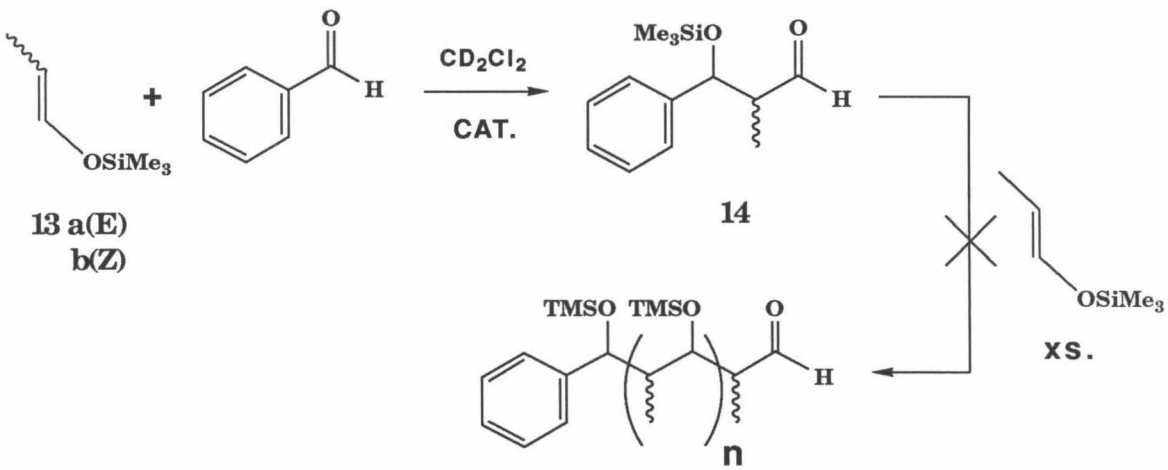


**Figure 14. Attempted polymerization of *Z* and *E*-1-trimethylsilyloxypropene.**

This probably reflects the much lower reactivity of the monomer towards the newly formed aldehyde in this system as a result of methyl substitution on the enol ether. The reaction of the *E* isomer proceeded with 7 catalytic turnovers and a diastereoselectivity of 2.7:1 (anti:syn). The reaction of the *Z* isomer proceeded with 5.7 catalytic turnovers and a diastereoselectivity of 1.8:1 (anti:syn). These results are consistent with the open transition state model due to the lack of steric interactions between R groups in transition state $\mathbf{S^2}$ (Scheme 2).

**Summary.** In summary, magnesium chloride supported titanium tetrachloride catalysts show catalytic activity for the Mukaiyama reaction with some examples giving up to 140 catalytic turnovers. The catalyst shows little diastereoselection with anti:syn ratios suggesting an open transition state is operative. The number of turnovers is directly related to the activity of the enol silanes and aldehyde substrates. Attempts to modify the catalyst surface via ligand poisoning and direct alkoxide formations have thus far proven unsuccessful. The supported catalysts are not effective for the group transfer polymerization of methylmethacrylate, however, they show activity for the aldol group transfer polymerization of *t*-butyldimethylsilyloxyethene. The polymerizations are limited by the conversion of monomer to initiator by the supported catalyst. These results are encouraging in that supported catalysts show activity in other Lewis acid catalyzed reactions. There is a great deal that is not known about these catalysts, however, as more information is obtained concerning the structure and reactivity of such systems, the potential applications should expand.

## Experimental Section

**General Considerations.** All air-sensitive manipulations were carried out under argon using standard Schlenk techniques or in a nitrogen-filled glove box (Vacuum Atmospheres DC-882) equipped with MO-40-1 purification train, DK-3E Dri-Kool conditioner, and Dri-Cold freezer. Flash chromatography was performed by the procedure of Still *et al.*, using silica Woelm 32-63(32-63mm). Thin layer chromatography was performed on EM Reagents 0.25mm silica gel 6-f plates and visualized with iodine vapor or *p*-anisaldehyde dip. Argon was purified by passage through columns of BASF RS-11 (Chemlog) catalyst and Linde 4Å molecular sieves. Benzene, diethyl ether, hexane, pentane (HPLC grade), THF, toluene, and NMR solvents were stirred over $CaH_2$ and transferred onto sodium benzophenone ketyl. All solvents were vacuum transferred and stored under argon in flasks equipped with teflon screw valves. Methylene chloride was dried over $P_2O_5$, vacuum transferred, and degassed by successive freeze-thaw pump cycles. Mesitylene was dried over $CaH_2$, vacuum transferred, and stored in the drybox. NMR spectra were recorded on Varian EM-390 (90 MHz, $^1H$), Jeol FX-90Q (89.60 MHz, $^1H$), and Jeol 400GX (399.65 MHz, $^1H$; 100.4 MHz, $^{13}C$) spectrometers. Chemical shifts are reported versus residual solvent signals ($^1H$: $C_6D_6$, δ 7.15; $CDCl_3$, δ 7.24; $C_7D_8$, δ 2.09; $^{13}C$: $C_6D_6$, δ 128.0; $CDCl_3$, δ 77.0; $C_7D_8$, δ 20.9;). Data are reported as follows: chemical shift, multiplicity (s=singlet, d=doublet, t=triplet, q=quartet, m=multiplet, br=broad), coupling constant (Hz), integration, and assignment. Measurement of weight was conducted after minimizing static interference through the use of Staticmaster ionizing unit (Nuclear Products Company). All reaction temperatures were

measured externally. Elemental analysis were performed at the California Institute of Technology Analytical Facility. Gas Chromatography was performed on a Shimadzu GC-mini 2 equipped with a Quadrex 50m SE-30 capillary column. Infrared spectra were recorded as nujol mulls or in solution in $CDCl_3$ on a Perkin-Elmer 1600 instrument. Gel permeation chromatography (GPC) was performed utilizing Shodex KF-803, 804, 805, and 805.4 columns with toluene as solvent. The polymer was detected with a Spectroflow variable wavelength absorbance detector and a Knauer differential refractometer. Samples for analysis were prepared between 0.2-0.4% by weight in toluene. The molecular weights were referenced to narrow-dispersity polystyrene samples (polysciences) ranging from MW = 3550 tp 1,300,000. All aldehydes were either passed through basic alumina or washed with aqueous bicarbonate and dilute mineral acid, dried with $MgSO_4$, and distilled. *E* and *Z* -1-[(trimethylsilyl)oxy]-1-propene **13 a,b**, *Z* -1-phenyl-1-[(trimethylsilyl)oxy]-1-propene **1**, *Z* -1-phenyl-1-[(*t*-butyl-dimethylsilyl)oxy]-1-propene **2**, 1-phenyl-1-(*t*-butyldimethylsilyl)-oxyethene **6**, and *t*-butyldimethylsilyloxy-1-ethene **11** were prepared using the known methods.[6c,18] Dimethyl ketene methyl trimethylsilylacetal **8** (Petrarch), 1-trimethylsilyloxy-1-cyclohexene **4** (Petrarch), $d_9$-chlorotrimethylsilane (MSD), and $d_5$-propiophenone(MSD) were used as received. Catalysts $TiCl_3$ (AA) **a**, $TiCl_3$ $(AlCl_3)_x(R_2O)_y$ **b**, $TiCl_4$ +E.B.+$MgCl_2$ **c**, $TiCl_4$ +DiBP+$MgCl_2$ **d**, $TiCl_2$ $OR(R_2O)_x(MgCl_2)_y$ **e**, $TiCl_3$ H **f**, $TiCl_4$ **g**,$MgCl_2$ **h** , and $TiCl_3$Ophenyl +E.B.+$MgCl_2$ **i** were provided by the Sumitomo Chemical Company.

**General Procedure for NMR Tube Reactions.** An NMR tube was first weighed under static-free conditions in a nitrogen atmosphere. Solids were loaded into the tube, static was removed, and weight was recorded. Solvent

(400 μl) was added and a latex septum was fitted onto the NMR tube and sealed with parafilm. The tube was cooled to the appropriate temperature and liquid substrates and integration standards added via syringe. The reaction vessel was then warmed to the required temperature and shaken vigorously for a specified time. The tube was inverted and the solids transferred to the top by centrufigation.

**Reaction of *Z* -1-phenyl-1-[(trimethylsilyl)oxy]-1-propene (1) with propionaldehyde, product (3a), catalyst C.** $^1$H NMR analysis with internal standard showed that the yield was 38% indicating 3.8 catalytic turnovers with a 2:1 (anti:syn) mixture of diastereomers . $^1$H NMR ($CD_2Cl_2$) Major isomer (*anti*) δ 7.92 (d, 2H, Ph), 7.50 (m, 3H, Ph), 3.95 (m, 1H, $H_a$), 3.49 (m, 1H, $H_b$), 1.40 (m, 2H, Et), 1.19 (d, $J$ = 6.8 Hz, 3H, Me), 0.86 (t, $J$ = 7.3 Hz, 3H, Et), 0.07 (s, 9H, $SiMe_3$). $^1$H NMR ($CD_2Cl_2$) of the hydrolysis product δ 7.95 (d, 2H, Ph), 7.50 (m, 3H, Ph), 3.92 (m, 1H, $H_a$), 3.66 (m, $J_{HaHb}$= 6.8 Hz, 1H, $H_b$), 2.88 (d, 1H, OH), 1.47 (m, 2H, Et), 1.24 (d, $J$ = 7.3 Hz, 3H, Me), 0.98 (t, $J$ = 7.3 Hz, 3H, Et). (*syn*) δ 7.92 (d, 2H, Ph), 7.50 (m, 3H, Ph), 3.95 (m, 1H, $H_a$), 3.46 (m, 1H, $H_b$), 1.40 (m, 2H, Et), 1.19 (d, $J$ = 6.8 Hz, 3H, Me), 0.86 (t, $J$ = 7.3 Hz, 3H, Et), 0.07 (s, 9H, $SiMe_3$). $^1$H NMR ($CD_2Cl_2$) of the hydrolysis product δ 7.95 (d, 2H, Ph), 7.50 (m, 3H, Ph), 3.92 (m, 1H, $H_a$), 3.46 (m, $J_{HaHb}$= 2.9 Hz, 1H, $H_b$), 3.09 (d, 1H, OH), 1.59 (m, 2H, Et), 1.23 (d, $J$ = 7.3 Hz, 3H, Me), 0.98 (t, $J$ = 7.3 Hz, 3H, Et).

**Reaction of *Z* -1-phenyl-1-[(trimethylsilyl)oxy]-1-propene (1) with *iso*-valeraldehyde, product (3b), catalyst C.** $^1$H NMR analysis with internal standard showed that the yield was 40% indicating 4.0 catalytic turnovers with a 2:1 (anti:syn) mixture of diastereomers . $^1$H NMR ($CD_2Cl_2$) Major isomer (*anti*) δ 7.90 (m, 2H, 2Ph), 7.45 (m, 3H, 2Ph), 4.08 (m, 1H, $H_a$), 3.51

(m, 1H, $H_b$),2.16 (m, 2H, *i*-Pr $CH_2$), 1.35 (m, 1H, *i*-Pr CH), 1.17 (d, $J$ = 7.0 Hz, 3H, Me), 0.88 (d, $J$ = 6.2 Hz, 3H, *i*-Pr Me), 0.87 (d, $J$ = 6.6 Hz, 3H, *i*-Pr Me), 0.03 (s, 9H, $SiMe_3$). (*syn*) δ 7.90 (m, 2H, 2Ph), 7.45 (m, 3H, 2Ph), 4.08 (m, 1H, $H_a$), 3.63 (m, 1H, $H_b$),2.16 (m, 2H, *i*-Pr $CH_2$), 1.35 (m, 1H, *i*-Pr CH), 1.08 (d, $J$ = 7.0 Hz, 3H, Me), 0.92 (d, $J$ = 6.6 Hz, 3H, *i*-Pr Me), 0.84 (d, $J$ = 6.6 Hz, 3H, *i*-Pr Me), -0.27 (s, 9H, $SiMe_3$).

**Reaction of *Z* -1-phenyl-1-[(trimethylsilyl)oxy]-1-propene (1) with cyclohexanecarboxaldehyde, product (3c), catalyst C.** $^1H$ NMR analysis with internal standard showed that the yield was 60% indicating 6 catalytic turnovers with a 3:1 (anti:syn) mixture of diastereomers . $^1H$ NMR ($CD_2Cl_2$) Major isomer (*anti*) δ 7.90 (d, 2H, Ph), 7.46 (m, 3H, Ph), 3.87 (m, 1H, $H_a$), 3.69 (m, 1H, $H_b$), 1.8-0.89 (brm, 11H, Cyclohexyl), 1.15 (d, $J$ = 7 Hz, 3H, Me), 0.02 (s, 9H, $SiMe_3$). (*syn*) δ 7.91 (d, 2H, Ph), 7.55 (m, 3H, Ph), 3.89 (m, 1H, $H_a$), 3.76 (m, 1H, $H_b$), 1.8-0.89 (brm, 11H, Cyclohexyl), 1.05 (d, $J$ = 7 Hz, 3H, Me), -0.11 (s, 9H, $SiMe_3$).

**Reaction of *Z* -1-phenyl-1-[(trimethylsilyl)oxy]-1-propene (1) with benzaldehyde, product (3d), catalyst C.** $^1H$ NMR analysis with internal standard showed that the yield was 66% indicating 6.6 catalytic turnovers with a 1.5:1 (anti:syn) mixture of diastereomers . $^1H$ NMR ($CD_2Cl_2$) Major isomer (*anti*) δ 7.40 (m, 10H, 2Ph), 4.83 (d, $J$ = 9.5 Hz, 1H, $H_a$), 3.81 (m, 1H, $H_b$), 0.82 (d, $J$ = 7 Hz, 3H, Me),- 0.21 (s, 9H, $SiMe_3$). (*syn*) 7.40 (m, 10H, 2Ph), 4.98 (d, $J$ = 7.3 Hz, 1H, $H_a$), 3.81 (m, 1H, $H_b$), 1.23 (d, $J$ = 6.6 Hz, 3H, Me),- 0.05 (s, 9H, $SiMe_3$).

**Reaction of *Z* -1-phenyl-1-[(*t*-butyldimethylsilyl)oxy]-1-propene (2) with propionaldehyde, product (3e), catalyst C.** $^1H$ NMR analysis with internal

standard showed that the yield was 80% indicating 8.0 catalytic turnovers with a 1:1 (anti:syn) mixture of diastereomers. $^1$H NMR ($CD_2Cl_2$) Major isomer (*anti*) δ 7.92 (m, 2H, Ph), 7.46 (m, 3H, Ph), 4.04 (d, 1H, $H_a$), 3.62 (m, 1H, $H_b$), 2.43 (m, 2H, Et), 0.98 (d, $J$ = 6.2 Hz, 3H, Me), 0.88 (t, $J$ = 7.3 Hz, 3H, Et), 0.86 (s, 9H, Si*t*-But), -0.04 (d, 6H, $SiMe_2$). (*syn*) δ 7.92 (m, 2H, Ph), 7.46 (m, 3H, Ph), 4.04 (d, 1H, $H_a$), 3.74 (m, 1H, $H_b$), 2.43 (m, 2H, Et), 1.18 (d, $J$ = 7.0 Hz, 3H, Me), 1.07 (t, $J$ = 7.7 Hz, 3H, Et), 0.71 (s, 9H, Si*t*-But), -0.10 (d, 6H, $SiMe_2$).

**Reaction of *Z* -1-phenyl-1-[(*t*-butyldimethylsilyl)oxy]-1-propene (2) with benzaldehyde, product (3f), catalyst C.** $^1$H NMR analysis with internal standard showed that the yield was 92% indicating 9.2 catalytic turnovers with a 1:1.7 (anti:syn) mixture of diastereomers . $^1$H NMR ($CD_2Cl_2$) Minor isomer (*anti*) δ 7.38 (m, 10H, 2Ph), 4.84 (d, $J$ = 9.5 Hz, 1H, $H_a$), 3.82 (m, 1H, $H_b$), 0.81 (d, $J$ = 7 Hz, 3H, Me), 0.59 (s, 9H, Si*t*-But), -0.27 (d, 6H, $SiMe_2$). (*syn*) δ 7.38 (m, 10H, 2Ph), 4.98 (d, $J$ = 7.3 Hz, 1H, $H_a$), 3.82 (m, 1H, $H_b$), 1.27 (d, $J$ = 7 Hz, 3H, Me), 0.86 (s, 9H, Si*t*-But), -0.16 (d, 6H, $SiMe_2$).

**Reaction of 1-trimethylsilyloxy-1-cyclohexene (4) with benzaldehyde, product (5), catalyst C.** $^1$H NMR analysis with internal standard showed that the yield was 43% indicating 4.3 catalytic turnovers with a 1.3:1 (anti:syn) mixture of diastereomers . $^1$H NMR ($CD_2Cl_2$) Major isomer (*anti*) δ 7.30 (m, 5H, Ph), 5.03 (d, $J$ = 7.7 Hz, 1H, $H_a$), 2.6-1.4 (brm, 9H, Aliphatic CH), 0.02 (s, 9H, $SiMe_3$). (*syn*) δ 7.30 (m, 5H, Ph), 5.28 (d, $J$ = 4.4 Hz, 1H, $H_a$), 2.6-1.4 (brm, 9H, Aliphatic CH), -0.05 (s, 9H, $SiMe_3$).

**Reaction of *t*-butyldimethylsilyloxy-1-ethene (6) with benzaldehyde, product (7), catalyst C.** $^1$H NMR analysis with internal standard showed

that the yield was 89% indicating 140 catalytic turnovers . $^1$H NMR ($CD_2Cl_2$) δ 7.45 (m, 10H, 2Ph), 5.36 (m, 1H, $H_a$), 3.56 (dd, $J$ = 6.6 Hz,$J$ = 15.3 Hz, 1H, $H_{b1}$), 3.00 (dd, $J$ = 4 Hz,$J$ = 15.3 Hz, 1H, $H_{b2}$), 0.75 (s, 9H, Si*t*-But), -0.14 (d, 6H, $SiMe_2$).

**Reaction of dimethyl ketene methyl trimethylsilylacetal (8) with benzaldehyde, product (9), catalyst C.** $^1$H NMR analysis with internal standard showed that the yield was 81% indicating 8 catalytic turnovers. $^1$H NMR ($CD_2Cl_2$) δ 7.24 (m, 5H, Ph), 4.94 (s, 1H, $H_a$), 3.65 (s, 3H, OMe), 1.09 (s, 3H, Me), 0.96 (s, 3H, Me), 1.03 (s, 3H, Me), -0.07 (s, 9H, $SiMe_3$). Analysis by chiral G.C., 25 M Chirasil-Val cap. col., shows no enantioselectivity using 0.5 equivalents of chiral amine or phosphine.

**Reaction of dimethyl ketene methyl trimethylsilylacetal (8) with R-(-)-myrtenal, product (10), catalyst C.** $^1$H NMR analysis with internal standard showed that the yield was 87% indicating 8.7 catalytic turnovers with only one diastereomer. $^1$H NMR ($CD_2Cl_2$) δ 5.37 (m, 1H, $H_b$), 4.35 (s, 1H, $H_a$), 3.60 (s, 3H, $Me_a$), 2.39 (m, 1H), 2.29 (m, 1H), 2.05 (m, 1H), 1.26 (s, 3H, Me), 1.14 (d, J=8.4Hz, 1H), 1.10 (s, 3H, Me), 1.03 (s, 3H, Me), 0.82 (s, 3H, Me),0.05 (s, 9H, $SiMe_3$).

**Deuterium double-label crossover experiment .** An NMR tube was charged with 14.4 mg ($2.9x10^{-6}$ mol) of catalyst **C** and suspended in 0.4 mL of $CD_2Cl_2$. After cooling to -78 °C, 2.3 μL of propionaldehyde (3.2 μmol) and 7.1 μL of a 50:50 mixture of the (**1**) and Z -1-$d_5$-phenyl-1-[($d_9$-trimethylsilyl)oxy]-1-propene were added via syringe. The temperature was raised to 25 °C slowly and the solids were transferred to the bottom by centrufigation. After small scale purification with Florisil, the crude

product was analyzed by VPC at 170 °C. The cap GC showed 8 peaks in the product region corresponding to a 2:1 mixture of the 4 possible products.

**X-ray powder diffraction of catalyst C before and after reaction.** The catalysts were loaded into 0.3 mm capillary tubes in the dry box and sealed with a microtorch on the bench. The samples were placed in a modified Phillips camera and runs made at 45 kV, 22 mA of Cu radiation for 4 to 15 hours. The film was developed and analyzed by a Brumma Ultrascan XL laser densitometer. The major peaks at $\theta$ = 16.04, 31.23, 35.99, 50.14, and 61.89 appeared in samples before and after with no indication of change.

**Preparation of $SnCl_4 \cdot MgCl_2$ catalyst.** A Schlenk tube was charged with 52 mg of $MgCl_2$ and suspended in 10 mL of hexane. An excess of tin tetrachloride was added and the mixture was stirred for 6 hours. The color changed from white to gray. The solvent was decanted and the residue washed 3X10 mL of hexane before pumping dry.

**Polymerization of *t*-butyldimethylsilyloxy-1-ethene (11) with catalyst C.** The catalyst was weighed into a Schlenk tube under nitrogen and suspended with 10 mL of methylene chloride. After cooling to -78 °C, a mixture of the monomer and the aldehyde initiator were added via syringe while stirring. The temperature was raised to 25 °C slowly. After one hour, the solvent was decanted from the catalyst, filtered through Florisil, and concentrated to afford the crude silylated polyvinyl alcohol. In most cases, the catalyst turned from yellow to pale yellow. During the control reaction in the absence of aldehyde, the catalyst turned blue-green indicating the presence of titanium(III). The resulting crude polymers were colorless, clear, tacky solids that could be drawn easily. $^1H$ NMR

($CDCl_3$) δ 9.78 (brs, 1H, Ald. H), 7.30 (m, 5H, Ph), 3.84 (brm, 1H, CH), 1.55 (brm, 2H, $CH_2$), 0.83 (brs, 9H, Si*t*-But), 0.03 (brd, 6H, $SiMe_2$). The aldehyde and aromatic peaks gave an integration of 1:30 versus all other peaks.

**Reaction of *E*-trimethylsilyloxy-1-propene (13a) with benzaldehyde, product (14), catalyst C.** $^1H$ NMR analysis with internal standard showed that the yield was 70% indicating 7 catalytic turnovers with a 2.7:1 (anti:syn) ratio. $^1H$ NMR ($CD_2Cl_2$) (anti) δ 9.72 (s, 1H, Aldehyde H), 7.32 (m, 5H, Ph), 4.78 (d, *J*=7Hz, 1H, $H_a$), 2.60 (m, 1H, $H_b$), 0.86 (d, *J*=7 Hz, 3H, Me), -0.02 (s, 9H, $SiMe_3$). (syn) δ 9.72 (s, 1H, Aldehyde H), 7.32 (m, 5H, Ph), 5.18 (d, *J*=4.4Hz, 1H, $H_a$), 2.60 (m, 1H, $H_b$), 0.97 (d, *J*=7 Hz, 3H, Me), 0.02 (s, 9H, $SiMe_3$).

**Reaction of *Z*-trimethylsilyloxy-1-propene (13b) with benzaldehyde, product (14), catalyst C.** $^1H$ NMR analysis with internal standard showed that the yield was 57% indicating 5.7 catalytic turnovers with a 1.8:1 (anti:syn) ratio. $^1H$ NMR ($CD_2Cl_2$) (*anti*) δ 9.72 (s, 1H, Aldehyde H), 7.32 (m, 5H, Ph), 4.78 (d, *J*=7Hz, 1H, $H_a$), 2.60 (m, 1H, $H_b$), 0.86 (d, *J*=7 Hz, 3H, Me), -0.02 (s, 9H, $SiMe_3$). (*syn*) δ 9.72 (s, 1H, Aldehyde H), 7.32 (m, 5H, Ph), 5.18 (d, *J*=4.4Hz, 1H, $H_a$), 2.60 (m, 1H, $H_b$), 0.97 (d, *J*=7 Hz, 3H, Me), 0.02 (s, 9H, $SiMe_3$).

## References and Notes

1. a) Mukaiyama, T.; Banno, K.; Narasaka, K. *J. Am. Chem. Soc.* **1974**, *96*, 7503-7509. b) Mukaiyama, T. *Angew. Chem. Int. Ed. Engl.* **1977**, *16*, 817-826. c) Evans, D.A.; Nelson, J.V.; Taber, T.R. *Top. Stereochem.* **1982**, *13*, 55-59. d) Heathcock, C.H. "Asymmetric Synthesis V. 3" (Morrison, J.D. Ed.) Academic Press, Orlando, **1983**.

2. Heathcock, C.H.; Davidsen, S.K.; Hug, K.T.; Flippin, L.A. *J. Org. Chem.* **1986**, *51*, 3027-3037.

3. Brownbridge, P. *Synthesis* **1983**, 1-28.

4. Yamamoto, Y.; Maruyama, K.; Matsumoto, K. *J. Am. Chem. Soc.* **1983**, *105*, 6963-6965.

5. a) Dubois, J.; Axiotis, G; Bertounesque, E. *Tetrahedron Lett.* **1984**, *25*, 4655-4658. b) Chan, T.H.; Brook, M.A. *ibid.*, **1985**, *26*, 2943-2946.

6..a) Kleschick, W.A.; Buse, C.T.; Heathcock, C.H. *J. Am. Chem. Soc.* **1977**, *99*, 247. b) Noyori, R.; Nishida, I.; Sakata, J. *ibid.* **1981**, *103*, 2106. c) Heathcock, C.H.; Buse, C.T.; Kleschick, W.A.; Pirrung, M.C.; Sohn, J.E.; Lampe, J. *J. Org. Chem.* **1980**, *45*, 1066. d) Nakamura, E.; Shimizu, M.; Kuwajima, I. *tetrahedron Lett.* **1976**, 1699. e) Noyori, R.; Yokahama, K.; Sakata, J.Nakamura, E.; Shimizu, M.; Kuwajima, I. *J. Am. Chem. Soc.* **1977**, *99*, 1265.

7. a) Reetz, M.T. *Angew. Chem. Int. Ed. Engl.* **1984**, *23*, 556. b) Reetz, M.T.; Kesseler, K.; Schmidtberger, S.; Wenderoth, B.; Steinbach, R. *Angew. Chem.* **1983**, *95*, 1007. c) Reetz, M.T.; Kesseler, K.; Jung, A.

*Tetrahedron* **1984**, *40*, 4327. d) Reetz, M.T.; Kesseler, K.; Jung, A. *Tetrahedron Lett.* **1984**, *25*, 729. e) Gennari, C.; Colombo, L.; Bertonlini, G.; Shimperna, G. *J. Org. Chem.* **1987**, *52*, 2754-2760.

8. a) Sato, S.; Matsuda, I.; Izumi, Y. *J. Organometal. Chem.* **1988**, *352*, 223-238. b) Reetz, M.T.; Vougioukas, A.E. *Tetrahedron Lett.* **1987**, *28*, 793-796. c) Reetz, M.T.; Kyung, S.; Bolm, C.; Zierke, T. *Chemistry and Industry* **1986**, 824. d) Reetz, M.T.; Kunisch, F.; Heitman, P. *Tetrahedron Lett.* **1986**, *27*, 4721-4724. e) Vougioukas, A.E.; Kagan, B. *ibid.*, **1987**, *28*, 5513-5516. f) Sato, S.; Matsuda, I.; Izumi, Y. *ibid.*, **1986**, *27*, 5517-5520.

9. a) Webster, O.W.; Hertler, W.R.; Sogah, D.Y.; Farnham, W.B.; Rajanbabu, T.V. *J. Macromol. Sci. Chem.* **1984**, *A21 (8&9)*, 943. b) Sogah, D.Y.; Hertler, W.R.; Webster, O.W. *Macromolecules* **1987**, *20*, 1473.

10. a) Barbe, P.C.; Cecchin, L.; Noristi, L. *Adv. Polym. Sci.* **1986**, *81*, 1-81 and references therein. b) Boor, J.; "Ziegler-Natta Catalysts and Polymerization," Academic Press, New York, **1979**. c) Kashiwa, N.; Yoshitake, J. "Transition Metal Catalyzed Polymerizations," Quirk, R.P. Ed., Cambridge University Press, Cambridge, **1988**, 240-254. d) Soga, K.; Shiono, M.C. *ibid.* 266-279. e) Busico, V.; Corradini, P. *ibid.* 551-562.

11. Information provided by Dr. Toshio Sasaki of the Sumitomo Chemical Company.

12. The infrared spectrum of the catalyst showed an absence of bidentate ligation of ethyl benzoate to titanium. The IR, however, showed bidentate ligation of ethyl benzoate to magnesium.

13. Reetz, M.T.; Jung, A. *J. Am. Chem. Soc.* **1983**, *105*, 4833.

14. A similar project using supported catalysts for Diels-Alder reactions was attempted by Dr. Andreas Endesfelder of this research group. His catalysts were prepared using intensive ball milling procedures which resulted in samples with about a 200 Å particle size. These catalysts gave no enantioselectivity with Diels-Alder reactions. Some of these catalysts were screened for activity with the Mukaiyama reaction, however, they were plagued by poor yields and gave large amounts of ethyl benzoate in solution indicating poor mechanical properties.

15. The number of titanium atoms on the surface edges of the magnesium support can be calculated using the following scheme:

Cl-Mg-Cl = 3.6Å

(100)/(110) = 50/50

$$\#\text{Ti atoms} = \frac{33.5\text{Å} \times 12}{3.6\text{Å}} = 112$$

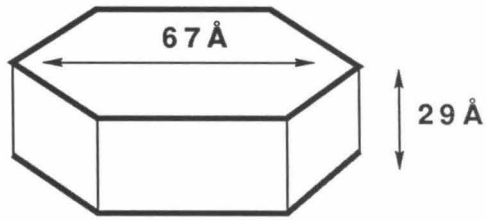


(100)

$$\text{wt. Ti} = \frac{112}{6.02 \times 10^{23}} \times 47.9 = 8.9 \times 10^{-21}(\text{g})$$

$$\text{wt. MgCl2} = \frac{33.5 \times 10^{-8} \times \frac{\sqrt{3}}{2} \times 33.5 \times 10^{-8} \times 6 \times 29 \times 10^{-8}}{2} \times 2.33\ \text{g/cm}^{-1}$$

$$= 2.0 \times 10^{-19}(\text{g})$$

$$\text{Ti Cont.} = \frac{\text{wt. of } TiCl_4}{\text{wt. of } MgCl_2} \times 100 = 2.2\ \text{wt.\%}$$

16. a) Ackerman, E. *Acta Chem. Scand.* **1957**, *11*, 373. b) Corey, E.J.; Snider, B.B. *J. Am. Chem. Soc.* **1972**, *94*, 2549.

17. a) Heathcock, C.H.; Flippin, L.A. *J. Am. Chem. Soc.* **1983**, *105*, 1667. b) Reetz, M.T.; Jung, A. *Tetrahedron* **1984**, **21**, 4327. c) Yammamoto, Y., Yatagia, H.; Naruta, Y.; Maruyama, K. *J. Am. Chem. Soc.* **1980**, *102*,

7107-7109. d) Murata, S.; Suzuki, M.; Noyori, R. *J. Am. Chem. Soc.* **1980**, *102*, 3248-3249.

18. Sogah, D. Y. *Polymer Preprints* **1986**, *27(1)*, 163-164.

19. Jung, M.E.; Blum, R.B. *Tetrahedron Lett.* **1977**, 3791.